GLASSES AND GLASS-CERAMICS FOR NUCLEAR WASTE MANAGEMENT

Scientific Editor: J.Ma. RINCON

Edited by : CENTRO DE INVESTIGACIONES ENERGETICAS MEDIOAMBIENTALES Y TECNOLOGICAS (CIEMAT)

and

INSTITUTO DE CERAMICA Y VIDRIO, C. S. I. C.

Madrid, 1987

GLASSES AND GLASS-CERAMICS FOR NUCLEAR WASTE MANAGEMENT

Scientific Editor: J.Ma. RINCON

Edited by : CENTRO DE INVESTIGACIONES ENERGETICAS
MEDIOAMBIENTALES Y TECNOLOGICAS (CIEMAT)

and

INSTITUTO DE CERAMICA Y VIDRIO , C. S. I. C.

Madrid, 1987

FOREWORD

This book documents a Seminar hold in Madrid of the use of glasses and glass-ceramics in nuclear waste management for the purpose of inmobilizing the radioactives isotopes used or generated in the nuclear industry. Nowadays, it is well known and accepted the critical problem which represent the nuclear wastes in the countries where the nuclear industry is being used for power production, research of military purposes. Therefore, since a few years a lot of technical and scientific and attention from the Governments research is being dedicated to solve this problem, giving rise to a wide spectrum of proposed solutions. Among them the ceramics and glasses can afford one of the most valuables. Furthermore , the glass-ceramics as intermediate material between the glasses and the ceramics are also candidate materials for inmobilizing the nuclear wastes.

The Seminar covered the glass structure, inmiscibility problems, materials design, leaching, thermal conductivity and radiation damage. This book should probe to be of value to both ceramic, glass, and nuclear researches and engineers.

The table of contents is organized in such a way as to serve as a subject index and provides easy to the information contained in the book.

Finally, this book is the first one published in Spain dedicated to applications of ceramics for nuclear waste management with a large contribution of spanish scientifics interested in this field. Hence, it is hope will promote this scientific research in Spain and serve to the European Community and other world scientifics in knowing the spanish researches working in glasses or ceramics related with nuclear waste inmobilization. Otherwise, the valuable contribution of Profs. from the University of California and Lawrence Berkeley Lab. on glass structure, radiation damage in glasses and leaching problems in geological environments will be very useful for specialist.

The Scientific Editor

Dr. JESUS Mª RINCON LOPEZ
CHAIRMAN OF THE
PHYSIC-CHEMISTRY METHODS DEPARTMENT
AT THE INSTITUTO DE CERAMICA Y VIDRIO,
C.S.I.C.

ACKNOWLEDGEMENTS

This monograph is a consequence of the "Seminario sobre Aplicación de los Vidrios y Materiales Vitrocerámicos en el almacenamiento de Residuos Radiactivos" hold in the Junta de Energía Nuclear, Madrid, in May, 21-22, 1985. This Seminar, the first one in this field hold in Spain, woke up a great interest between scientifics, technologists and managers involved in Spain un nuclear industry, ceramics and materials science research. It was sponsored by the:

- Centro de Investigación Energética, Medioambiental y Tecnológica (CIEMAT) (Junta de Energía Nuclear).
- Instituto de Cerámica y Vidrio and Comité de Ciencia de Materiales from the C.S.I.C. and
- Hispano-USA Joint Commitee for Scientific and Technical Cooperation.

Therefore, thanks are due to these Goverment research organizations for interest making possible to joint in Madrid the different spanish specialists and the valuable contribution of the visiting specialist, from USA, VIZ: prof. J.F. Schackelford and Dr. De Natale from the Department of Materials Science, University of California, Davis and prof. J.A. Apps from the Lawrence Berkeley Laboratory, University of California, Berkeley.

Scientific Editor

Dr. Jesús Ma. Rincón

CONTENTS

HIGH LEVEL NUCLEAR WASTES

B. López Pérez
Centro de Investigación Energética, Medioambiental y Tecnológica (CIEMAT), Instituto de Tecnología Nuclear, Madrid (Spain)

ABSTRACT.- The transformations involved in the nuclear fuels during the burn-up at the power nuclear reactors for burn-up levels of 33.000 MWd/tn are considered. Graphs and data on the radioactivity variation with the cooling time and heat power of the irradiated fuel are presented. Likewise, the cycle of the fuel in light water reactors is presented and the alternatives for the nuclear waste management are discussed.
A brief description of the management of the spent fuel as a high level nuclear waste is shown, explaining the reprocessing and giving data about the fission products and their radioactivities, which must be considered on the vitrification processes.
On the final storage of the nuclear waste into depth geological burials, both alternatives are coincident. The countries supporting the reprocessing are indicated and the spanish programm defined in the Plan Energético Nacional (PEN) is shortly reviewed.

RESUMEN.- Se estudian las transformaciones que experimentan los combustibles nucleares en los reactores nucleares de potencia para grados de quemado de 33.000 MWd/tn. Se presentan gráficas sobre la variación de la radioactividad y la potencia calorífica del combustible irradiado con el tiempo de enfriamiento. Se dá un esquema del ciclo del combustible nuclear de los reactores de agua ligera resumiento las dos alternativas que se contemplan actualmente para la gestión del combustible irradiado. Se explica la alternativa de la reelaboración y se dan datos sobre productos de fisión que habría que tener en cuenta en los procesos de vitrificación. Se hace un breve resumen sobre la convergencia de las dos alternativas existentes a la hora del almacenamiento final de los resíduos de alta actividad en capas geológicas profundas, y se señalan los países que han elegido la reelaboración, enumerándose las razones que aducen para ello. Se presenta brevemente el programa español definido en el PEN.

The fuel elements used in a nuclear central have a limitation in the burn-up level after that are discharged from the core of the reactor. This fuel yet contains Uranium-235 without be fissioned and also contains Plutonium generated by neutron absoption and the nuclear fission products which constitute the 99,5 % of generated radioactivity equivalent to several millions of curies per ton. of fuel.

Nowadays,in order to solve the problem of high radioactivity of these spent fuels, two solutions or "options" have been considered.

The first option is to consider the spent fuels as a high lever nuclear waste (HLNW) and to evaluate the possibility of its log-term storage into depth geologic burials, isolated of the environment and man. This solution is named as the "open cycle option"

The second option is named as the reprocessing. The reprocessing is the dissolution in nitric media of the burn-up material contained into the spent fuel and the separation by selective extraction of Uranium, Plutonium and the fission products in three different parts.

The Uranium and Plutonium could be reused in the energy generation cycle; so, they would be profitable fission materials and the fission products, and only them, would constitute the high level nuclear waste in liquid state. This solution is the "closed cycle option."

The reprocessing is a difficult technology which it is not today economically justifiable, implying high costs with losses of 1500 $ per kg of treated Uranium. In spite of, some countries as the Germany Federal Republic, France, United Kingdom and Japan are in favor of the commercial reprocessing. One of the arguments is that the separation of a current shortens the radioactive decay time of the nuclear waste. That is to say, the necessary time for reaching the innocuousness decreases. This is due to the big difference between the desintegration periods of the fission products, about 30 years and in the Plutonium one approximately 25,000 years. This Plutonium, with so longer half-life time, would be recycled and burned in the thermal or breeder reactors being the best procedure for eliminating it.

For the purpose of this Seminar, I think it can be interesting to indicate that in both options, ""open" and "closed" cycle, the glasses and ceramics can play an important role.

When the "open cycle", the burn-up nuclear level is going to be store temporally for a period until 50 years. Later, its dismantling and capsuling in a cylindric container is prevented by adding a filling material which transmits the heat. Copper, lead and ceramic-metal composites (Cermets) are the candidate materials.

In the reprocessing solution the high level liquid wastes are solidified by introducing into glass materials.

The glass for its stability in front of the radiation, in special to the alfa radiation, and due to its low leaching rate was selected. The borosilicate glasses are adequated because of their higher devitrification temperatures, which garantize the stability in longer-time storages, since the generated heat on the radioactive desintegration must be dispersed through the own glass which get a low thermal conductivity.

The Frech Commisariat of Atomic Energy and the Nuclear Center of Karlsruhe in the Germany Federal Republic have developed vitrification procedures which are being used on industial scale, viz:

The french in Marcoule (Attelier de Vitrification de Marcoule, AVM) and the german one in Mol, Belgium (PAMELA method).

Otherwise, the solidification in the glass-ceramics composites have been considered and the possibility of synthesizing natural rocks for their higher stability (SYNROC method).

The glasses manufactured can incorporate until 20 % weight of the fission products. They are poured in cylindric containers and maintained in short-term storages, eliminating the generated heat with air current. In this storage the nuclear waste forms will stay for 40-50 years before its final or long-term isolation into burials of depth geological layers. The following figures show data and technical details wich will contribute to the best comprehension of the focus of this Seminar, the first one of this type developed in Spain. Likewise, an Appendix with the chemical and radioactive characteristics of the HLNW is included.

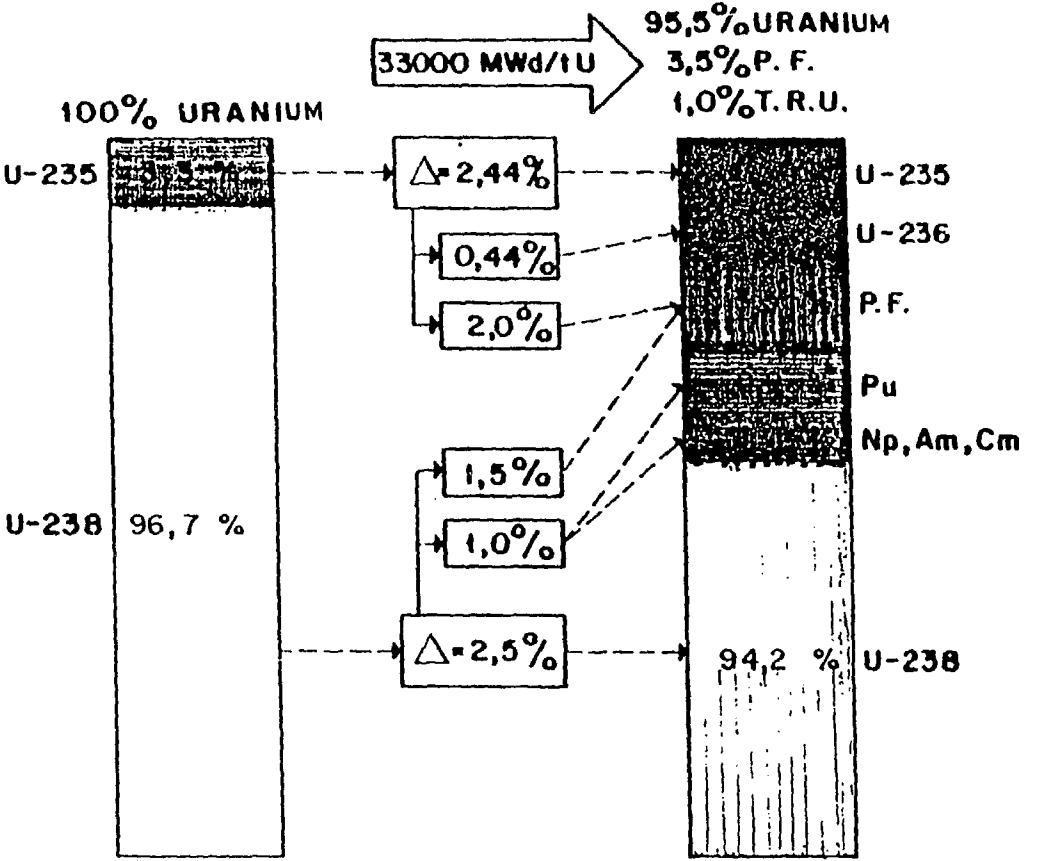

Fig. 1.- Nuclear fuel transformations in a PWR reactor.

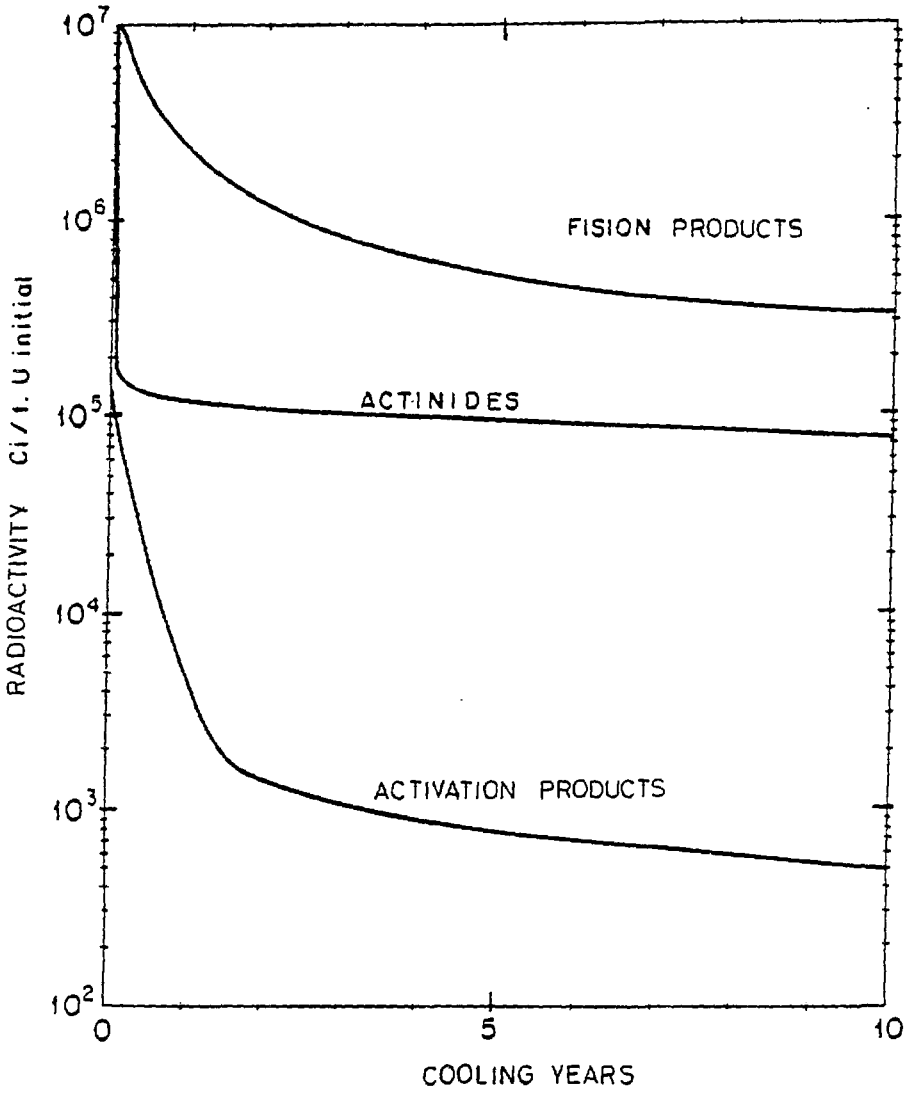

Fig. 2.- Radioactivity of irradiated PWR fuels. Burnup level = 33,000 MWd/t.U. Initial enrichment = 3.3% U-235.

TABLE I

THERMAL CHARACTERISTICS AND RADIOACTIVES OF A PWR FUEL ELEMENT IRRADIATED

Initial enrichment : 3,3% U-235
Burnup level : 33000 MWd/tU

Cooling time	Thermal power (*) vats element	Radiactivity (*) curies element	Surface dosis rem/hour
1	4800	$2,5 \times 10^6$	234.000
5	930	$6,0 \times 10^5$	46.800
10	550	$4,0 \times 10^5$	23.400
50	250	$1,0 \times 10^5$	8.640
100	110	$5,0 \times 10^4$	2.150
500	45	$2,5 \times 10^3$	58
1.000	26	$1,7 \times 10^3$	9,6
5.000	15	$6,0 \times 10^2$	2,5
10.000	6,4	$4,5 \times 10^2$	1,8

(*) Multiply by 2,2 to obtain vats, or curies per t.U.

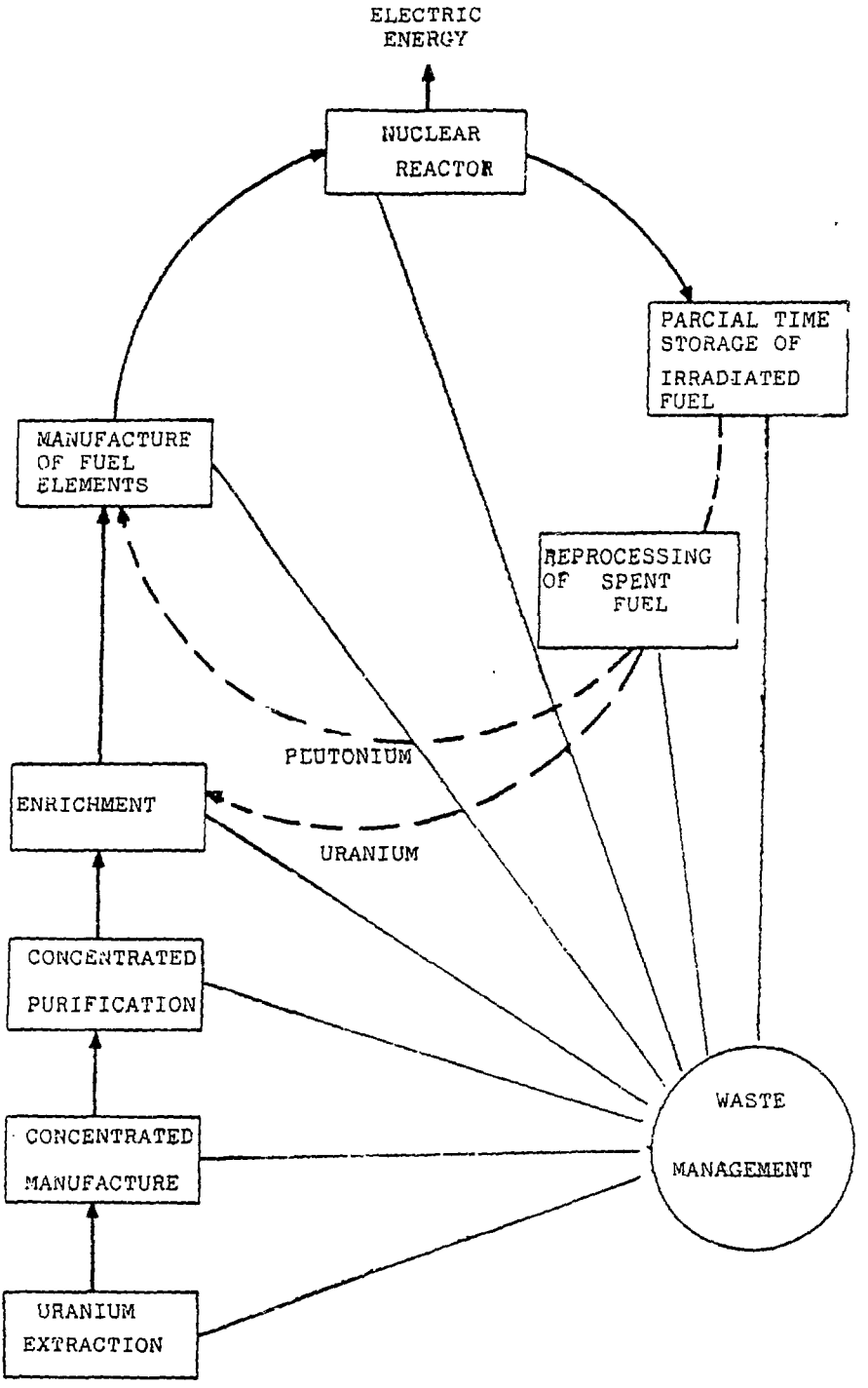

Fig. 3.- Nuclear fuel cycle with reprocessing and enriched Uranium.

TABLE II. NEXT FUTURE (1995) REPROCESSING CAPACITY

COUNTRY	t. U / YEAR
BELGIUM	60 - 300 ?
UNITED KINGDOM	1.200
FRANCE	2.400
G.F.R.	350
JAPAN	1.000
INDIA	200
U.S.A.	¿

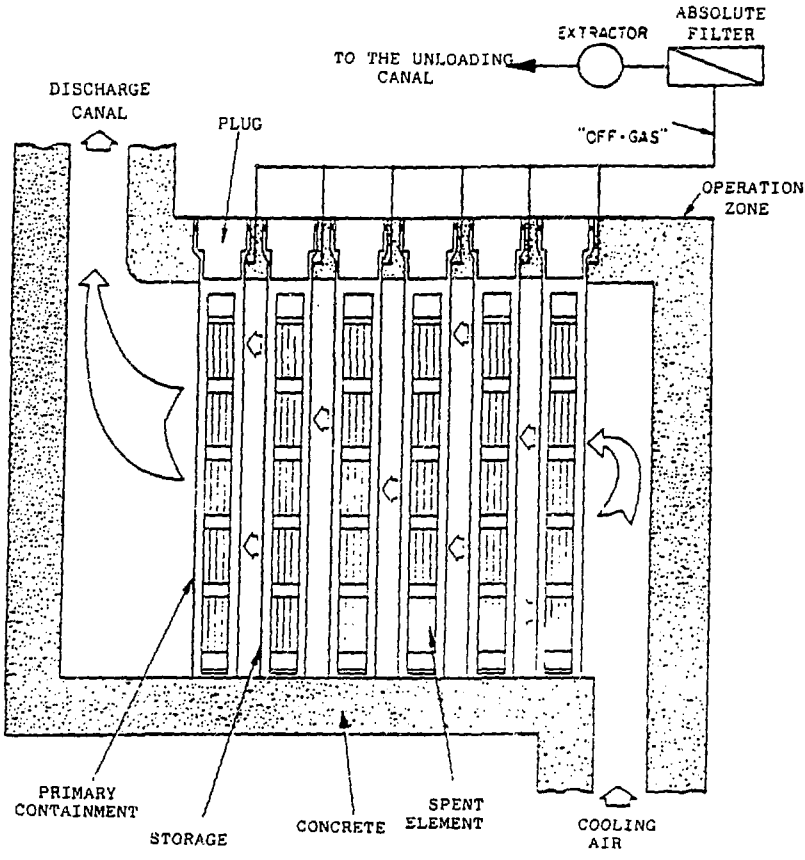

Fig. 4.- Drawing of the system for dry storage of spent nuclear fuel.

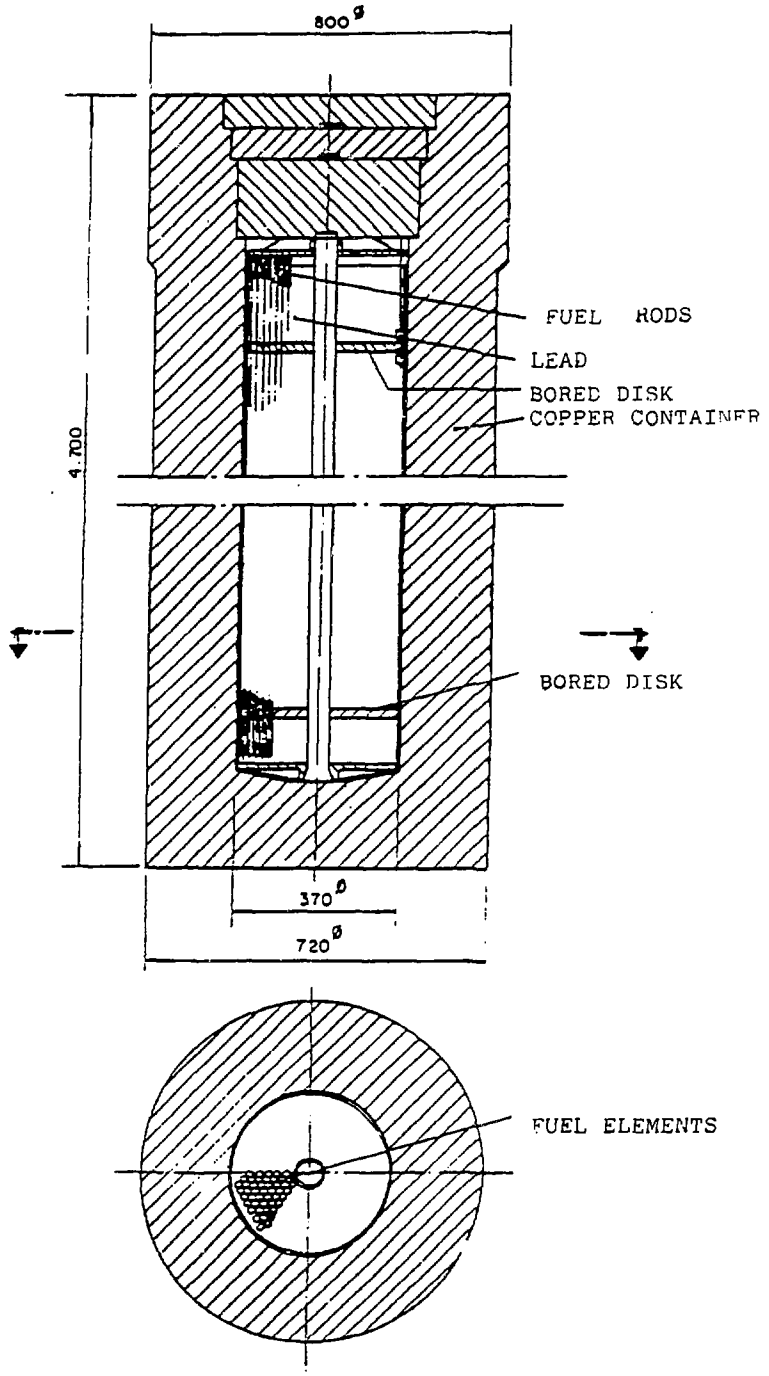

Fig. 5.- Long-term storage in Copper container of PWR fuel elements.

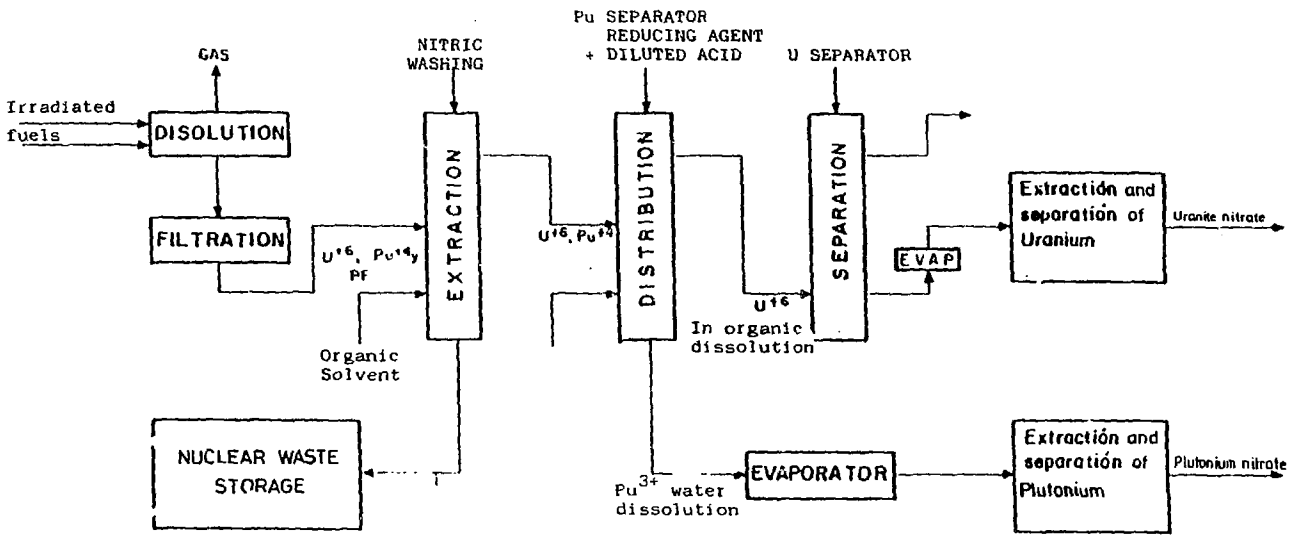

Fig. 6 .- Flux diagram of the Purex process.

TABLE III

Composition of a vitrified nuclear waste.

SiO_2	47,6%
B_2O_3	18,6%
Na_2O	12,9%
Fe_2O_3	5,6%
Other oxides (Al,Cr,Ni,..)..	1,4%
Actinides oxides and fission products	13,9 %

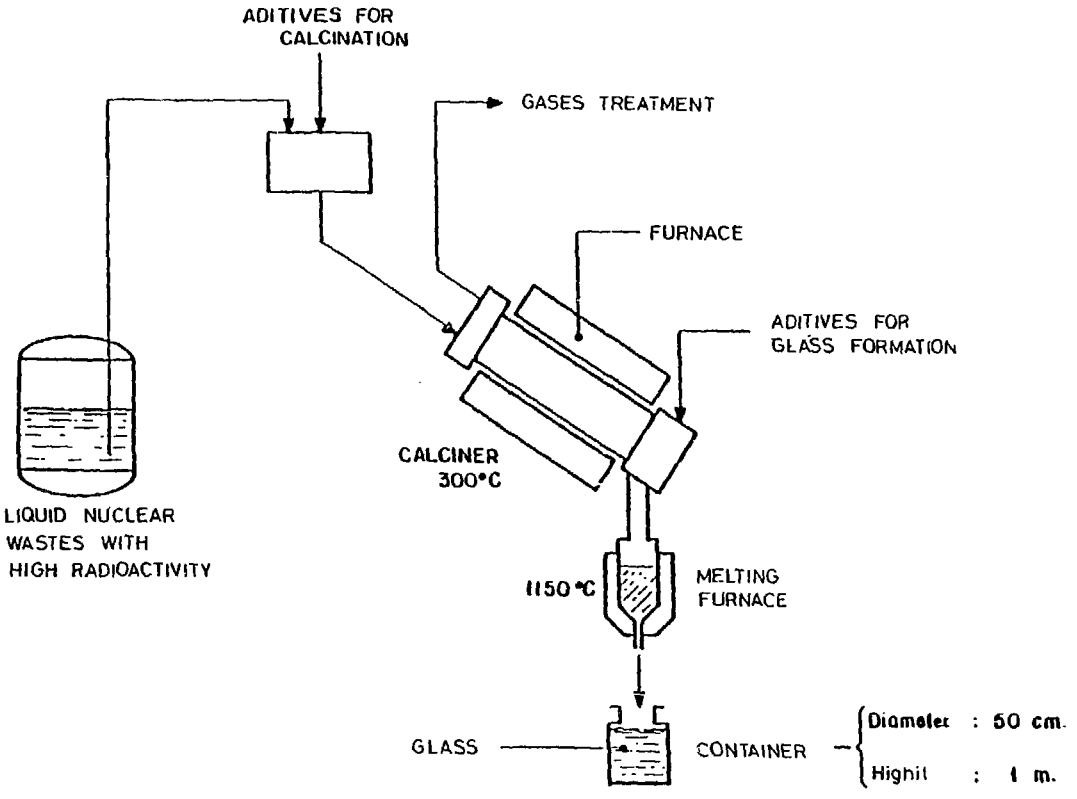

Fig. 7 .- Drawing of the solidification and glass formation.

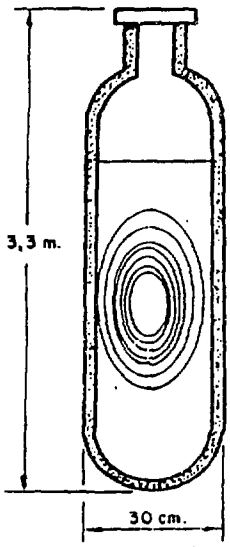

Cooling time years	heat generation Kw	Cumulative radiations per gr.	Dosis R/h. a 30 cm.
1	22	1.0×10^{17}	$1. \times 10^{6}$
5	~4.4		
10	3.1	2.5×10^{17}	6.2×10^{4}
100	0.36	7.1×10^{17}	5.8×10^{3}
1,000	0.02	1.5×10^{18}	1.6
10,000	0.006	3.0×10^{18}	1.3
100,000	0.003	6.1×10^{18}	0.6

Material	304L SS	160 Kg.
Volume	210 lirs.	
Content	630 Kg.	(equivalent to 2,5 I.U.)

Fig. 8 .- Container for NW glass.

NUCLEAR CHARACTERISTICS AND RADIOACTIVES OF HIGH LEVEL NUCLEAR WASTES

Base : 1 t. U INITIAL CHARGED IN A PWR REACTOR
BURNUP LEVEL : 33.000 MWD/t. U
ENRICHMENT : 3,3 % U-235
RECOVERING TREATMENT : 99,9 % U - 99,5 % Pu
VOLUME : 0,25 m^3/t. U INITIAL
HNO_3 FREE : 3 - 4 M

ELEMENTS RADIACTIVES NUCLEIDES	SEMIDESINTEGRATION TIME YEARS	RADIATION TYPE	COOLONG TIME (TOTAL) 10 YEARS	20 YEARS
H - 3 (tritio)	12,3	β	$4.03 \cdot 10^{2}$	$2,30 \cdot 10^{2}$
SELENIUM	—	—	52,1	52,1
Se - 79	$6,5\ 10^{4}$	β	0,40	0,40
RUBIDIO	—	—	347	354
Rb - 87	$5,0 \cdot 10^{10}$	β	$1,96 \cdot 10^{-5}$	$1,96 \cdot 10^{-5}$
ESTRONCIUM ←	—	—	779	685
Sr - 90	28	β	$6,07 \cdot 10^{4}$	$4,74 \cdot 10^{4}$
YTRIUM	—	—	467	467
Y - 90	65 h	β	$6,07 \cdot 10^{4}$	$4,74 \cdot 10^{4}$
CIRCONIUM ←	—	—	3780	3870
Zr - 93	$1,1 \cdot 10^{6}$	β	1,89	1,89
MOLIBDENUM ←	—	—	3470	3470

ELEMENTS RADIACTIVES NUCLEIDES	SEMIDESINTEGRATION TIME YEARS	RADIATION TYPE	COOLONG TIME (TOTAL) 10 YEARS	20 YEARS
TECNECIUM	—	—	841	841
Tc - 99	$2,3 \cdot 10^{5}$	β	1,43 10	1,43 10
RUTENIUM ←	—	—	2150	2150
Ru - 106	1,0	β	$5,52\ 10^{2}$	$5,60\ 10^{-1}$
RODIUM	—	—	388	388
Rh - 106	30 S	β, γ	$5,52\ 10^{2}$	$5,60\ 10^{-1}$
PALADIUM ←	—	—	1410	1410
Pd - 107	$7,0\ 10^{6}$	β	$1,10\ 10^{-1}$	$1,10\ 10^{-1}$
PLATA	—	—	59,7	59,7
Ag - 110 m	253 d	β, γ	$1,67 \cdot 10^{-1}$	$7,59\ 10^{-6}$
Ag - 110	24,4 S	β, γ	$2,17 \cdot 10^{-2}$	$9,86 \cdot 10^{-7}$
CADMIUM	—	—	83,9	83,9
Cd - 113 m	14	β, γ	6,40	3,90
	—	—	51,0	51,0
S - 126	$\sim 10^{5}$	β	$5,46 \cdot 10^{-1}$	$5,46 \cdot 10^{-1}$
ANTIMONIUM	—	—	10 7	10,7
Sb - 125	2,73	β, γ	$6,79 \cdot 10^{2}$	$5,22 \cdot 10^{1}$
Sb - 126 m	19 m	β, γ	$5,46 \cdot 10^{-1}$	$5,46 \cdot 10^{-1}$
Sb - 126	12,5 d	β, γ	$5,41 \cdot 10^{-1}$	$5,41 \cdot 10^{-1}$
TELURUM	—	—	570	571
Te - 125 m	—	γ	$2,81 \cdot 10^{2}$	$2,16 \cdot 10^{1}$
IODUM	—	—	270	270
I - 129	$1,6 \cdot 10^{7}$	β, γ	$3,74 \cdot 10^{-2}$	$3,74 \cdot 10^{-2}$
CESIUM ←	—	—	2320	2120
Cs - 134	2,05	β, γ	$8,40 \cdot 10^{3}$	$2,86 \cdot 10^{2}$

ELEMENTS RADIACTIVES NUCLEIDES	SEMIDESINTEGRATION TIME YEARS	RADIATION TYPE	COOLONG TIME (TOTAL) 10 YEARS	20 YEARS
Cs - 135	$2,0 \cdot 10^{5}$	β	$2,86 \cdot 10^{-1}$	$2,86 \cdot 10^{-1}$
Cs - 137	29,8	β	$8,56 \cdot 10^{4}$	$6,79 \cdot 10^{4}$
BARIUM ←	—	—	1790	2000
Ba - 137 m	2,6 m	γ	$8,00 \cdot 10^{3}$	$6,35 \cdot 10^{4}$
LANTANUM ←	—	—	1270	1270
CERIUM ←	—	—	2480	2480
Ce - 144	277 d	β, γ	$1,50 \cdot 10^{2}$	$2,03 \cdot 10^{-2}$
PRASEODIMIUM ←	—	—	1200	1200
Pr - 144	17,3 m	β, γ	$1,50 \cdot 10^{2}$	$2,03 \cdot 10^{-2}$
NEODIMIUM	—	—	$4,12 \cdot 10^{3}$	$4,12 \cdot 10^{3}$
PROMECIUM	—	—	8,36	0,60
Pm - 147	2,67	β	$7,77 \cdot 10^{3}$	$5,52 \cdot 10^{2}$
SAMARIUM	—	—	901	905
Sm - 151	93	β	$1,16 \cdot 10^{3}$	$1,07 \cdot 10^{3}$
EUROPIUM	—	—	156	166
Eu - 152	12,5	β, γ	7,04	3,95
Eu - 154	16	β, γ	$4,53 \cdot 10^{3}$	$2,94 \cdot 10^{3}$
Eu - 155	1,81	β, γ	$1,63 \cdot 10^{2}$	3,55
URANIUM ←	—	—	956	956
NEPTUNIUM	—	—	762	762
Np - 237	$2,20 \cdot 10^{6}$	α, γ	$5,4 \cdot 10^{-1}$	$5,4 \cdot 10^{-1}$
Np - 239	2,35 d	$\beta+\gamma$	$1,82 \cdot 10$	$1,81 \cdot 10$
PLUTONIUM	—	—	42,95	41,70
Pu - 238	86,4	α, γ	$1,35 \cdot 10$	$1,25 \cdot 10$
Pu - 239	$2,44 \cdot 10^{4}$	α, γ	1,62	1,62

ELEMENTS RADIACTIVES NUCLEIDES	SEMIDESINTEGRATION TIME YEARS	RADIATION TYPE	COOLONG TIME (TOTAL) 10 YEARS	20 YEARS
Pu - 240	$6,6 \cdot 10^3$	α, γ	2,40	2,40
Pu - 241	13,2	β	$3,27\ 10^2$	$2,03 \cdot 10^2$
AMERICIUM	—	—	145	145
Am - 241	$4,58 \cdot 10^2$	α, γ	$1,41 \cdot 10^3$	$2,21 \cdot 10^3$
Am - 242 m	$1,52 \cdot 10^2$	γ	8,75	8,36
Am - 242	16 h	β, γ	8,75	8,36
Am - 243	$7,65 \cdot 10^3$	α, γ	$1,81 \cdot 10^1$	$1,81 \cdot 10^1$
CURIUM	—	—	22,8	16,2
Cm - 242	1,63 d	α, γ	7,18	6,86
Cm - 243	32	α, γ	2,99	2,41
Cm - 244	17,6	α, γ	$1,67 \cdot 10^3$	$1,14 \cdot 10^3$
TOTAL ELEMENT (Kg)				
fission products			29.1	29.1
Actinides			2.015	2.249
TOTAL RADIOACTIVITY (Ci)				
fission products			$3.12 \cdot 10^5$	$2,32 \cdot 10^5$
Actinides			$2,4 \cdot 10^3$	$1,63\ 10^3$
THERMAL POWER (vots)				
fission products			$1,04 \cdot 10^3$	$7,37 \cdot 10^2$
Actinides			70,6	40,0

THE NATURE OF THE GLASSY STATE - IMPLICATIONS FOR RADIOACTIVE WASTE STORAGE

James F. Shackelford

Division of Materials Science and Engineering
University of California
Davis, CA 95616

Abstract

Glass is a primary candidate for the storage of radioactive waste. The glassy state is defined in terms of atomic-scale structure, viz., short-range order (building blocks) and long-range randomness. On the microstructural-scale, these non-crystalline solids may exhibit phase separation. Optical and mechanical properties are central to the general structural applications of glasses. Transport properties are of special importance to the use of glasses for nuclear repository. Both gaseous and ionic diffusion can be involved.

1. Introduction

Glass is a primary candidate for the storage of radioactive waste. This paper will review the nature of the structure and properties of this material with a special emphasis on their implications for this critical application. Glasses can be defined as "non-crystalline solids with compositions comparable to the crystalline ceramics."[1] We can consider three aspects of the glassy state. First would be a glassy phase in a predominantly crystalline ceramic. Second would be a completely non-crystalline material, i.e., a true glass. And third would be a glass-ceramic in which the glassy state is primarily a precursor to a final, fully-crystallized product.

A significant glassy phase at the grain boundaries of a crystalline ceramic is largely associated with traditional ceramic technology, e.g., relatively large impurity levels and/or a significant amount of silica in the material composition.[2] More sophisticated "high technology" ceramics are structurally more similar to common metals, in which crystallinity of the grains extends completely up to the grain boundary.[3] The structure of such interfacial regions can be modelled with tools developed for characterizing non-crystalline solids, but the regions do not represent a bulk glassy phase.[4] This review will not treat further the subject of glass-ceramics. That material is discussed by Martinez, et al. in this Proceedings.[5]

Traditional glasses involve a silica-based chemistry. Non-silicate oxide glasses are generally of little commercial value. However, there is currently substantial interest in various nonoxide glasses. Rapid

solidification techniques developed for amorphous metals allow virtually any material composition to be formed in a non-crystalline or glassy state. Nonetheless, the primary examples to be used in this review for illustration of the nature of the glassy state will be vitreous silica and related silicate glasses. These serve as classic examples of glasses and cover the majority of the commercial glass industry, including various candidates for radioactive waste storage.

This review paper is an extension of a more general discussion of the glassy state.[6] Various monographs are available for more detailed study. The field of "glass science" was systematically reviewed by R.H. Doremus in 1973.[7] Four volumes in the monograph series entitled "Treatise on Materials Science and Technology" have been subtitled "Glass I, "Glass II, "Glass III," and "Glass IV"[8] and contain several review articles edited by M. Tomozawa and R.H. Doremus. An ambitious series of monographs entitled "Glass: Science and Technology" has been undertaken by editors D.R. Uhlmann and N.J. Kreidl. The first of twelve planned volumes has been published covering the area of "Elasticity and Strength in Glasses."[9] Finally, an extensive collection of data in glass systems from the Russian literature is being translated into English. The first volume has been published under editor O.V. Mazurin.[10]

2. Structure

In Section 1, the basic definition of glass centered on its lack of crystalline order. The primary statement of the nature of this non-crystallinity was given in the classic paper of Zachariasen.[11] The

famous Zachariasen schematic is shown in Figure 1(a) in contrast to the corresponding crystalline structure in Figure 1(b). The key features of the non-crystalline schematic are (i) AO_3 triangular "building blocks" comparable to those in the crystalline material and (ii) an irregular connectivity of the building blocks in contrast to the regular connectivity in the crystalline material. The building block is a component of short-range order (sro) in a material lacking in long-range order (lro). Zachariasen argued that the connectivity of building blocks is essentially random in nature. This "long-range randomness" (lrr) can be specified in terms of distributions of structural parameters such as the A-O-A bond angle, the n-membered oxygen ring, and interstitial size. The significance of Zachariasen's achievement in providing a useful working definition of glass structure, which is still widely used over 50 years later, is especially impressive in that it was solely an intellectual exercise based on his understanding of the principles of crystal chemistry. Zachariasen's "random network theory" became widely accepted following the publication of supporting experimental evidence by Warren and co-workers in 1936.[12] Their early use of the Fourier transform of X-ray scattering data confirmed the presence of SiO_4 tetrahedra in vitreous silica with an apparently random linkage of those tetrahedra. Figure 2 represents an extended Zachariasen schematic[13] with enough interstices (oxygen rings in this two-dimensional schematic) to allow a statistical analysis of the distribution of their size (Figure 3). The histogram of interstitial size (Figure 3(a)) shows a large, single bar for the 3-coordinated interstices associated with the AO_3 building block and a distribution of sizes for the randomly-generated

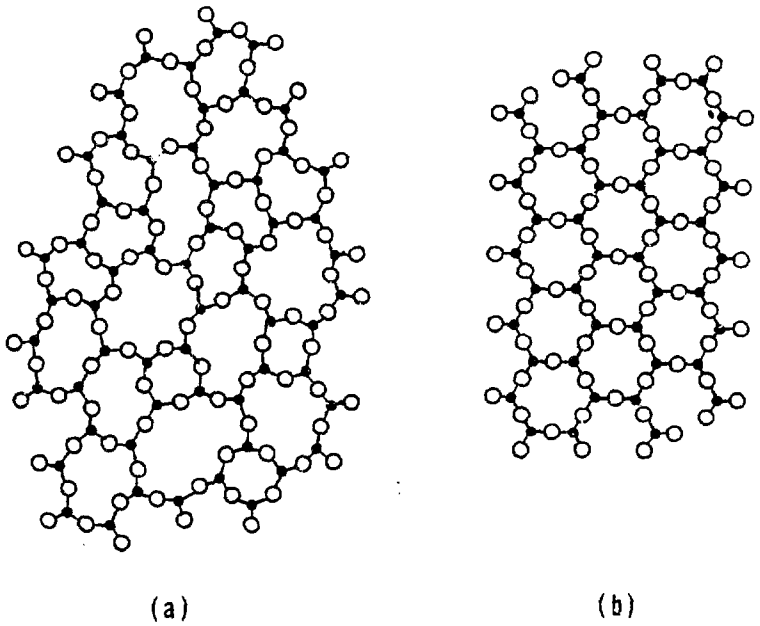

Fig.1. Schematic of the structure of (a) a glass compared to (b) a crystal of the same composition. The two structures have the same building block (short-range order), but the glass lacks long-range order (after Zachariasen[11]).

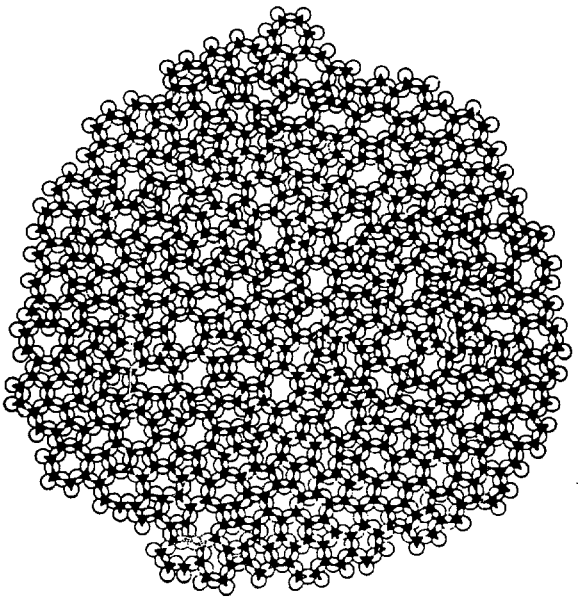

Fig. 2. A 300-ring "triangle raft" is an extended Zachariasen schematic that allows statistical analysis of structural parameters (after Shackelford[13]).

rings. A best-fit of the continuous distribution of interstitial size (Figure 3(b)) becomes a sharp spike representing the 3-coordinated A^{3+} ion (short-range order) and a lognormal distribution representing the long-range randomness. This overall distribution (Figure 3(b)) is, then, a working definition of an ideally random structure. The random network theory has been a widely used and generally adequate model of the structure of vitreous silica. There has been, however, an ongoing debate about the ideality of the randomness. Substantial discussion has been given to experimental evidence for ordering in this non-crystalline material.[14] Various spectroscopic techniques have been effective in providing this more complete structural picture. Although the validity of the random network model is the source of substantial debate and current research for vitreous silica, structural studies on more chemically-complex silicate glasses during the past two decades have shown the random network model to be inadequate for such materials. As a simple example, a random network model of an alkali modified silicate (such as $xNa_2O \cdot (1-x)SiO_2$) would involve a random distribution of "modifier" Na^+ ions within the silica network (shown schematically in Figure 4[15]). However, X-ray diffraction studies of such glasses (using the techniques pioneered by Warren[12]) indicate that the average Na^+-Na^+ separation distance is substantially less than would be the case for random distribution.[16] The structural ordering in these relatively simple model glasses is an indication of the inadequacy of the random network model for general, commercial glass compositions.

Our discussion of glass structure has centered on atomic-scale geometry consistent with the definition of glass in terms of its non-crystallinity.

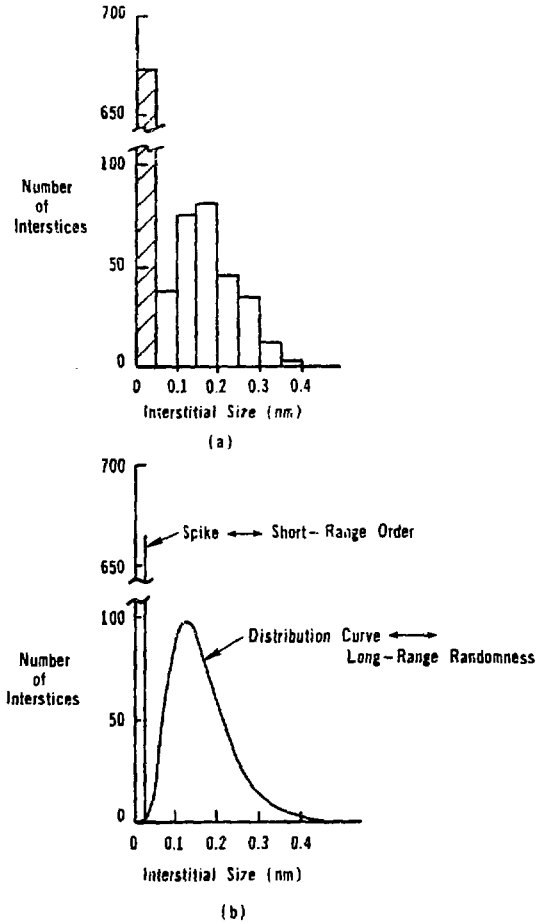

Fig. 3. (a) Histogram of interstitial size (defined as an inscribed circle) for the triangle raft of Figure 2. There is a large bar associated with the 3-membered rings of the AO_3 building blocks. (b) A best-fit of the continuous distribution of interstitial size serves as a working definition of an ideally random structure (after Shackelford[13]).

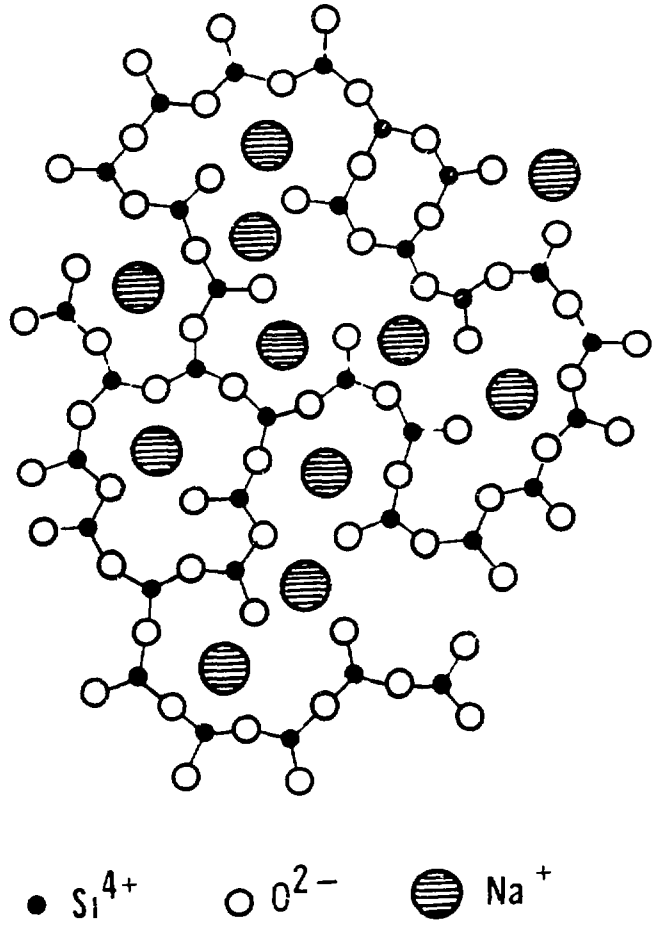

Fig.4. A schematic of an ideally random "modified" silicate network structure (after Warren[15]).

It is also important to note that, on the microstructural-scale, many glasses show a tendency to phase separate.[17] Figure 5 illustrates a typical phase-separated microstructure. This phenomenon, analogous to liquid-liquid immiscibility, can be modelled in terms of both thermodynamic principles and structural considerations derived from crystal chemistry. The practical significance of this phenomenon is the effect of the resulting microstructure on certain properties, especially within the optical and transport categories. The specific structural implications for radioactive waste glass storage center on transport properties, such as leaching[18] and fission gas release. The microstructural distribution of a high-diffusivity phase (in a phase separated glass) will determine the overall performance of that material. In turn, the diffusivity of a given phase can be strongly affected by ordering phenomena described earlier in this section.

3. Properties

With an understanding of the nature of the atomic and microscopic-scale structure of glasses, we can proceed with a systematic discussion of their key properties as relevant to radioactive waste storage. We will consider optical, mechanical, and transport properties with an emphasis on the last category.

3.1. Optical

Perhaps the most distinctive feature of traditional glass-ware is its optical transparency. This and related optical properties are at the

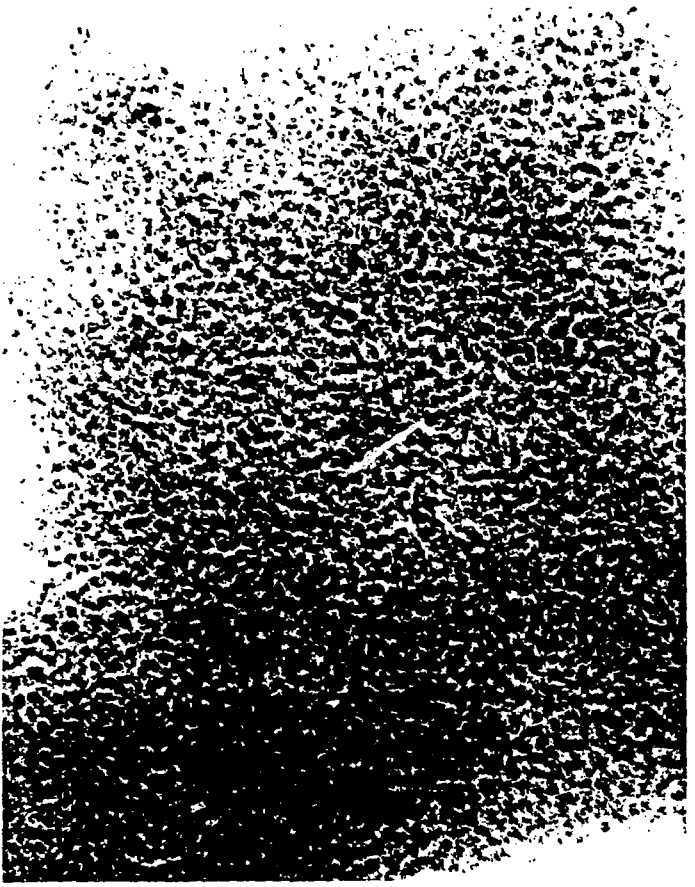

Fig. 5. Transmission electron micrograph of phase separation in a 20 mole percent Al_2O_3 - 80 mole percent SiO_2 glass, 100,000 X. (Courtesy of P.J. Hood)

foundation of many of the contemporary applications of glasses, such as windows, lenses, containers, filters, lasers, and waveguides.[19] Various applications are dependent on the percentage transmission as a function of wavelength within (i) the visible region (0.4 - 0.7 μm wavelength), (ii) the ultraviolet (< 0.4 μm), and (iii) the infrared (> 0.7 μm). Figure 6 shows a typical transmission curve in the infrared region for vitreous silica, which is, of course, transparent in the visible range but drops sharply in transmission for wavelengths between 4 and 5 μm. The various absorption peaks between 1 and 3 μm are associated with chemically dissolved water (in the form of unassociated OH groups). Especially distinctive is the 2.73 μm peak associated with a fundamental vibrational mode. The magnitude of this peak is the basis for determining the "water" content of this glass. The coloration of glasses results from similar, selective absorption bands within the visible range. The specific mechanism for such absorption is the excitation of 3d electrons in partially filled inner shells of transition metal elements. Phase separation can be the source of light scattering due to different indices of refraction associated with each phase.[17] A quantitative analysis of scattering can be an effective tool for identifying the immiscibility region in binary or multi-component glasses.[20]

Optical behavior is not a primary consideration in the evaluation of candidate materials for radioactive waste storage. Of more direct importance is the wide use of optical transmission behavior to characterize the structural effects of radiation exposure. Friebele and Griscom[21] have thoroughly reviewed the literature in this area. They have systematically cataloged the various types of local structural defects produced by radiation in a wide range of glass compositions.

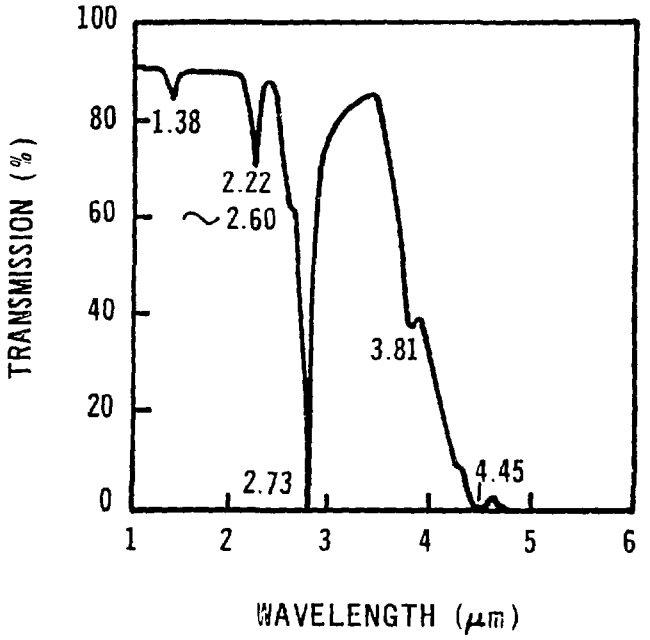

Fig. 6. Typical transmission curve for vitreous silica in the infrared region.

Mechanical

As with optical properties, mechanical behavior is not generally the primary consideration in evaluating a glass for waste storage. The design philosophy for typical storage systems involves the encapsulation of the glass within a container vessel. The structural integrity of the container vessel is, of course, of paramount importance. To provide a comprehensive view of the mechanical behavior of glass, it is necessary to consider a wide temperature range. Glasses are characteristically brittle at moderate temperatures but readily deformable at elevated temperatures. Waste storage can involve temperatures over this full range. Recent years have seen rapid progress in understanding and controlling these mechanical properties.[22]

Substantial practical information about the mechanical behavior of structural glasses has been obtained within the past decade by the application of fracture mechanics,[23] which can be defined as the introduction of a large crack into the material followed by analysis of material resistance to propagation of the crack under various environments and stresses. Knowledge of the nature of crack propagation and flaw geometry provides for the prediction of strength and/or lifetime of given structures. The most general fracture mechanics parameter is the "fracture toughness," or K_{IC}, which is the critical value of the stress intensity factor for a slit crack in an infinitely wide plate loaded under a tensile stress (perpendicular to the crack face). In general, the value of fracture toughness is approximated by

$$K_{IC} \cong \sigma_f \sqrt{\pi a} \qquad (1)$$

where σ_f is the applied tensile stress at failure and a is the length of a surface crack. In general, relatively "brittle" ceramics and glasses have relatively low values of K_{IC}.[24] The predominant source of failure in glass is surface flaws produced by machining or handling. The distinctive fracture surface emerging from the initiating crack permits detailed "failure analysis" of a structural piece. A precise mechanism of fracture can generally be assigned using microscopic inspection. This technology has been reviewed by Frechette.[25] Of special importance in the prediction of structure lifetimes is consideration of delayed failure, or "static fatigue." Fracture mechanics has helped to identify this phenomenon with a mechanism of subcritical growth of cracks, usually in the presence of water.[23]

As noted earlier, glass exhibits viscous deformation at relatively high temperatures (above the glass transition temperature, T_g). The viscosity of a typical sode-lime-silica glass from room temperature to 1500°C is summarized in Figure 7. A good deal of useful processing information is contained in such a plot relative to the manufacture of glass products. The annealing point (at which the viscosity is $10^{13.4}$ poise) corresponds approximately to the glass transition temperature. Above T_g, the viscosity data follow an Arrhenius form with

$$\eta = \eta_0 e^{+Q/RT} \qquad (2)$$

where η_0 is the preexponential constant, Q is the activation energy for viscous deformation, and RT has the usual meaning. Viscosity deviates from this Arrhenius form below T_g as elastic deformation mechanisms come into play, and a plateau of 10^{20} poise is reached near room temperature.

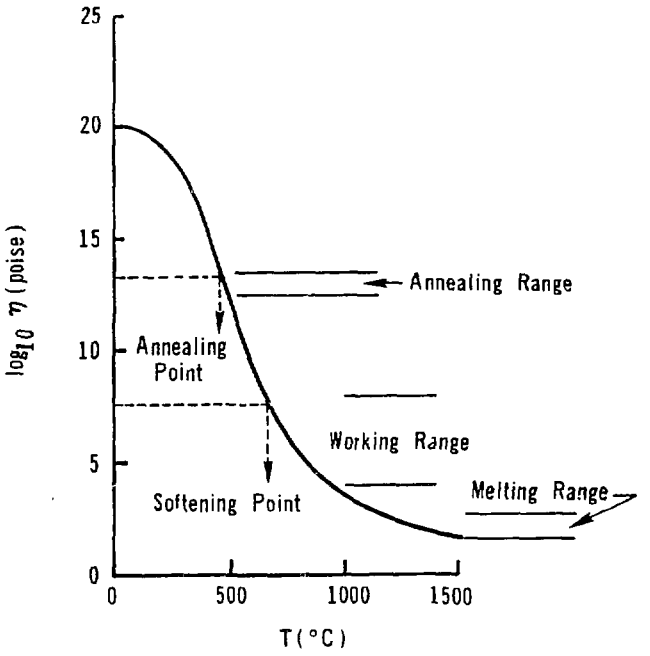

Fig. 7. Viscosity of a typical soda-lime-silica glass from room temperature to 1500°C (after Shackelford[1]).

3.3 Transport

Frequently, the applications of glasses are dependent on certain transport properties. Alternately, applications may be limited by such transport properties. The safe application of glass for radioactive waste storage is an important example.

A relatively simple transport system is the diffusion and solution of unreactive gases in glass. Studies of these systems have been reviewed by Shelby[26] and Shackelford.[27,28] The relatively open structure of silica-based glasses permits measurable diffusion of numerous gases. Substantial structural information is available from the careful analysis of this transport, as indicated schematically by Figure 8. An important, practical example of this transport system relative to radioactive waste storage is fission gas release. An example of the correlation of transport parameters with a phase separation boundary is illustrated by the Na_2O–SiO_2 system in Figure 9. Rothman et al.[29] have shown that, for small concentration levels, modifier ion diffusion can be modelled as an interstitial mechanism through the silicate network structure (analogous to unreactive gas atom transport). The general case of ionic transport in high modifier concentration glass systems has been reviewed by Doremus[7] and Kingery et al.,[30] including the relationship of ionic diffusion to the electrical conductivity of these materials. The important relationship of ionic diffusion to the chemical durability of glass has also been reviewed by Doremus.[31] He has discussed the reaction of typical alkali silicate glasses with water in terms of the interdiffusion of alkali and hydronium ions. The effect of glass composition on chemical durability can, in turn, be discussed in terms of

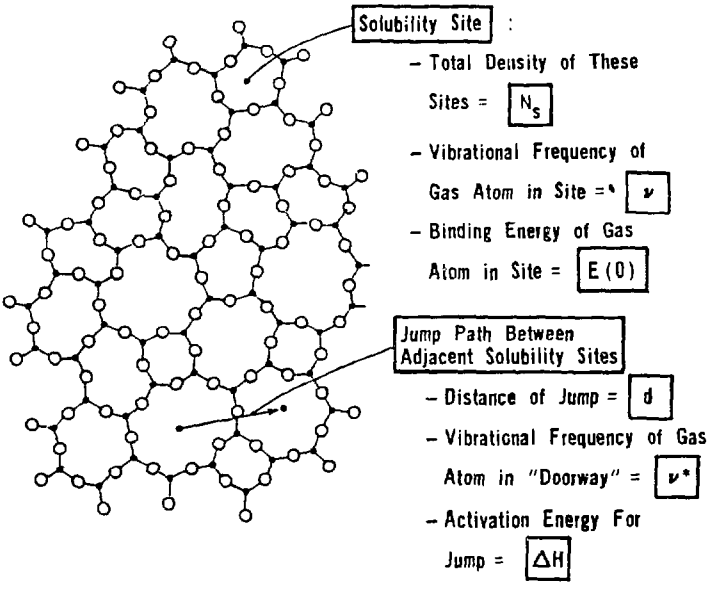

Fig. 8. Solubility and diffusion parameters for inert gas transport are related to the structure of the glass network (after Shackelford[27]).

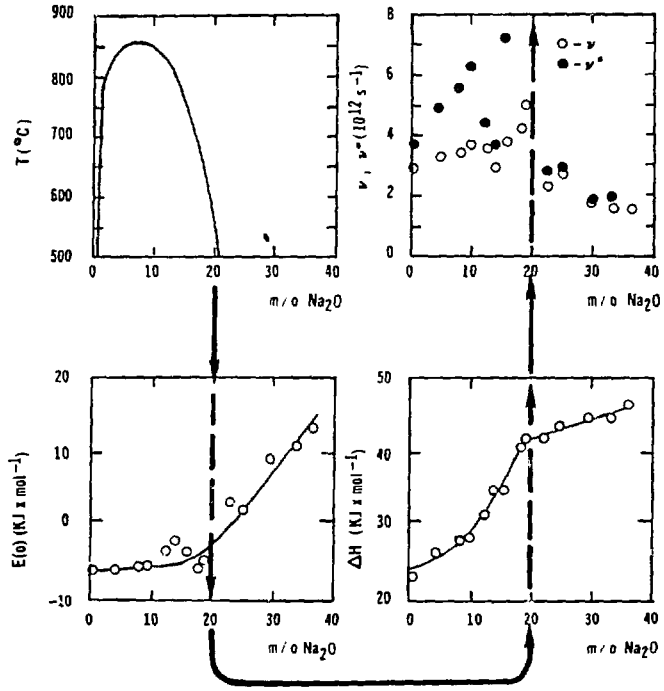

Fig. 9. The transport parameters defined in Figure 8 correlate with phase separation in the Na_2O - SiO_2 system (after Shackelford[27]).

changes in the diffusion coefficients for these ionic species. As with other properties, phase separation can have a strong influence. McElfresh[32] has succesfully modelled ionic transport by an interstitial mechanism in relation to the problem of leaching of radioactive waste storage glasses.

Acknowledgements

This work has been made possible with the support of National Science Foundation Grant DMR 82-04394 and the U.S.-Spain Joint Committee on Scientific and Technological Cooperation.

References

1) Shackelford, J.F.: Introduction to Materials Science for Engineers, Macmillan, New York (1985) Chapter 8.

2) Stuijts, A.L.: "Ceramic microstructures" in Ceramic Microstructures '76 (Fulrath, R.M. and Pask, J.A., eds.) Westview Press, Boulder, Colorado (1977) 1-26.

3) Balluffi, R.W., Bristowe, P.D. and Sun, C.P.: "Structure of high-angle grain boundaries in metals and ceramic oxides," J. Amer. Ceram. Soc., 64 (1981) 23-34.

4) Shackelford, J.F.: "A canonical hole model of grain boundaries and interfaces in oxides" in Advances in Ceramics, Vol. 6: Character of Grain Boundaries (Yan, M.F. and Heuer, A.H., eds.) Amer. Ceram. Soc., Columbus, Ohio (1983) 96-101.

5) Martinez, S., Alfonso, P., de la Fuente, C., and Queralt, I.: "Materiales vitroceramicos obtenidos a partir de rocas basalticas de las Islas Canarias," to be published in this Proceedings.

6) Shackelford, J. F.: "The Glassy State" to be published in Fine Ceramics - Annual Reviews Vol. 1., Ohmsha, Tokyo.

7) Doremus, R.H.: Glass Science, John Wiley and Sons, New York (1973).

8) Tomozawa, M. and Doremus, R.H., eds.: Glass I: Interaction with Electromagnetic Radiation; Glass II; Glass III; and Glass IV, Academic Press, New York (1977, 1979, 1982, and 1985).

9) Uhlmann, D.R. and Kreidl, N.J., eds.: Glass: Science and Technology, Vol. 5 Elasticity and Strength in Glass, Academic Press, New York (1980).

10) Mazurin, O.V., Streltsina, M.V. and Shvaiko-Shvaikovskaya, T.P.: Handbook of Glass Data, Part A: Silica Glass and Binary Silicate Glasses, Elsevier Science Publishers, New York (1983).

11) Zachariasen, W.H.: "The atomic arrangement in glass," J. Amer. Chem. Soc., 54 (1932) 3841-3851.

12) Warren, B.E., Krutter, H. and Morningstar, O.: "Fourier analysis of X-ray patterns of vitreous SiO_2 and B_2O_3," J. Amer. Ceram. Soc., 19 (1936) 202-206.

13) Shackelford, J.F.: "Triangle rafts -- Extended Zachariasen schematics for structure modeling," J. Non-Cryst. Solids, 49 (1982) 19-28.

14) Proc. Intl. Symp. on Bonding and Structure in Non-Crystalline Solids, Wash., D.C., May 1983, to be published by Plenum Press, New York.

15) Warren, B.E.: "Summary of work on atomic arrangement in glass," J. Amer. Ceram. Soc., 24 (1941) 256-261.

16) Porai-Koshits, E.A.: "The possibilities and results of X-ray methods for investigation of glassy substances" in The Structure of Glass, Vol. 1, Consultants Bureau, New York (1958) 25-35; Ohlberg, S.M. and Parsons, J.M.: "The distribution of sodium ions in soda-lime-silica glass" in Proc. Conf. on Physics of Non-Cryst. Solids (Prins, J.A., ed.) John Wiley and Sons, New York (1965) 31-40; Carraro, G. and Domenici, M., cited in Wright, A.C.: "The structure of amorphous solids by X-ray and neutron diffraction" in Advances in Structural Research by Diffraction Methods (Hoppe, W. and Mason, R., eds.) Pergamon Press, New York (1974) 59.

17) Tomozawa, M.: "Phase separation in glass" in Glass II (Tomozawa, M. and Doremus, R.H., eds.) Academic Press, New York (1979) 71-113.

18) Apps, J.: "Leaching problems in nuclear waste repositories," to be published in this Proceedings.

19) Sigel, G.H., Jr.: "Optical absorption of glasses" in Glass I (Tomozawa, M. and Doremus, R.H., eds.) Academic Press, New York (1977) 5-89.

20) Schroeder, J.: "Light scattering of glass" in Glass I (Tomozawa, M. and Doremus, R.H., eds.) Academic Press, New York (1977) 157-222.

21) Friebele, E.J. and Griscom, D.L.: "Radiation effects in glass" in Glass II (Tomozawa, M. and Doremus, R.H., eds.) Academic Press, New York (1979) 257-351.

22) Uhlmann, D.R. and Kreidl, N.J. in the preface to Glass: Science and Technology, Vol. 5 (Uhlmann, D.R. and Kreidl, N.J., eds.) Academic Press, New York (1980) page x.

23) Freiman, S.W.: "Fracture mechanics of glass" in Glass: Science and Technology, Vol. 5 (Uhlmann, D.R. and Kreidl, N.J., eds.) Academic Press, New York (1980) 21-78.

24) Ashby, M.F. and Jones, D.R.H.: Engineering Materials - An Introduction to Their Properties and Applications, Pergamon Press, Elmsford, N.Y. (1980).

25) Frechette, V.D.: "The fractography of glass" in Introduction to Glass Science (Pye, L.D., Stevens, H.J. and La Course, W.C., eds.) Plenum Press, New York (1972) 433-450.

26) Shelby, J.E.: "Molecular solubility and diffusion" in Glass II (Tomozawa, M. and Doremus, R.H., eds.) Academic Press, New York (1979) 1-40.

27) Shackelford, J.F.: "The potential of structural analysis from gas transport studies," J. Non-Cryst. Solids, 42 (1980) 155-174.

28) Shackelford, J.F.: "Structural implications of gas transport in amorphous solids" to be published in Proc. Intl. Symp. on Bonding and Structure in Non-Crystalline Solids, Wash., D.C., May 1983, to be published by Plenum Press, New York.

29) Rothman, S.J., Marcuso, T.L.M., Nowicki, L.J., Baldo, P.M. and McCormick, A.W.: "Diffusion of alkali ions in vitreous silica," J. Amer. Ceram. Soc., 65 (1982) 578-582.

30) Kingery, W.D., Bowen, H.K. and Uhlmann, D.R.: Introduction to Ceramics, 2nd ed., John Wiley and Sons, New York (1976).

31) Doremus, R.H.: "Chemical durability of glass" in Glass II (Tomozawa, M. and Doremus, R.H., eds.) Academic Press, New York (1979) 41-69.

32) McElfresh, D. K.: "Diffusion in glass" Ph.D. thesis, University of California, Davis, December 1984.

LIQUID INMISCIBILITY IN GLASSES AND NUCLEAR WASTE MANAGEMENT

J.Mª Rincón
Instituto de Cerámica y Vidrio, CSIC
Arganda del Rey, Madrid, Spain

ABSTRACT.-

The glass-in-glass phase separation or liquid inmiscibility in glasses has been widely investigated in the past due to its applications in glazes, opal glasses and glass-ceramics. Since time , the thermodinamics of the miscibility domes in equilibria diagrams, binaries or ternaries, has been established. Nowadays, the inmiscibilities studies are emerging due to the vitrification of the nuclear wastes and location in adequate geological burial for longer time. The focus of recent researchs is to determine the partition ratio of radioelement between diferent phases separated with differents chemical leaching, as well as the miscibility gaps in the Na_2O-B_2O_3--SiO_2 system including one or several elements which could be contained in a high or low level nuclear waste.

RESUMEN.-

El fenómeno de inmiscibilidad líquida en vidrios ha sido ampliamente estudiado desde hace unos años por sus aplicaciones en la producción de vidriados, vidrios opales y materiales vitrocerámicos. La base termodinámica de las zonas o cúpulas de inmiscibilidad en diagramas de equilibrio en sistemas binarios o ternarios de óxidos está establecida desde hace tiempo. Actualmente, el estudio de la inmiscibilidad en vidrios está resurgiendo debido a su posible aplicación en la inmovilización química de residuos radiactivos para su almacenamiento en un enterramiento geológico adecuado por tiempo indefinido. Las investigaciones más recientes tratan de determinar la relación de partición de radioisótopos entre las diferentes fases que tienen distinta resistencia a la lixiviación química, así como las zonas de inmiscibilidad líquida en el sistema Na_2O-B_2O_3-SiO_2 incluyendo uno o varios elementos químicos que podrían formar parte de un residuo de alta o de baja actividad.

1. INTRODUCTION.-

The nuclear waste (NW) management by chemical inmobilization in

a glass, ceramic or cement matrix have been the aim of a tremendeous research in the last years (1). The matrices more investigated have been the ceramics, such as the SYNROC or the glass-ceramics such as basalts, sphene or pollucite compositions, however a little work - has been dedicated to the fully glassy matrices. In fact, there are nuclear wastes management plants in France and Canada that enclose the NW on glassy matrices based on the $Na_2O-B_2O_3-SiO_2$ composition - system (2).

The sodium borosilicate glasses are easily fusibles and are obtained with avalaible and cheap raw materials; therefore these glasses are a good melter in order to enclose the wide range of NW produced in research or in the nuclear industry. Nevertheless, they show a low level of chemical durability due to the wide area of liquid--liquid inmiscibility in the $Na_2O-B_2O_3-SiO_2$ ternary system (3). This liquid phase separation produces a microstructure of separated or - interconnected droplets facilitating the leaching of the interconnected matrix in water, alkalis or acids depending on the phase separated composition.

The addition of elements coming from a NW to a phase separated glass can be critical on the performance of these kind of glassy matrices:

a) Because of the harmful increased leaching, for the final product
b) Conversely, it would be used to include some elements in the dispersed phase designing conveniently the glass-in-glass inmiscibility degree.

Hence, is the aim of this paper to show the general principles of the liquid inmiscibility on glasses and reviewing the main papers carried out over the effect of additives in the liquid inmiscibility of the $Na_2O-B_2O_3-SiO_2$ glasses.

2. BASIS OF THE LIQUID INMISCIBILITY IN GLASSES.-

2.1. THERMODINAMICS.

Generally, on the glasses the compositions which produce liquid phase separation are include in a convex curve on the Temperature--Composition diagrams named "inmiscibility dome". This "dome" appears above or below the liquidus curve on binary silicate systems. If the "dome" is located above the liquidus, a "stable inmiscibility" area

is defined. If the "dome" is located below the liquidus, frequent - situation on systems with S elongated liquidus curve, the inmiscibility is a "metastable inmiscibility" or subliquidus inmiscibility.

The Fig. 1 shows the subliquidus inmiscibility in a binary - phase diagram showing the areas, viz:

- The I area is named the metastability area, where $\delta^2G/\delta X^2 > 0$. Therefore, spontaneous phase separation does not exist in this - area since to overcome a potentital barrier ΔG^* is required.
- The II area is the unstability area or spinodal decomposition - area, where $\delta^2G/\delta X^2 < 0$. In this area the phase separation is produced spontaneously if the mobility is high enough.

The temperature where both curves are tangents are situated in the top of the dome is the T_m named "miscibility temperature" or T_c "consolute temperature". Above this temperature it must not exist phase separation.

The Fig. 2 show the stable inmiscibility dome located above the liquidus in a model binary silicate system. For $T=T_1$, the stable equilibrium give rise to two liquid phases with e and h compositions. For $T=T_2$ the coexisting phases are one solid p and one liquid k and at the eutectic temperature two solids and one liquid are in equilibrium.

Charles (4) has calculated the inmiscibility curves on R_2O-SiO_2 binary systems from the chemical activities and assuming a subregular solution for the glass. Some assymetry of these curves are proved - because the critical composition appears at $X \approx 0.1$ in spite of $X = 0.5$ as would be theoretically prevented.

2.2. CALCULATION CRITERIA.-

There are some simple formulations which allow to calculate the T_m or T_c and some points of the miscibility curves. This, near the critical point is accoplished the following expression:

$$|c_e - c_c| \approx \sqrt{T - T_c}$$

here c_e is the equilibrium composition for each temperature T and c_c and T_c the critical composition and temperature (3).

Galakhov (5) relates the phase separation area with the ionic

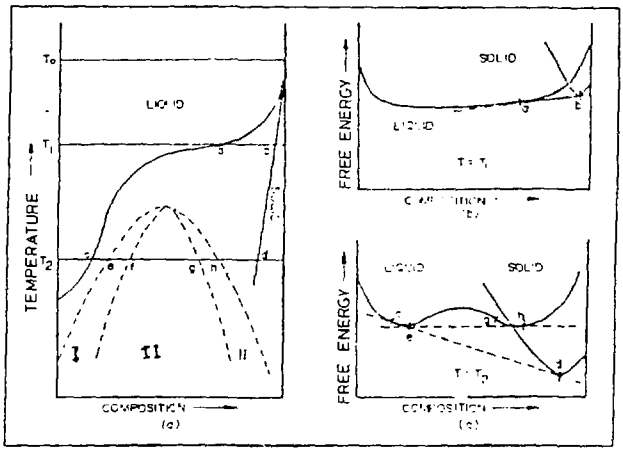

Fig. 1.- a) Phase diagram with subliquidus inmiscibility: b) and c) free energy curves corresponding to T_1 and T_2 temperatures (3).

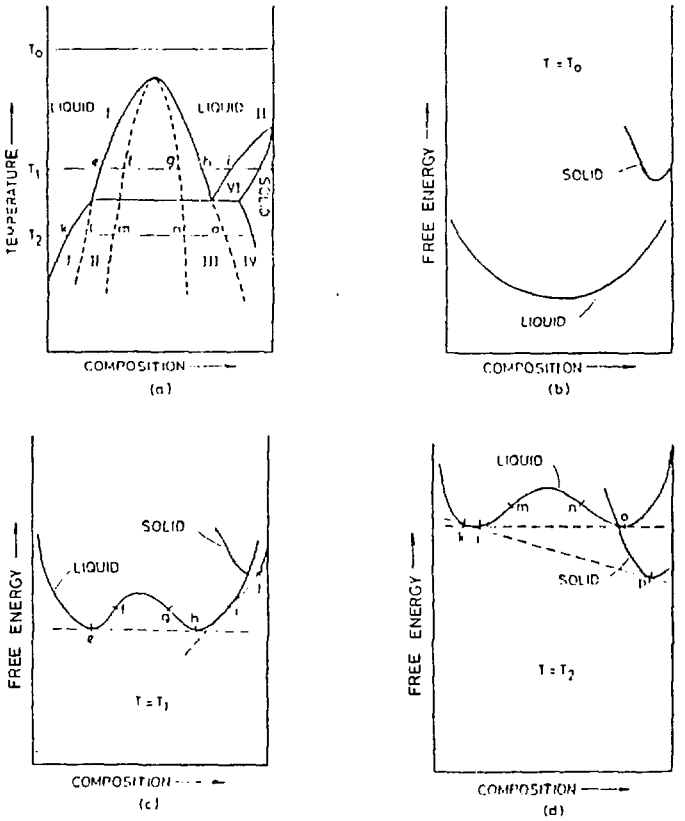

Fig. 2.- a) Phase diagram with stable inmiscibility area; b) c) and d) free energy curves for T_0, T_1 and T_2 (3).

potential (Z/r^2) at the temperature T(°K)/2 by using the expression:

$$\Delta_{0.5} = 28.5 + 8.5\ (Z/r^2)$$

On the other hand, Filipovich (6) obtains: $T_c = 6500\ Z/a^2$ where a = = r + 1.40 (r: ionic radius of modifier oxide in $RO-SiO_2$ systems) being this coefficient 5500 for Li_2O-SiO_2 and $MgO-SiO_2$ systems.

Other procedure, develloped by Cook and Hilliard (7) prcpose to determine the spinodal curve with the approximate expression:

$$\Delta C_S = \Delta C_e / \sqrt{3}$$

where ΔC_S is the c_s-c_c difference on each spinodal point and ΔC_e is the c_e-c_c difference on the bimodal points.

The calculations of phase separation based in structural arrangement use the Levin and Block (8) structural considerations. These authors have calculate the inmiscibility limit in practically all the binaries: R_2O-SiO_2; $RO-SiO_2$; $R_2O-B_2O_3$; $RO-B_2O_3$ ... formed with almost the R elements of the Periodic Table of Elements. Levin and Block (3) (8) determined the limit composition of inmiscibility (x: mol%) according to the expression:

$$X = \frac{3400}{(17+S^3-6.195r^3)n}$$

where r is the ionic radius of modifier; n, the cations number in - the oxide and S, the distance between the modifier cations. This -- distance, S, depends strongly of the coordination number of the modifier cations (3) (8). By representing the limit composition versus the modifier cations radius (Fig. 3), it can be seen that the inmiscibility in borate systems is larger than in the silicate. In other cases, such as Mn^{2+} or Sc^{3+} the oxigen number per modifier cation is more significant in order to compare the miscibility trend.

3. LIQUID PHASE SEPARATION IN BORATE SYSTEMS.-

3.1. BINARY SYSTEMS.-

The binary systems of alcali-borate show a wide inmiscibility - area at low temperature as is shown in Fig. 4. With an increase of the ionic radius of modifier cation from Li_2O to K_2O a decrease on - the critical miscibility temperature (T_m) is produced with a simulta

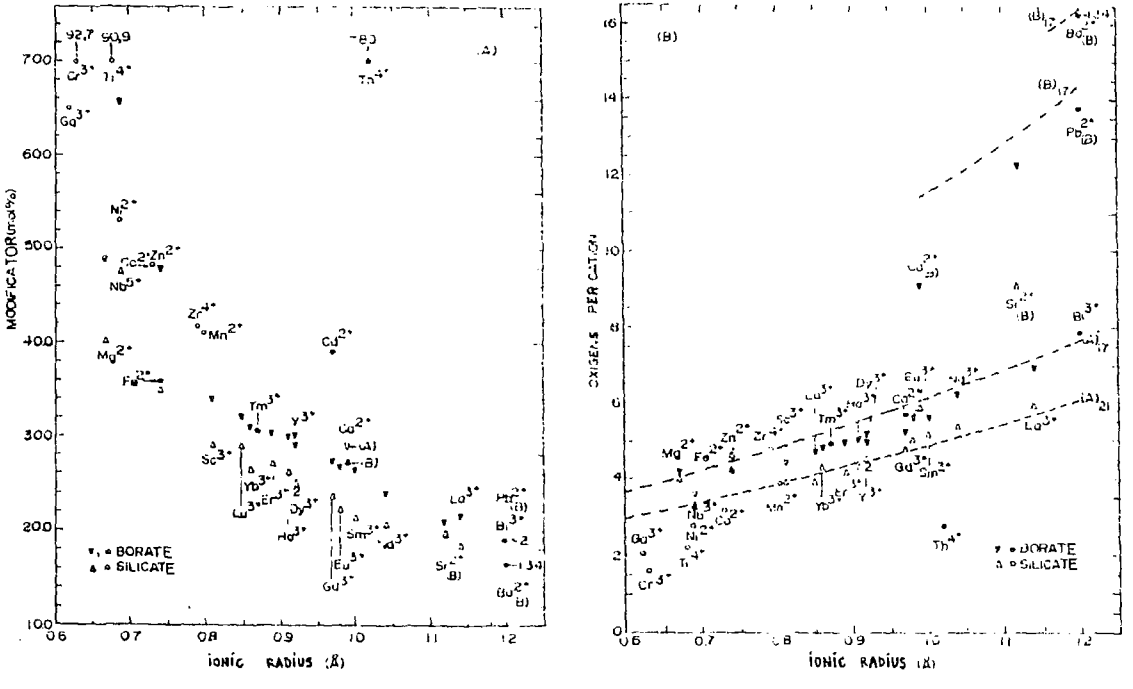

Fig. 3.- Extension of the inmiscibility (A) and the oxigen number per cation (B) versus the ionic radius (3)(8).

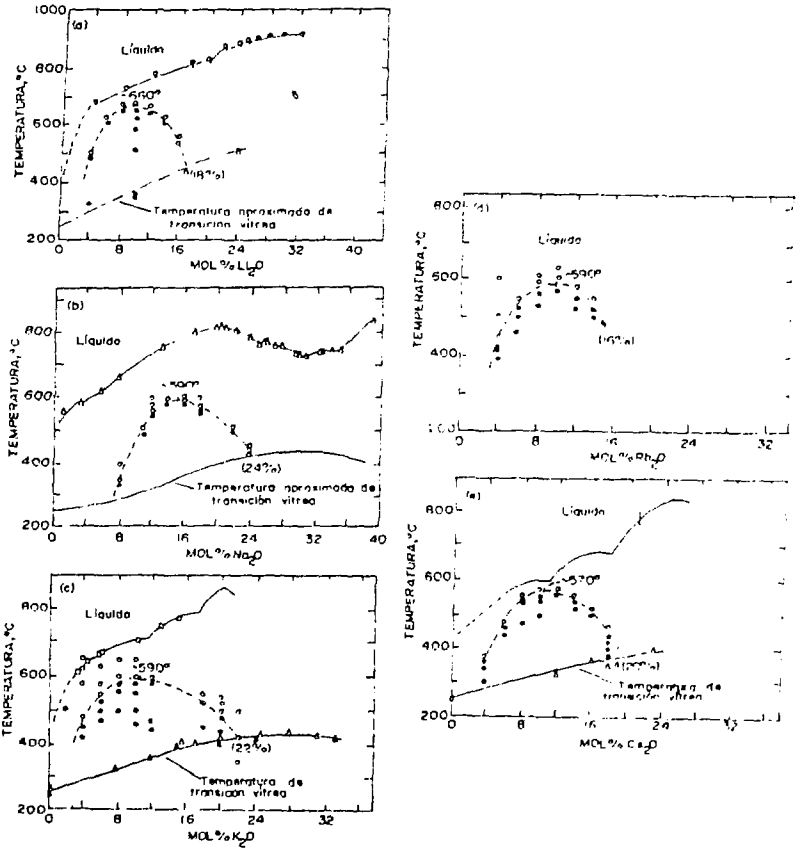

Fig. 4.- Inmiscibility curves in the R_2O-B_2O_3 systems (R=Li, Na, K, Rb and Cs) (3).

neous widen of the inmiscibility dome. When Rb_2O or Cs_2O is added to the B_2O_3 the T_m decreases. It is worth to point out that these curves are subliquidus, therefore, adding B_2O_3 to the Cs_2O or Rb_2O -- which be in a NW we can obtain glasses with phase separation, inmobilizating these elements into one of the liquid separated phases.

In the binary boron oxide systems the superior miscibility -- limit increases with ion size. Thus, the B_2O_3 mol % limits are:

61% in the $MgO-B_2O_3$; 72% in the $CaO-B_2O_3$;
79% in the $SrO-B_2O_3$ and 81% in the $BaO-B_2O_3$.

In the $ZnO-B_2O_3$ system this limit are located in the 50% B_2O_3 (9). The $PbO-B_2O_3$ has been studied extensively because the formulation of glazes. It shows a subliquidus phase separation with a high level of inmiscibility only with the 2wt% PbO in a lower range of temperatures being probed by electron microscopy.

3.1.1. Additives effect on binary systems.-

The addition of a third component on the liquid phase separation in binary systems has been investigated by Tomozawa (10), which deduces the following equation for determination of the change in the -- miscibility temperature (ΔTm):

$$\Delta Tm \approx \Delta T_L \frac{S(T_L)}{S(T_m)} + (T_L - T_m) \frac{\Delta S}{S(Tm)}$$

where $S(T_L)$, $S(T_m)$ and ΔS are the entropies for the liquidus, miscibility temperatures and the entropy change by the addition of the -- third component. ΔT_L is the change of the liquidus temperature.

When a component is added to a glass with liquid phase separation it must take account the effect on the surface tension (σ) (11) as indicated on the tabla I. Thus, the variation of σ with respect the matrix produce droplets of inmiscibility. As an example, the - MoO_3 and WO_3 additions promotes greatly the phase separation. Likewise Rincón and col. (12) have observed by transmission and scanning electron microscopy and increase of the inmiscibility on Li_2O-SiO_2 glasses with small additions of V_2O_5 and Cr_2O_3 which reduce the σ as can be seen on table I.

3.2. TERNARY SYSTEMS.-

Briefly the occurrence of liquid inmiscibility will be review in

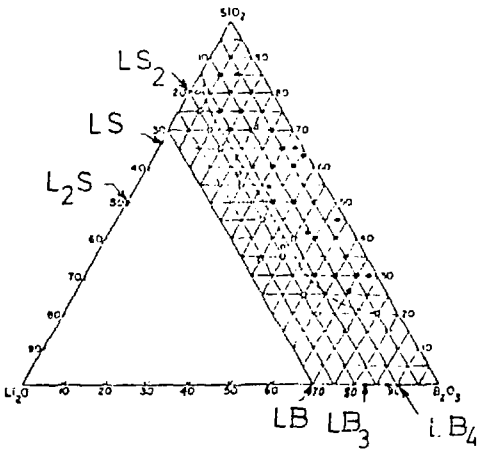

Fig. 5.- Inmiscibility area in the Li_2O-B_2O_3-SiO_2 system (13).

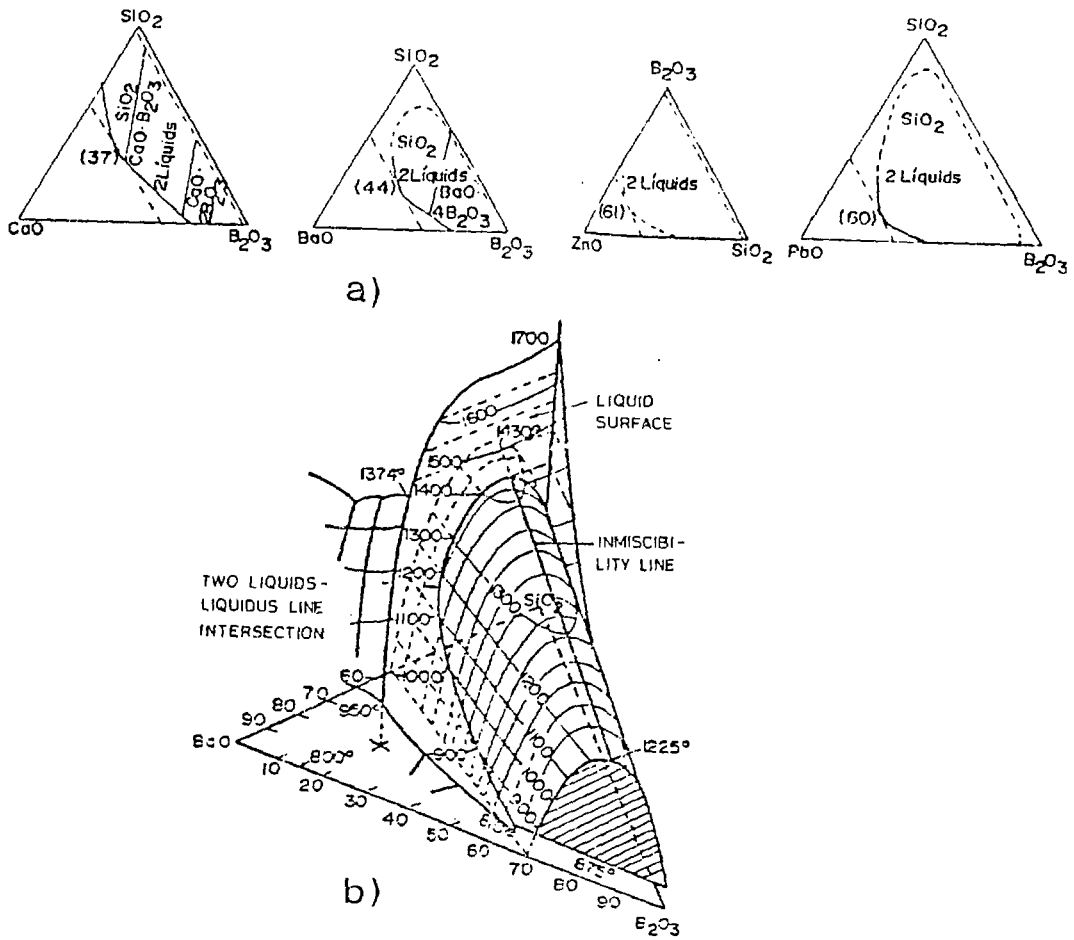

Fig. 6.- a) Types of inmiscibility in the ternary system BaO-,CaO-,ZnO- - and PbO-B_2O_3-SiO_2 (15); b) Tridimensional representation of the miscibility gap in the BaO-B_2O_3-SiO_2 system.

this part, considering in a different part the most important and studied $Na_2O-B_2O_3-SiO_2$ system.

The $Li_2O-B_2O_3-SiO_2$ system shows a wide area of inmiscibility near the binary $SiO_2-B_2O_3$. This is a typical case where the electron microscopy has been applied in order to know the phase separation - microstructure and to determine the miscibility gap. Sastry and Hummel (13) have obtained the area showed in the Fig. 5. Clear or transparent glasses are obtained in the area less than 25.6% Li_2O and white and opal glasses are obtained by thermal treatment of the same glasses at 550°-880°C temperature range.

The subliquidus miscibility gap in the $K_2O-B_2O_3-SiO_2$ system has been determined by Taylor and Owen (14) at temperatures higher than 550°C and mole ratios $SiO_2/B_2O_3 < 2$. The miscibility extension is - lower in this case than in the Li_2O-or Na_2O-similar systems. The critical temperature is $T_m = 629°C$ and is located at the $4K_2O.30B_2O_3.66SiO_2$ composition.

In the bivalent cation oxides-silicoborate systems such as CaO, BaO, ZnO and PbO the miscibility area is bigger than in the former - systems. As is shown in Fig. 6, when the ionic radius of the alkalin-earth oxide increases, the tighting of the miscibility gap is produced. In the case of $ZnO-B_2O_3-SiO_2$ and $PbO-B_2O_3-SiO_2$ systems these -- gaps are almost the same, and the critical miscibility composition - is practically the same in both cases. The $BaO-B_2O_3-SiO_2$ system miscibility has been extensively studied by Levin (15) over more than 70 compositions. The Fig. 6b shows the tridimensional gap miscibility in this system.

Likewise, this system and the PbO-containing system show secondary phase separation in large droplets enclosing inside small droplets. This phenomenon has been studied by Vogel and col (16). In some cases as in the $0.5PbO.7B_2O_3.92.5SiO_2$ composition heat treated at 600-650°C. The phase separation nucleates crystallizations (17) which can be used conveniently to isolated radioisotopes of a nuclear waste.

4. THE LIQUID INMISCIBILITY IN THE $Na_2O-B_2O_3-SiO_2$ SYSTEM.-

The sodium-borosilicate ternary glassy system has been the most widely studied giving rise to a tremendeous research due to its - applications on:

- Low thermal coefficient glasses

- Production of silica glass, such as Vycor
- Opal glasses and
- Lately, nuclear waste management.

This composition system constitues the basis for the NW vitrification in France and Canada which prepare waste forms by mixing the NW with a sodium-borosilicate glass.

This system shows a wide inmiscibility gap with elongated shape parallel and near the B_2O_3-SiO_2 binary with a critical temperature about 755°C (3).

Taylor and col (18) have examinated by SEM the microstructure of glasses located inside the miscibility gap in the Na_2O-B_2O_3-SiO_2 system and heat treated at 650°, 700° and 750°C. The "tie" lines determination inside the miscibility area for each temperature gives rise to experimental difficulties and frequent errors in the litterature. These authors have considered 24 glassy compositions near the 750°C isotherme containing a "silica enriched phase" and other "poor silica phase". By combining the opalescence with de SEM observations it was possible to estimate the plait points in this system in the above indicated temperatures (Fig. 7).

In spite of lack of precision in the litterature with respect the T_m or critical composition determination, the T_m temperature value in the Na_2O-B_2O_3-SiO_2 system is intermediate between the T_m in the corresponding Li_2O-and K_2O-systems. Table II shows comparatively these values. The trend to phase separation follows the sequence Li > Na > K, likely as happen in the binary silicate systems (3)(15) and is related with the decreasing ionic field intensity of alkalin metal cation.

4.1. Effect of additives on the liquid inmiscibility in the Na_2O-B_2O_3-SiO_2 system.-

The Canada Atomic Energy Commission has developped a wide research program with the aim of to elucidate the liquid inmiscibility extension in quaternary or multicomponent systems formulated from the Na_2O-B_2O_3-SiO_2 system. The substitution of monovalent metal oxides such as Li,K and Cs by Na_2O in a sodium borosilicate glass has been investigated by Taylor and Owen (21). A $5Na_2O.23B_2O_3.72SiO_2$ composition close to the critical point (table II) has been probed. The Fig.

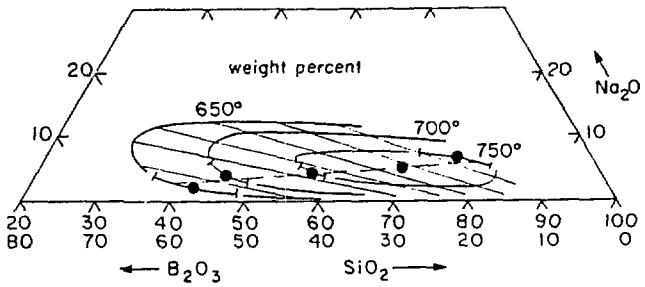

Fig. 7.- Miscibility tie-lines at 650°, 700° and 750°C in the ternary Na_2O-B_2O_3-SiO_2 system (19).

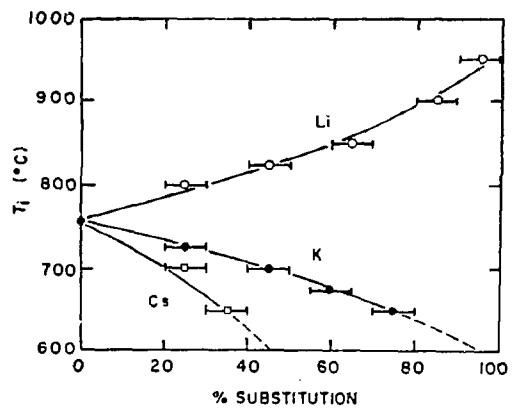

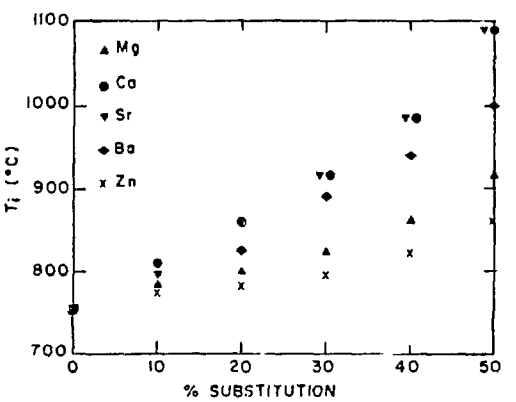

Fig. 8.- a) Clearing or consolute temperature of inmiscibility versus the R_2O% substitution and b) the similar versus the RO% substitution in the $5Na_2O.23B_2O_3.72SiO_2$ glass (21).

TABLE I

Effect of oxides on the Glass Surface Tension (11)

Group	Oxide	σ(dyn/cm) at 1300°C
Increase the surface Tension	La_2O_3, MnO	610
	Al_2O_3	580
	MgO	520
	CaO	510
	SrO, FeO	490
	BaO	470
	ZnO, Li_2O	450
	CdO, CoO	430
	NiO	400
	BeO	390
	SnO_2, ZrO_2	350
	Na_2O	295
	SiO_2	290
	TiO_2	250
Decrease the surface Tension	As_2O_3	The σ value are variable and negativ
	V_2O_5	
	Cr_2O_3	
	MoO_3	
	WO_3	
	SO_3	

TABLE II

Critical miscibility composition and temperature in the R_2O-B_2O_3-SiO_2 systems (3)

System	mol % R_2O - B_2O_3 - SiO_2			T_c(°C)	Ref
Li_2O-B_2O_3-SiO_2	13	19	68	995	(13)
Na_2O-B_2O_3-SiO_2	5	21	74	755	(19)
	6	31	63	750	(20)
K_2O-B_2O_3-SiO_2	4	30	66	629	(14)

8a represents the variation of critical temperature (clearing temperature) versus the R_2O substitution by Na_2O being R = Li,K or Cs. The phase separation decreases or suppress in the case of K and Cs, respectively. Only the Li^+ addition increases the T_i and, therefore, the extension of inmiscibility.

The Fig. 8b shows that the alkalin-earth elements addition increases the T_i (clearing temperature). In this case does not exist relation between the phase separation enhancement and the ionic radius. CaO > SrO > BaO behaviour is as was prevented, but the MgO and ZnO show abnormal and lower enhancement of phase separation may be due to the partial lattice formator character of these oxides.

By considereing a SiO_2/B_2O_3 = 1.07 $\pm$ 0.05 (mol) the inmiscibility limits at 650°C are represented on the Fig. 9. It can be probed that an increase in the ionic radius which involves a decreasing - ionic field intensity (Z/r^2) produces a decreasing inmiscibility in both Na_2O-B_2O_3-SiO_2 and K_2O-B_2O_3-SiO_2 systems. The habit of this -- curve is different in both cases being wider in the Na_2O-than in the K_2O-system due to the tight relation between inmiscibility and ionic field intensity.

Actually, these curves (Fig. 9) are projection at different temperatures giving a more complete idea of the inmiscibility dome as is shown in Fig. 10. The T_S value or consolute temperature for these systems depend of the M cation and the SiO_2/B_2O_3 ratio considered.

It is interesting to note here the experimental procedure to - determine the miscibility areas. Firstable, a large number of transparent and opal glasses have been obtained, but according to Taylor and col (21) following preventions must be taken, viz:

1) To examine a few samples by SEM. A microstructure with phase -- domains larger than 100 nm in all the opalescent samples has been observed; however, no one microstructure on transparent samples - at ≈ 20 nm resolution was observed.
2) In order to confirm that opalescence must be due to amorphous -- phase separation and not to devitrifications the XRD has been used.
3) The experimental T_m is refered to the reversible phase separation measuring the critical miscibility temperatures in some glasses. The samples have been heated at sucessive temperatures in 10°C - ranges until opalescence dissappear.

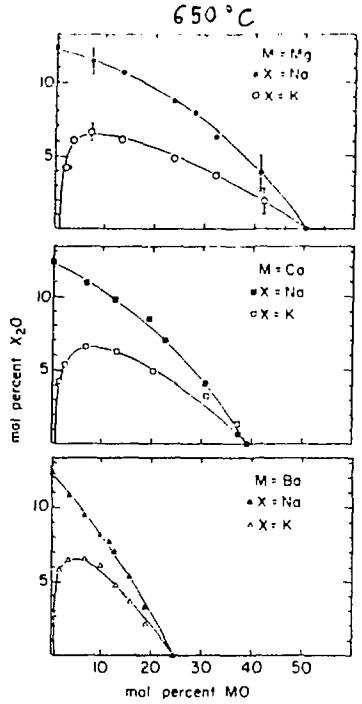

Fig. 9.- Miscibility areas at 650°C for the SiO_2/B_2O_3 = 1.07 ± 0.05 (mol) ratio in the R_2O- and $RO-B_2O_3-SiO_2$ systems (22).

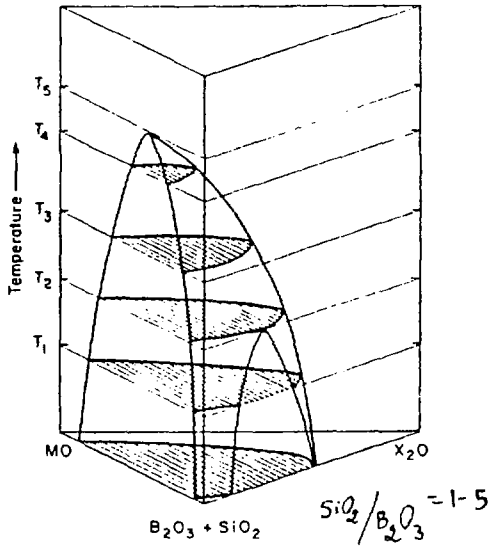

Fig. 10.- Cuts of the miscibility gap at diferent temperatures in the $X_2O-MO-B_2O_3-SiO_2$ system (22).

The $Na_2O-B_2O_3-SiO_2$ ternary system with ZnO additions shows a great interest fot the USA and Canada NW Research (21). The corresponding quaternary system shows a wide stable inmiscibility. The tie lines in the miscibility area on the $ZnO-B_2O_3-SiO_2$ subternary system is very similar to those with CaO-or SrO. Usually, the Zn enriched phase concentrates the Si on the particles larger than 10 μm. By superimposing the miscibility areas on the $Na_2O-B_2O_3-SiO_2$ and the $ZnO-B_2O_3-SiO_2$ systems (Fig. 11a) it may be visualize the turned location of the tie lines.

The miscibility contours for diferent X = Na_2O% values are represented on Fig. 11b. The 650°C contour increases when to the $Na_2O-B_2O_3-SiO_2$ system (X=1.0) is adding ZnO until sustituing all the Na_2O by ZnO (X=0). At 800°C and 950°C for X = 0.25 both contours are superimposed. Two areas rest unexplored in this system: the higher SiO_2 content area and the shape of the miscibility gap up to 950°C.

The MnO addition to the glasses of the $Na_2O-B_2O_3-SiO_2$ has been investigated (23) on twelve compositions along the tie-line crossing the 700°C isotherme on the inmiscibility gap. By adding between 0.1 and 6.0 % MnO to the selected compositions a whole of 40 glasses have been obtained. The large size of glass-in-glass droplets (2-10μm) in the $5Na_2O.50B_2O_3.45SiO_2$ composition glass has made possible the EDX microanalysis probing that MnO is strongly partioned in matrix phase and the effect of this additions on the tie-lines.

The Fig. 12 represents the inmiscibility isothermes obtained from the T_c experimental data. The MnO additions produces a sudden variation on T_c on the compositions with lower Na_2O content.The MnO addition produces also a high increase on the silica partioning between phases indicating a small expansion of the inmiscibility gap.

The CoO addition to the glasses on the $Na_2O-B_2O_3-SiO_2$ system has been studied by Ehrt and col (24).

The Nd_2O_3 addition (1.3%) to a phase separable $8.7Na_2O-40.4B_2O_3-49.6SiO_2$ glass has been studied by Villiers and col (25) with the aim to produce a SiO_2 rich sintered glass. It has been demonstrated by water and HCl leaching experiments that Nd_2O_3 is located in the borate phase preferentially. In water leached at 95°C for 24 hours, the 99% Nd_2O_3 is retained in the porous glass if the glass is heat treated at 550°C from 1 hour to 96 hours.

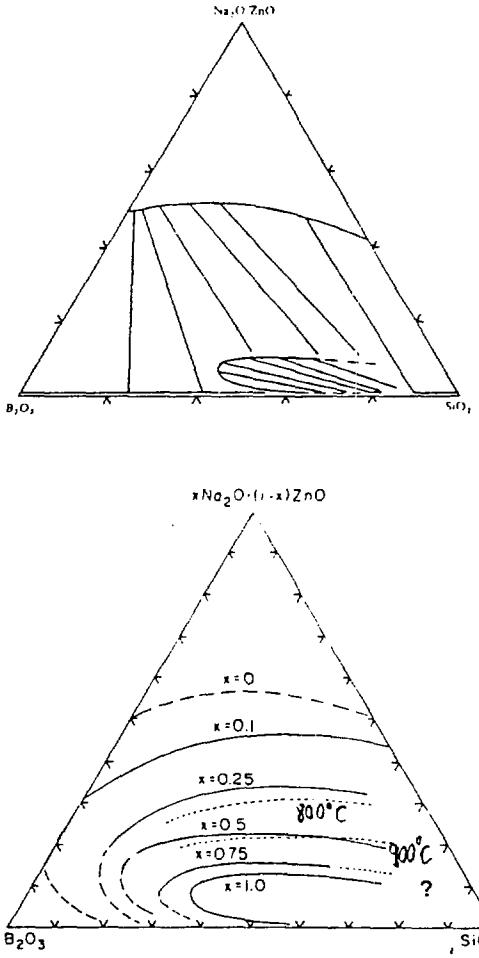

Fig. 11.- a) Superposition of known miscibility areas and tie lines for the Na_2O-B_2O_3-SiO_2 inner loop and ZnO-B_2O_3-SiO_2 systems. b) Miscibility isothermes at different x values in the $xNa_2O.(1-x)ZnO.B_2O_3.SiO_2$ system (22).

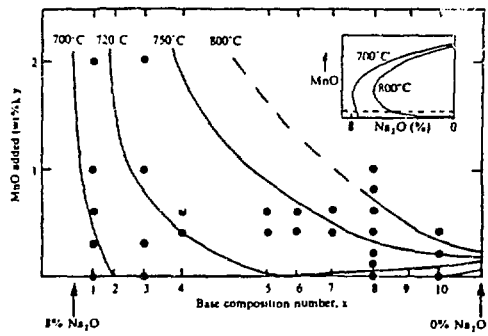

Fig. 12.- Miscibility isotherms determined from the T_c data showing - the probable form of the miscibility gap in the Na_2O-MnO-B_2O_3--SiO_2. The experimental isotherms are into the area indicated by dashed lines (23).

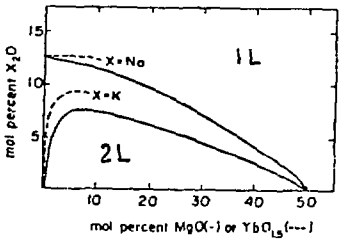

Fig. 13. Miscibility areas at 650°C in the pseudoternary X_2O-MgO-(0.48 B_2O_3.0.52SiO_2) and X_2O-Yb_2O_3-(0.33B_2O_3.0.67SiO_2) (X=Na,K) - system (26).

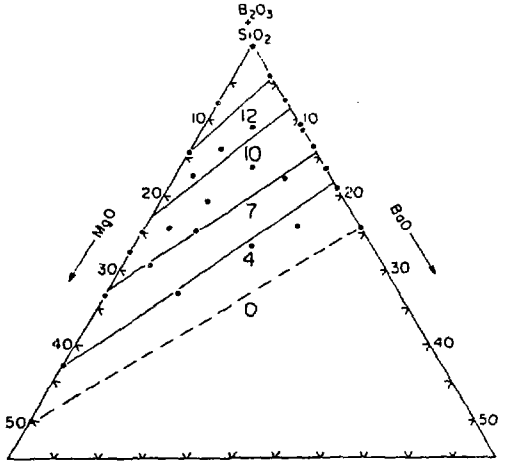

Fig. 14.- Limits of the miscibility in the Na_2O-MgO-BaO-B_2O_3-SiO_2 - system with SiO_2/B_2O_3 = 1.07 $\pm$ 0.05. The points locate the - composition of the MgO.BaO.(B_2O_3 + SiO_2). Numbering of contours represents the n' values (27).

The miscibility limits in the Na_2O-B_2O_3-SiO_2 and K_2O-B_2O_3-SiO_2 systems with Yb_2O_3 additions has been investigated in the 650°-800°C range for concentrations to 5 mol% Yb_2O_3 and a fixed ratio SiO_2/B_2O_3= =2.0 (26). The great interest of these experiments are that miscibility behaviour of lanthanides is hardly known and being lanthanides approximately 1/3 bulk of the nuclear waste fission products. Usually, the T_c is very sensitive to the X_2O and Yb_2O_3 contents on the glass, but additions can produce devitrifications masking the phase separation. For this reason only tne xX_2O. yYb_2O_3. (100-x-y) ($0.33B_2O_3$. .$0.67SiO_2$) compositions have been considered, specially for y < 5. The Fig. 13 represents the miscibility limits at 650°C in the pseudoternary system: X_2O-MgO-($0.48B_2O_3$.$0.52SiO_2$), and X_2O-Yb_2O_3-($0.33B_2O_3$. .$0.67SiO_2$) being observed that miscibility area extends more with -- Yb_2O_3 than with MgO additions. From a practical point of view the glass production up to 5 mol% Yb_2O_3 does not greatly affect the extend of the miscibility. But, only the T_m is greatly affected of low sodium compositions (x < 10). It seems that inmiscibility behaviour of lanthanides is similar to the corresponding alkalinearth containing systems, in spite of the charge-to-radius ratios of the La^{3+} ions are only -- slightly larger than those of the smaller M^{2+}.

In the fine components system resulting of MgO + BaO additions to the Na_2O-B_2O_3-SiO_2 system, the miscibility behaviour has been examinated by Taylor and col (27). The high sensibility of the critical miscibility with the Na_2O content produces variations to 100°C with 1mol% Na_2O. By first time, a different representation of the miscibility data on five components systems in a quaternary subsystem has been used (Fig 14), viz: the composition data are expressed as nX_2O. .m($MO.B_2O_3$).1.$07SiO_2$ molar. The m values for n=0 are defined as m_o and these values are normalized as $m' = m/m_o \times 100$. The X_2O content is expressed as n' (X_2O mol% that must be added to a composition in order to decrease 650°C the T_m):

$$n' = \frac{n \times 100}{m + 2.07}$$

Thus, the Na_2O data representation of X_2O mol% added vis a MO content normalized, m', gives a right line.

As a summary, it can be say that present stay of research in -- glass-in-glass miscibility allow us to prevent the microstructure --

resulting on the nuclear waste vitrification with Na_2O-B_2O_3-SiO_2 glass composition. The effect of some additions such as: K_2O, CaO, MgO, BaO, CoO, MnO, Yb_2O_3 or Nd_2O_3 is well established; however much more research is necessary on the additions with other important elements of the nuclear wastes.

Consequently, the effect of such additions on water leaching, thermal conductivity and radiaction damage of the waste forms must - be the aim of research in the next future.

Acknowledgements.-

Litterature information facilitated by P. Taylor of the Atomic Commission of Canada is sincerely appreciated.

REFERENCES

1. Scientific Basis for Nuclear Waste Mangement.VI, Editor D.G. Brookins, Material Research Soc.Symposia Proc. Vol.15, 1982, Ed. North Holland N.Y., Amsterdam, Oxfor.
2. G.M. Hughs, J.L. Knabenschuh, E.G. Hess and D.K. Pluetz, Concep tual design of high-level waste vitrification process at West Valley using a slurry-fed ceramic melter. Advances in Ceramics. Vol. 8. Nuclear Waste Management. Ed. Am.Cer.Soc., Columbus, Ohio, 1984,pp: 143-148.
3. J.Mª Rincón and A. Duran, Separación de Fases en Vidrios. El Sistema Na_2O-B_2O_3-SiO_2. Ed. Soc.Esp.Ceram.Vidr., 1982. Madrid.
4. R.J. Charles, Activities in Li_2O-Na_2O and K_2O-SiO_2 solutions, J. Am.Cer.Soc. 50 (1967) 631-641.
5. F.Y. Galakhov and B.G. Varshal, The Structure of Glass. Vol. 8. Ed. Porai-Koshits. Consultans Bureau, N.Y., 1973, pp: 7-11.
6. V.N. Filipovich. The Structure of Glass. Vol. 8. Ed. Porai-Koshits. Consultans Bureau. N.Y., 1973, pp: 12-22.
7. H.E. Cook and J.E. Hilliard. Trans. AIME 233 (1975) 12, 1066-1071.
8. E.M. Levin and S. Block, Structural Interpretation of Inmiscibility in oxide Systems: IV, Ocurrence, Extent and Temperature of the Monotectic, J.Am.Cer.Soc. 41 (1967) 1, 29-38.
9. M. Imaoka, Glass Formation Range and Glass Structure, International Congress of Glass, Washington, Advances in Glass Technology,Ed. Am.Cer.Soc., Columbus, Ohio, 1962, pp:149.
10. M. Tomozawa and R.O. Obara, Effect of Minor Third Components on Metastable Inmiscibility, Boundaries of Binary Glasses, J.Am.Cer. Soc., 56 (1973) 7, 378-381.
11. J.E. Flannery, W.H. Dunbaugh and G.B. Carrier, Improving the Opacity of Phase-Separated Opal Glasses by Alterations of the Interfacial Tension, Am.Cer.Soc.Bull. 54 (1975) 12, 1066-1071.
12. J.Mª Rincón, C.J.R. Gonzalez Oliver and P.F. James. Phase Separation in Li_2O-SiO_2 glasses with additions of V_2O_5, MnO_2 and Cr_2O_3. To be published.
13. B.S. Sastry and F.A. Hummel, Studies in Lithium Oxide Systems:VII, Li_2O-B_2O_3-SiO_2, J.Am.Cer.Soc. 43 (1960) 23-30.
14. P. Taylor and D.G. Owen, Liquid Inmiscibility in the System K_2O-B_2O_3-SiO_2, Comm. of the Am.Cer.Soc. C-158-159 (1981) Nov.
15. E.M. Levin, Liquid Inmiscibility in Oxide Systems.

On Phase Diagrams, Vol.III,Ed. Alper, Academic Press, 1970, pp:143.

16. W. Vogel, W. Schmidt and L. Horn, Neue Ergebnisse und Erkenntnisse zur Phasentrennung in Glase, 9^{e} International Congress of Glass, Versalles, 1971. Ed. Institut du Verre, Paris, pp: 425-450.
17. O.H. El-Bayoumi and K.N. Subramanian, Crystallization of borosilicate glass containing Lead Oxide, Mat.Res.Bull. 17 (1982) 1379--1384.
18. P. Taylor, A.B. Campbell, D.G. Owen, D. Simkin and P. Menassa, Microstructure of phase-separated sodium borosilicate glass. Advances Mat.Charact., 1983, Ed. D.R. Rossington, R.A. Condrate and R.L. Snyder. Ed. Plenum Publishing Corp.
19. W. Haller, D.H. Blackburn, F.E. Wagstaff and R.J. Charles, Metastable Inmiscibility Surface in the Na_2O-B_2O_3-SiO_2 system. J.Am. Cer.Soc. 53 (1970) 1, 34-39.
20. F. Ya. Galakhov and O.S. Alekseeva, The Structure of Glass, Vol.8, Ed. Consultans Bureau, 1973, pp: 80-83.
21. P. Taylor and D.G. Owen, Liquid Inmiscibility in Complex Borosilicate Systems, J.Non-Cryst.Solids 42 (1980) 143-150.
22. P. Taylor and D.G. Owen, Liquid Inmiscibility in the System Na_2O--ZnO-B_2O_3-SiO_2, J.Am.Cer.Soc. 64 (1981) 6, 360-367.
23. P.E. Menassa, D.J. Simkin and P. Taylor, Miscibility Limits and Microstructure of Glasses in the System Na_2O-MnO-B_2O_3-SiO_2, Phys. Chem.Glasses, 26 (1985) 5, 137-142.
24. D. Ehrt, H. Reiss and W. Vogel, Microstructural Study of CoO-containing Na_2O-B_2O_3-SiO_2 Glasses, Silikattechnik 28 (1977) 359.
25. D.R. Villiers, M.A. Res and R.O. Heckroodt, High Silica Glass Doped with Nd_2O_3 from a Phase Separated Na_2O-B_2O_3-SiO_2-Nd_2O_3 glass, Physics and Chem. of Glasses, 26 (1985) 5, 187-188.
26. P. Taylor, Sh. D. Ashmore and A.B. Campbell, Liquid Inmiscibility in the System Na_2O-Yb_2O_3-B_2O_3-SiO_2 and K_2O-Yb_2O_3-B_2O_3-SiO_2, Comm. of the Am.Cer.Soc. (1984) Sept, C-186-188.
27. P. Taylor, A.B. Campbell and D.G. Owen, Liquid Inmiscibility in the System X_2O-MO-B_2O_3-SiO_2 (X=Na,K; M=Mg,Ca,Ba) and Na_2O-MgO-BaO--B_2O_3-SiO_2, J.Am.Cer.Soc. 66 (1983) 5, 347-351.

GLASS CERAMIC MATERIALS FROM SPANISH BASALTS

Salvador Martínez Manent
Pura Alonso Abella
Carlos de la Fuente Cullell
Ignacio Queralt Mitjans

Instituto de Geología "Jaime Almera", CSIC, Barcelona
Facultad de Geología. Universidad de Barcelona

SUMMARY

In this paper we are described the chemical and mineralogical composition of the spanish basalt-rocks from Catalonia and Canary Islands like a raw material for the glass-ceramic production. Likewise, the main features of the thermal behaviour of glasses obtained from basalt melts are showed, trough their study by means of DTA, XRD, SEM and EDAX techniques.

RESUMEN

En este artículo se describen las composiciones químicas y mineralógicas de las rocas basálticas españolas de Cataluña y las Islas Canarias como materias primas para la obtención de vitrocerámicos. Asimismo, se muestran las principales características del comportamiento térmico de vidrios obtenidos a partir de fundidos basálticos por medio de técnicas de ATD, DRX, SEM y EDAX.

1. Introduction

A glass-ceramic material is a material obtained from a glass in which controlled nucleation and crystallization has been induced through heat treatment. In the last few years, research on several kinds of compositions has been done so as to get glass-ceramic products of specific characteristics, one of those being glass-ceramic materials obtained from basalts. Several authors have worked on that field, both from a general point of view and to obtain chemical and mechanical resisting materials, BAHL,D.(1); BANDYOPADHYAY,A.K.(2); BEALL,G.H.(3); GARCIA VERDUCH,A.(4); QUERALT,I.M.(5); THOMASSIN,J.H.(6); etc. as well as from the point of view of particular uses -like their possible applications to building materials- ABRAMYAN,A.V.(7); WATANABE,T.A.(8); etc.; to obtain enamel and glaze DIKEN,G.M.(9); DVORKIN,I.(10); or to inmobilize radioactive wastes, CHICK,L.A.(11); NEWKIRK,H.W.(12); SASAKI,N.(13); etc.

In this paper, we present a brief reference to the point we are now in the study os Spanish basalts to obtain glass-ceramic materials, and their possible applications.

2. Chemical and Mineralogical Study

In the first place, a study and a bibliographical compilation of the geology of the different areas studied was made, as well as the chemical and mineralogical analysis of the basalts sampled. As regards Catalonia and nearly all the Canary Islands, this stage is finished.

The classification of basalts is made according to two main factors: their chemical composition, and if there are some specific minerals. Due to the difficulties in determining quantitatively some minerals, like those in basalts, because of their great variability of composition, they are classified according to their chemical analysis, which is taken as the starting point to work out of petrological norms classification.

The procedures used here are the calculation rules for C.I.P.W. Norm (see MORSE,S.A., 1980), in which the final result is given in percentages of weight of several normative minerals or potential minerals resulting from their chemical analysis. Those minerals are feldspars, pyroxenes, olivines, ilmenite, magnetite, apatite and, in some cases, nefeline and quartz. The first three groups, which are solid solutions, are calculated in terms of their last terms; the normative composition of feldspars is recalculated as percentages of anortite, albite and ortose; the normative composition of pyroxenes in terms of wollastonite, enstatite and ferrosilite; and the normative compositon of olivine in terms of forsterite and fayalite.

YODER and TILLEY (1962) made a diagram to classify basaltic rocks starting from CIPW (fig. 1), using a tetrahedron of mineral compositions. This tetrahedron is just the quaternary system forsterite, diopside, nefeline, and quartz.

Thus, we have got five groups of basalts, based on their normative composition (fig. 2). Three of them occupy volumes in the tetrahedron and the two left are related to the plane of saturation and subsaturation of silica. The five groups are:

1. Toleite
2. Hypersthene basalt
3. Olivine toleite
4. Olivine basalt
5. Alkaline basalt

2.1 Chemical and Mineralogical composition of the Basalts of the Canary Islands.

Seven big islands and four small ones make up the Canary Islands. Those island emerge from the continental slope and glacis, in the area of the continental margin between the platform and the abyssal plain.

The Canary Islands are one of the most varied and complex volcanic areas known, not only because of their geological evolution, variability of volcanic phenomena and eruptive history, but also because of the diversity of geological material found there.

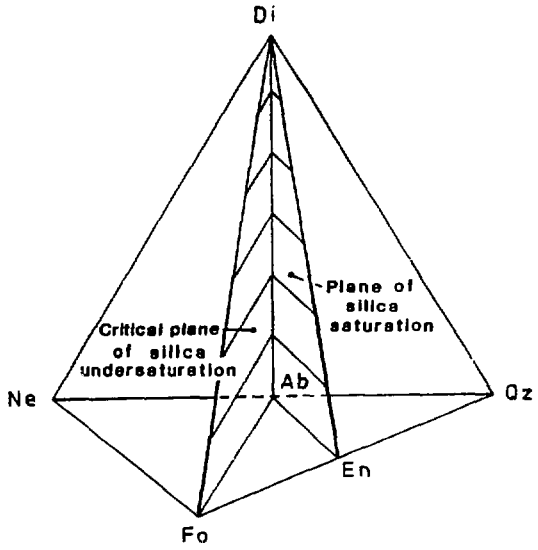

Fig. 1 The basalt tetrahedron of YODER and TILLEY. A classification model for basalt study.

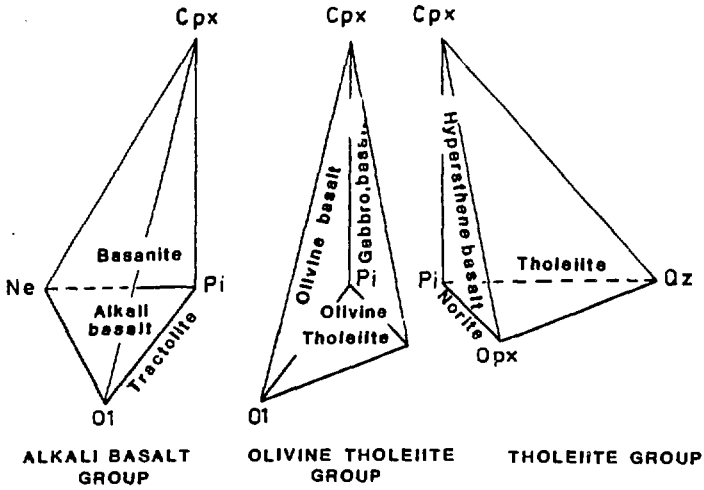

Fig. 2 The main basalt types nomenclature based on their normative compositon.

The studies of several authors on the petrological composition of the islands have allowed the grouping of materials, in a very general way and without taking into account the characteristics o each single island, into thre main groups: base complex, old basaltic series and new volcanic series. Our study is focused on the last group and, especially, on recent basalts (those of series IV).

At the present moment, nearly all the recent basalts of the Canary Islands are sampled, except those of Tenerife and Fuerteventura, which will be sampled in a next campaing.

As to the method of sampling, we have taken into account, apart from the geological criteria, the possibility of exploitation of the sampled lava flows. That is to say, the areas sampled are those liable to be exploited.

The mean chemical composition of the basalts of the islands can be seen in table I. According to the content of silica, we can see that, in general, the rocks are of basic type (45%-52% of Si and of ultrabasic type (45% of , and with high content of TiO_2 which, in some instances, are higher than 5%, like in some samples from the Canary Islands.

If we make the normative calculation through CIPW Norm, we see that they can be classified, in general, in the group of alkaline basalts, which agrees with the high content of Ti although, in this case, it is higher than the normal average for these materials.

The mineralogical analysis has been made through X ray diffraction and optical microscopy in thin sheet. This composition also agrees with than expected of alkaline basalts with olivine, plagioclase and pyroxene as principal minerals, and the content of magnetite is, in general, considerable.

2.2 Chemical and mineralogical composition of the Basalts of Catalonia.

As to the basalts in Catalonia, they are spread over La Garrotxa, Baix Empordà and La Selva (fig.3). Similar criteria to that used in the Canary Islands has been applied for the sampling.

Table I. Chemical compositions of basalt-rocks from Canary Islands

	SiO_2	Al_2O_3	TiO_2	Fe_2O_3	FeO	MnO	MgO	CaO	Na_2O	K_2O	P_2O_5	L.O.I.
La Gomera	46.8	15.8	3.9	9.7	3.9	0.2	5.3	10.6	3.4	1.0	1.3	0.8
Hierro	43.1	11.1	4.3	7.1	7.4	0.2	11.5	11.1	2.9	1.1	0.6	0.2
La Palma	45.3	13.9	3.7	5.1	6.4	0.2	7.6	11.1	4.2	1.7	0.8	0.2
Lanzarote	49.7	14.1	2.6	7.3	4.6	0.2	7.8	9.8	3.3	0.7	0.3	0.3
Gran Canaria	42.4	12.5	4.0	5.6	7.1	0.2	7.5	12.0	3.3	0.7	1.2	3.2

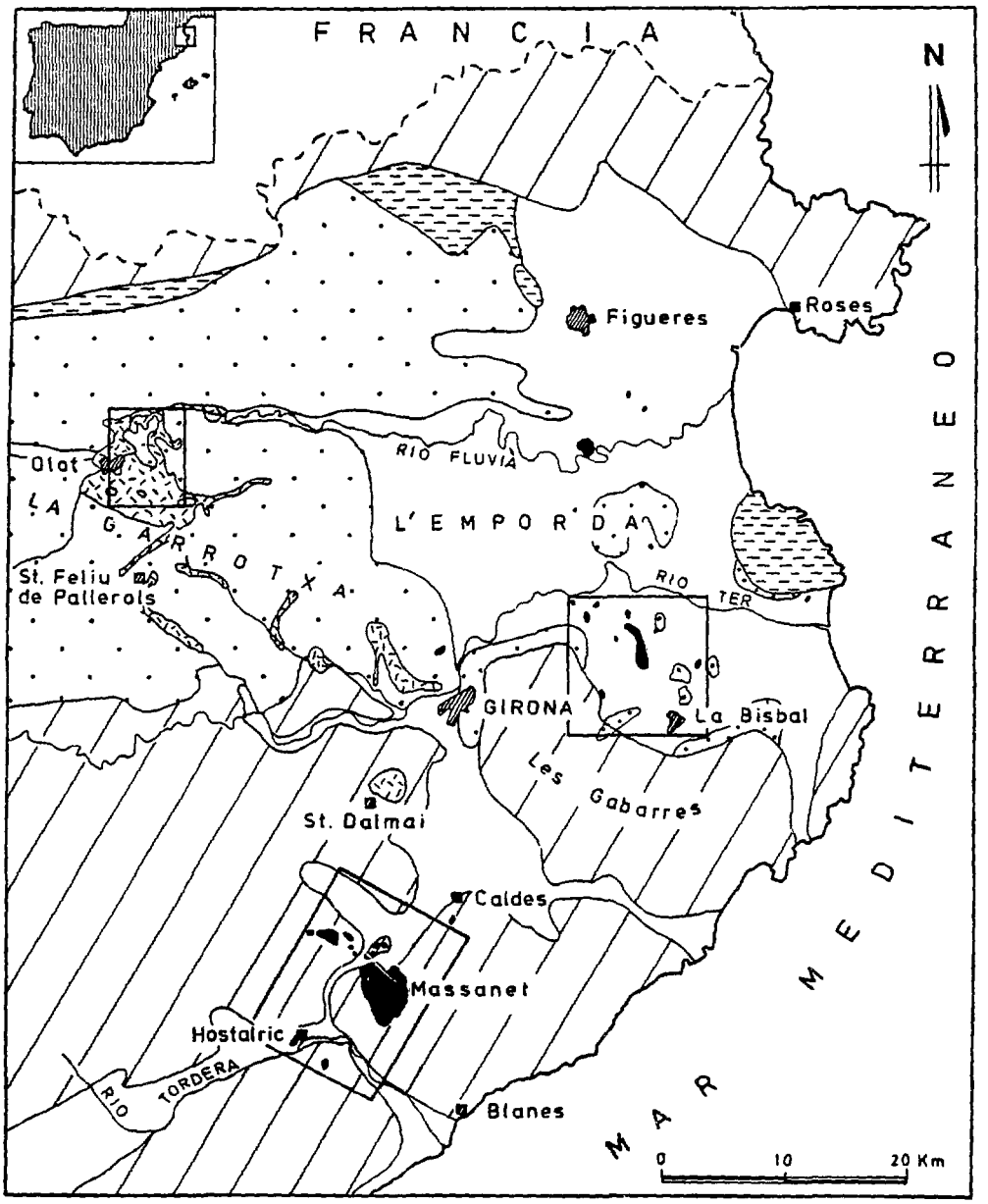

Fig. 3 Localization of basalts from Catalonia.

In table II, the mean composition of the samples of the main areas studied is shown. Those materials show very little difference in their chemical composition, being placed, according to their content of silica, betwen basic rocks and ultrabasic ones. As to the content of Titanium, it is also high, although much more in agreement with the mean content of that type of rocks.

If we make the normative analysis based on the chemical composition, we see that they are mainly made up of alkaline basalts and basanites (basalts of similar composition but somewhat more basic).

The mineralogical study was also made through X rays diffraction and optical microscopy in thin sheet.

Through the mineralogical study, we can see that they are made up of a porphyritic structure in which the phenocrystals are mainly of olivine and/or pyroxene, and which are immersed in a microlithic matrix rich in plagioclase. There is also magnetite.

Through the diagrams of diffraction, we have been able to determine the term of the series Fo-Fy to which the olivines belong, and their composition expressed in percentages of Fo is between Fo-66% and Fo-72%.

As to the pyroxenes, they are titanium augites, and as regards plagioclases, they are placed on the term labradorite, that is, anortite 55%-60%.

3. Study of the nucleation and crystallization through DTA, XRD, SEM and EDAX.

Once know the chemical and mineralogical compositon of the different samples, the process of nucleation and crystallization was studied. This part of the study has beguin with the basalts of Catalonia, because of their proximity to the centre of research, which makes it easier to get samples.

In the first place, through heating microscopy, the curves viscosity-temperature were obtained (fig.4). Although this method is

Table II.Chemical compositions of basalt-rocks from Catalonia

	SiO_2	Al_2O_3	TiO_2	Fe_2O_3	FeO	MnO	MgO	CaO	Na_2O	K_2O	P_2O_5	*L.O.I.*
Castellfollit	45.0	15.0	2.6	5.1	7.3	0.2	9.2	10.0	3.4	1.5	0.3	0.5
Batet	47.2	14.6	2.6	4.6	6.9	0.2	6.3	9.8	3.5	1.8	0.8	0.5
Cruscat	44.7	14.5	2.5	4.1	8.0	0.2	9.1	9.6	3.8	2.4	0.5	0.4
Rupià	44.8	16.1	2.4	3.2	8.1	0.2	8.0	10.3	3.5	1.0	0.4	2.4
Sant Corneli	46.8	16.5	1.8	3.0	6.9	0.1	6.8	9.2	4.3	1.9	0.3	1.8

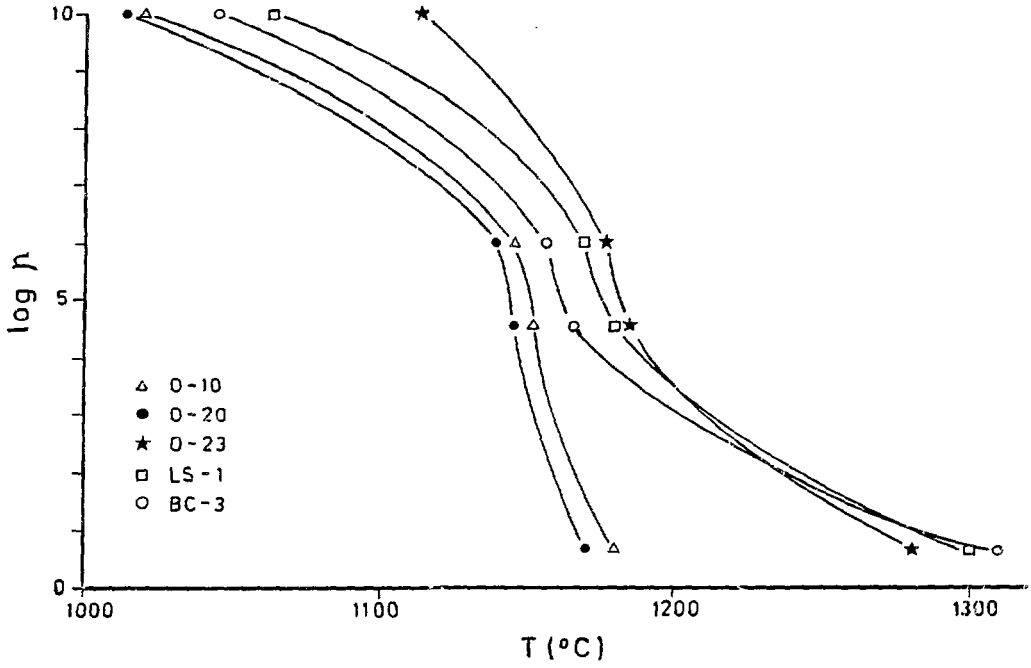

Fig. 4 Viscosity-temperature relations.

not very accurate, it gives a primary information about the reaction of basalt to temperature. Once determined the melting temperature, which is about I,280ºC, the process to obtain glass began through fusion in an electric furnace at I,350ºC in aluminous crucible. Later on the melt was poured on a metalic plate, and put into a furnace at 550ºC to reduce tensions and to avoid the breaking of glass.

Through the differential thermal analysis, we studied the reaction of glass to heat treatment, and the temperature of transformation and crystallization was determined. They are 700ºC, 835ºC and I,035ºC, respectively (fig.5).

To study nuceation we made heat treatment of the glasses at a temperature near that of transformation -and in different times. The temperatures were 680, 700, 720, 740, 760 and 770ºC, and the times were 0, 5, 1, 2, 4, 6 and 8 hours. The samples treated were studied through XRD, SEM and microanalysis through dispersive energies (EDAX).

By means of X-Ray Diffraction we checked the lack of diffraction in the different glasses when obtaining the diagrams in standard conditions.

Afterwards, we were able to make a diagram of the glass of one of the samples by using a lineal detector, and getting the diagram with intervals of 0.02º at a speed of 30 degrees/min. The scanning was repeated and the countings were accumulated during 8 hours. With this method, we could see various clear and defined mineral phases. Thus, it was determined that there was magnetite as the main phase forsterite, and a small quantity of quartz (fig.6). The fact that there is forsterite may be, on the one hand, because of the descomposition of olivine in oxidizing atmosphere:

$$(MgFe)_2SiO_4 \rightarrow Mg_2SiO_4 + SiO_2 + MgSiO_2 + Fe_3O_4$$

The metastable crystallization of SiO_2 when there is forsterite may because of the intense intergrowth in the first stages of the reaction.

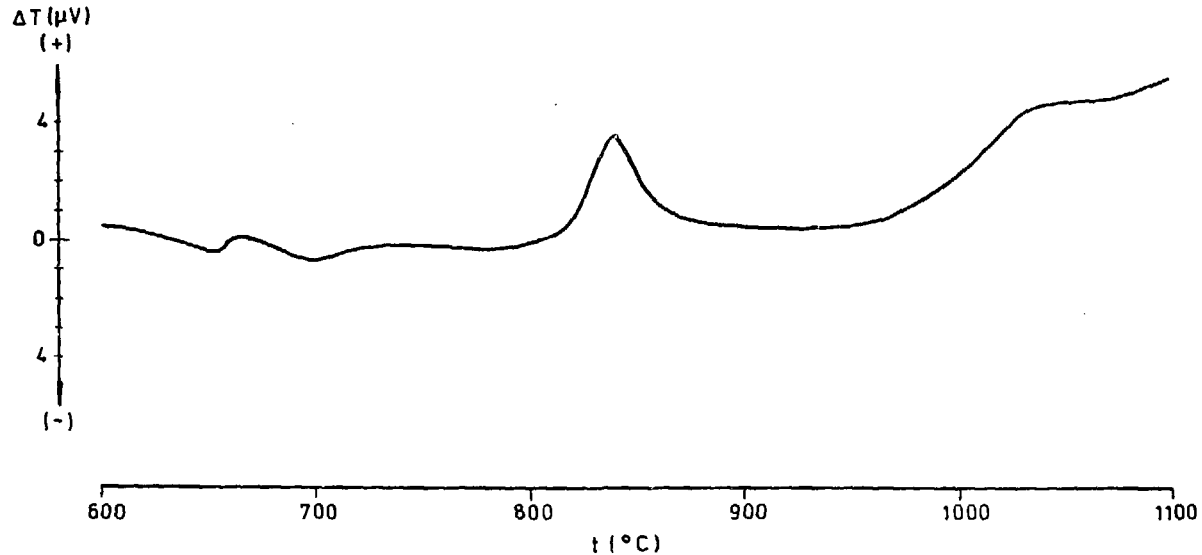

Fig. 5 D.T.A. of basalt glass

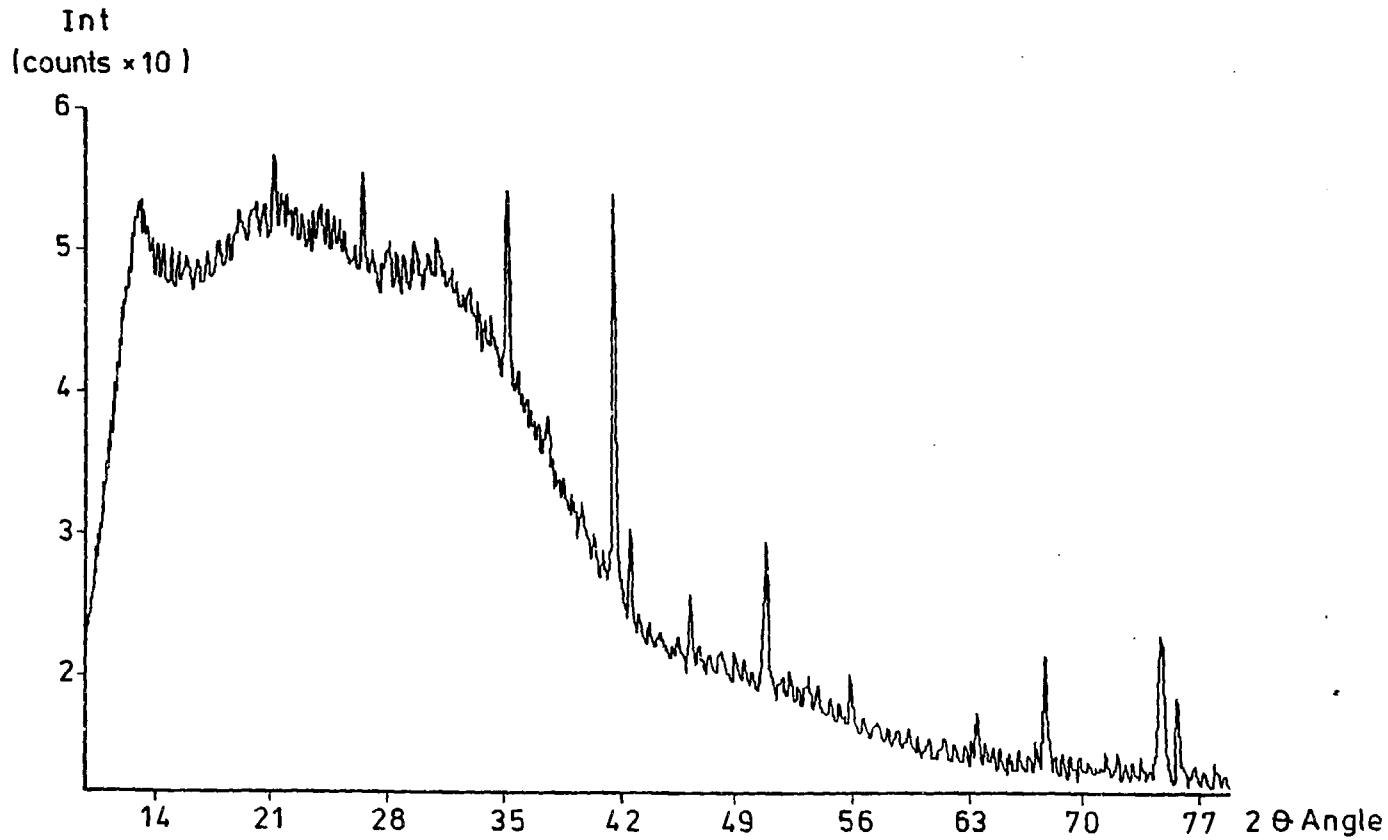

Fig. 6 Diffraction diagram obtained by means of lineal detector (Glass 0-10).

Here, enstatite must have melted incongruently, producing forsterite and liquid, and the phases kept in the melt are fosterite, magnetite and quartz.

On the other hand, if the temperature of liquidus was reached, we could explain the fact that there are fosterite and magnetite because, as Suleemenov et al. see through electron microscopy, in glasses obtained from basalts there is, during the heat treatment at the interval between 685 to 700ºC, a process of differentiation of glass with areas enriched with Fe, with composition similar to magnetite. In later increases of temperature, it is from those areas that magnetite is separated.

Apart from that, the fact that there is forsterite in the original "glass", could be explained starting from the theory of nucleation in silicate melts explained by R.J. Kirkpatrick (1983). In it, it's seen that silicate crystalline phases of less polimeryzed structures usually nucleate in metastable form, instead of stable phases of more polimeryzed structures. Thus, Kirkpatric et al. (1981) see that, in experiences with controlled cooling of melts with diopside compositions, the olivine nucleates sooner than clinopyroxene even if this is the equilibrium stable phase.

In this second assumption, it would not be explained the fact that there is SiO_2, so, it seems that the liquidus has not been reached, although it is also possible that part of the forsterite and magnetite is of new formation.

If we analyze through X-Ray Diffraction the nucleated samples, we see that the first mineral is magnetite; when the temperature rises or the time of treatment is longer, we have pyroxene, and the last phase is felsdpar (fig.7).

If we observe the variation of diffracted intensity through the lines 2.99Å of pyroxene, and the time for the different temperatures of treatment (fig.8), we see that there is a first interval in which the intensity of the formed phase is weak, as

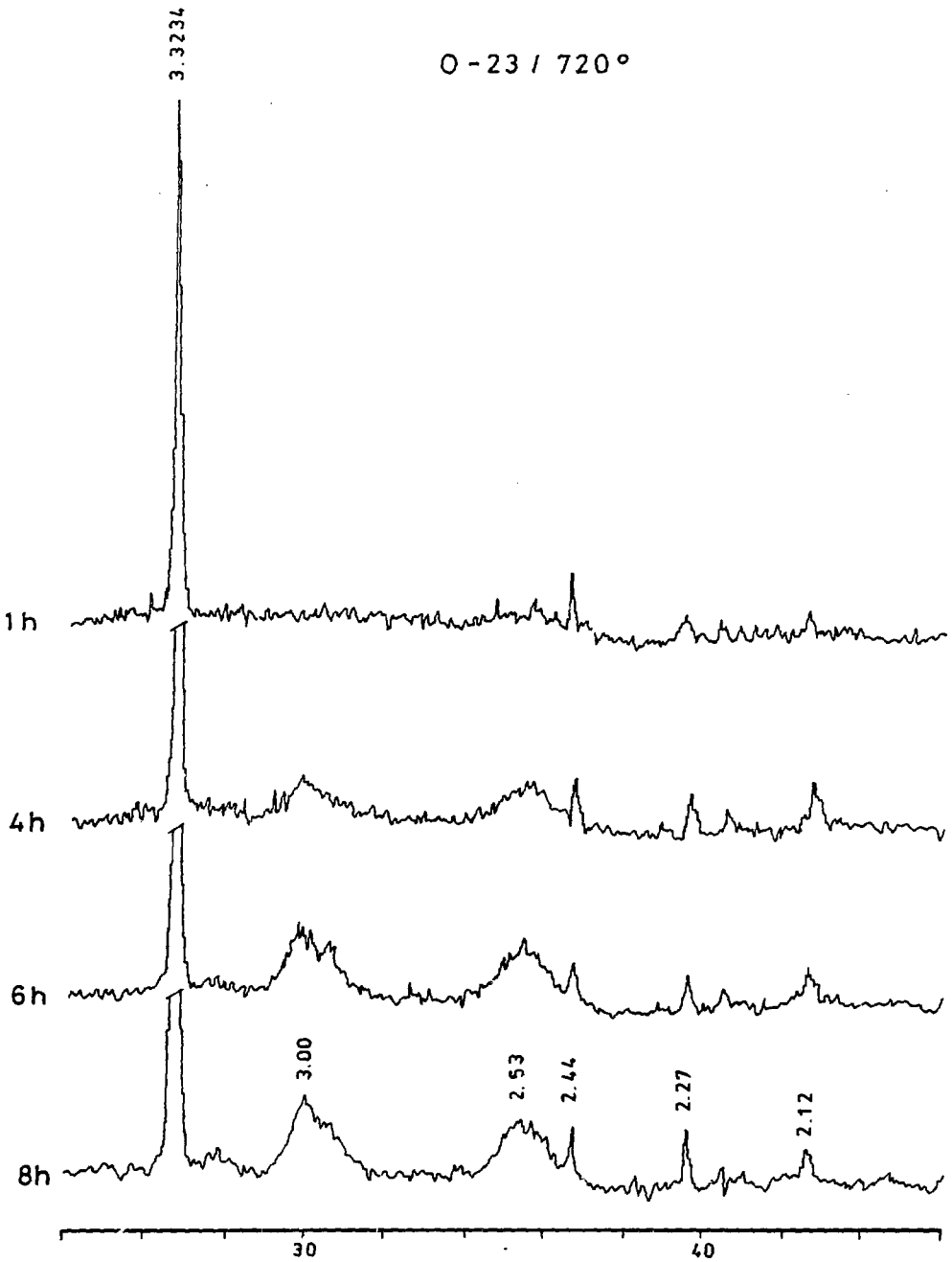

Fig. 7 Evolution of XRD analyses trough the time of treatment.

well as its crystallinity, because the spectrum is flat; a second interval in which there is an increase of intensity with a best definition of peaks. In the last stage, the stage formed has become stabilized again. On the other hand, the time of induction decreases with the rise of temperature of treatment.

The magnetite shows a similar behaviour, however, plagioclase does not increase its intensity with the time of treatement.

If we take the samples nucleated at 720º during 8 hours to the temperature of growth given by the two exothermic in the curve ATD, and they are kept at such temperature during 24 hours, it can be seen that the diagram obtained for the sample treated at 835ºC does not show notable differences in relation to that of the sample nucleated at 720ºC during 8 hours. There is just an increase in the intensity of pyroxene, and a greater crystallization. However, there is not variation in feldspar.

Taking the nucleated sample to the temperature of the second exothermic (1.035ºC), there is an increase in the crystallinity of the phase-minerals and, in addition, there is a very marked increase in feldspar (plagioclase). Fig.9.

Summarizing: At temperatures of nucleation, magnetite is formed in the first place, and once a time of induction is over, the pyroxene grows in a lineal way until it becomes stabilized. Plagioclase, however, the last stage coming at the temperature of nucleation, and that does not increase its intensity with time, does not grow until it is taken to the temperature of the second exothermic.

Before explaining the results obtained through SEM, let us see which is the function of some oxides or nucleating agents in the process of nucleation of glasses.

In works of several authors, it has been observed that the nucleating agents which have a greater influence on the process of nucleation of basalts are TiO_2, P_2O_5 and, above all, Fe^{2+}/Fe^{3+}.

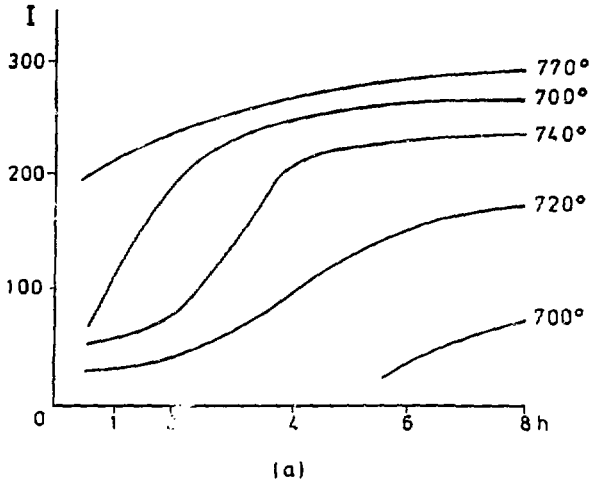

Fig. 8 Diffracted intensity-time of treatment relations for some temperatures. (Intensity of 2.99Å line of pyroxene. Glass 0-23).

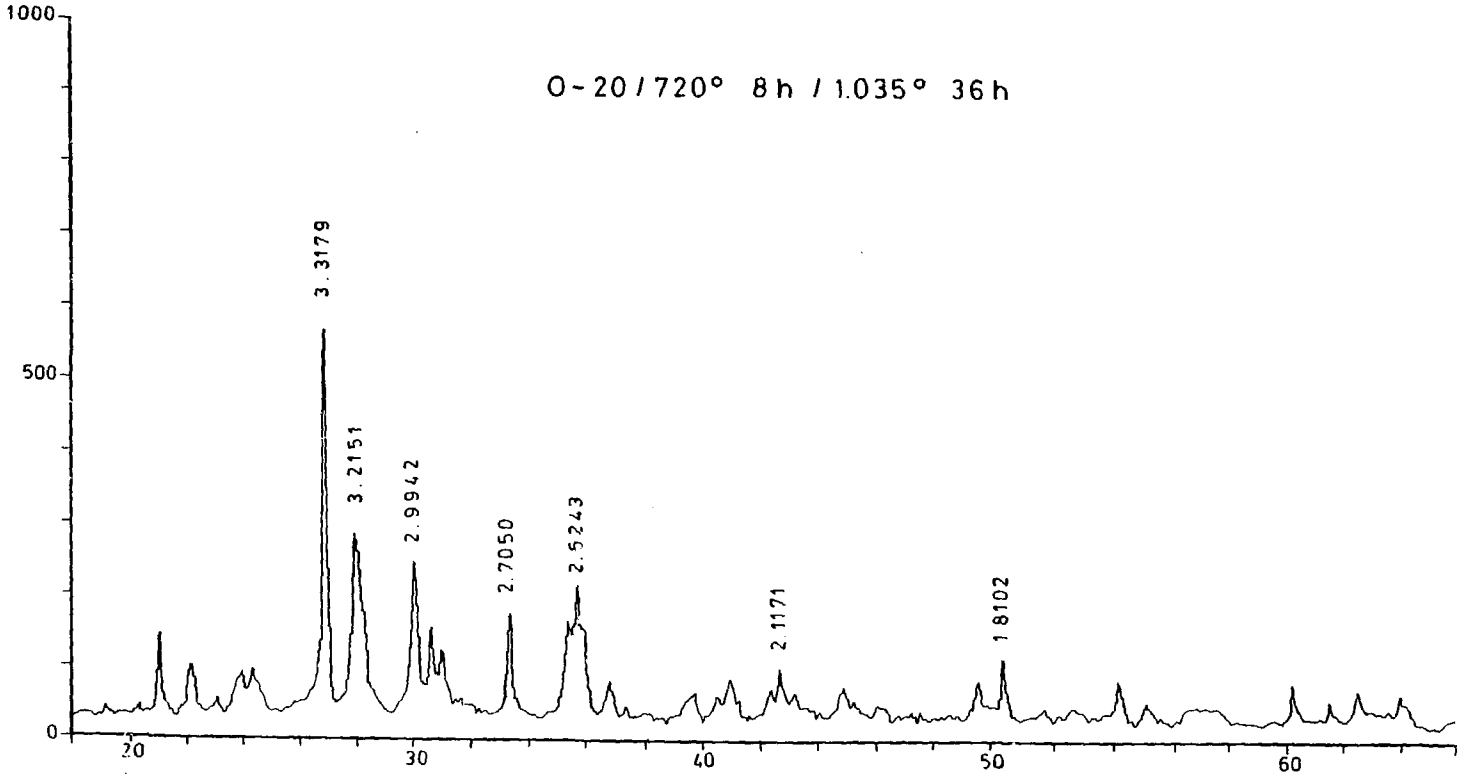

Fig. 9 Diffraction diagram of basalt glass-ceramic obtained from glass O-20.

TiO_2, as it is shown in several works, seems to make easy the nucleation of glasses through the induction of a separation of stages glass-glass. This process of separation of stages is explained by the structural role of titanium. Titanium, in terms of its relation of radious with oxygen, usually has the number of coordination 6, and it is with this octahedral coordination with which it is usually found in different compounds. Anyway, at nigh temperatures, Ti^{4+} can have coordination 4 with oxygen and, in this case, the groups Ti-O will be structurally compatible with Si tetrahedron. During the cooling, ion Ti tends to its coordination of equilibrium. If the struc[illegible] o. high temperature is freezed in the cooling, it becomes unstable at low temperatures and, therefore, a reheating of glass will produce a separation of stages.

Another of the oxids used as nucleating agent is P_2O_5. Ion P^{5+} shows tetrahedric coordination and, therefore, it provides an example of phase-separation due to the different charges between the main ion forming the network Si^{4+} and the ion P^{5+}. As we can see in figures 10, if the bonds P-O were all of then simple bonds, electric neutrality would not be ensured, except in the case that one of the bonds P-O was a double bond. This double bond creates the condition for a separation of stages. It is improbable that phosphorus comes off as phosphorus-pentoxide, but that is possible in combination with an alkaline or earth alkaline oxides.

Small concentrations, above 0.5%, are enough to induce the phase-separation necessary to help nucleation.

This tendency to phase-separation the glasses or melts phosphorus-pentoxide containing is reduced if the glass contains a high proportion of alumina. This reduction can be explained in terms of the roles of P^{5+} and Al^{3+} in the vitreous structure (fig.11). The ion aluminium is in the centre of a tetrahedron AlO_4, which takes part in the vitreous structure forming the network. Because of the changes of Al and O, this unity shows an excess of one negative charge. This charge can be neutralized by the alkaline and

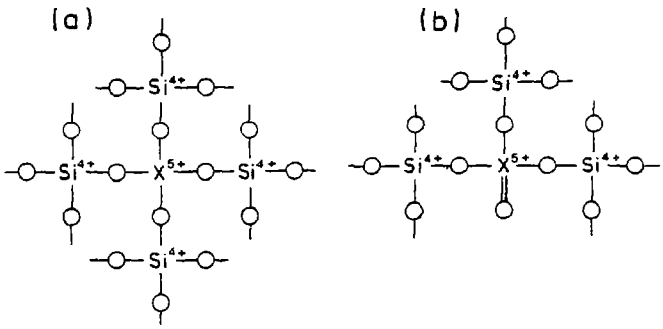

Fig. 10

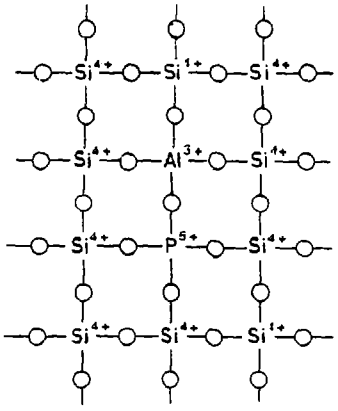

Fig.11

Fig. 10 and 11 Structural roles of P^{5+} and Al^{3+}

earth-alkaline ions. When there is also phosphorus in the glass, this excess of negative charge can be neutralized by linking the tetrahedron of Al to those of phosphorus. Thus, the excess of positive charge associated to the group PO_4 is used to neutralize the excess of negative charge in the group AlO_4.

On the other hand, the radius of the ions Al and P (0.5Å and 0.34Å are such that, when those ions are in the centre of adjacent tetrahedron groups, the total atomic space for those two groups is similar to that of and adjacent pair of groups SiO_4 in which the ion Si^{4+} has a radius of 0.41Å.

As we previously said, the samples have also been observed through SEM and EDAX. To do so, we have polished the samples in the first place, and, then, they have been etched by F_2H_2 at 4% during 30 seconds. The samples treated have been metallized to be observed.

Through microanalysis, we have observed that magnetite has a composition 93.4% Fe, 5.7% and Cr, 0.9% Ti. We have also made the mappings of the glasses of magnetite, and it has been observed that Cr is concentrated in them, while Ti, that can be combined with Fe^{2+} to produce ulvospinel (structurally equivalent to magnetite), is, at first sight, homogeneously distributed in the sample.

If we observe the preparation at 10,000x (fig.12), we see that there is a structure where we can distinguish a separation into two phases, and a matrix with a microestructure difficult to define. If we analyze each phase through EDAX, we see that there is an enrichment of Ti in the separate phases, being very reduced in the matrix 2.9% and 2.6% as opposed to 0.8%. Fe is similar: 14.4% and 13.7% as opposed to 10.6%.

On the other hand, the darkest phase has a strong reduction of Mg as opposed to the clear phase: 2.3% and 9.5% respectively. However, Na shows an opposite reaction, for it is hardly seen in the clear stage while the dark one has a 9%.

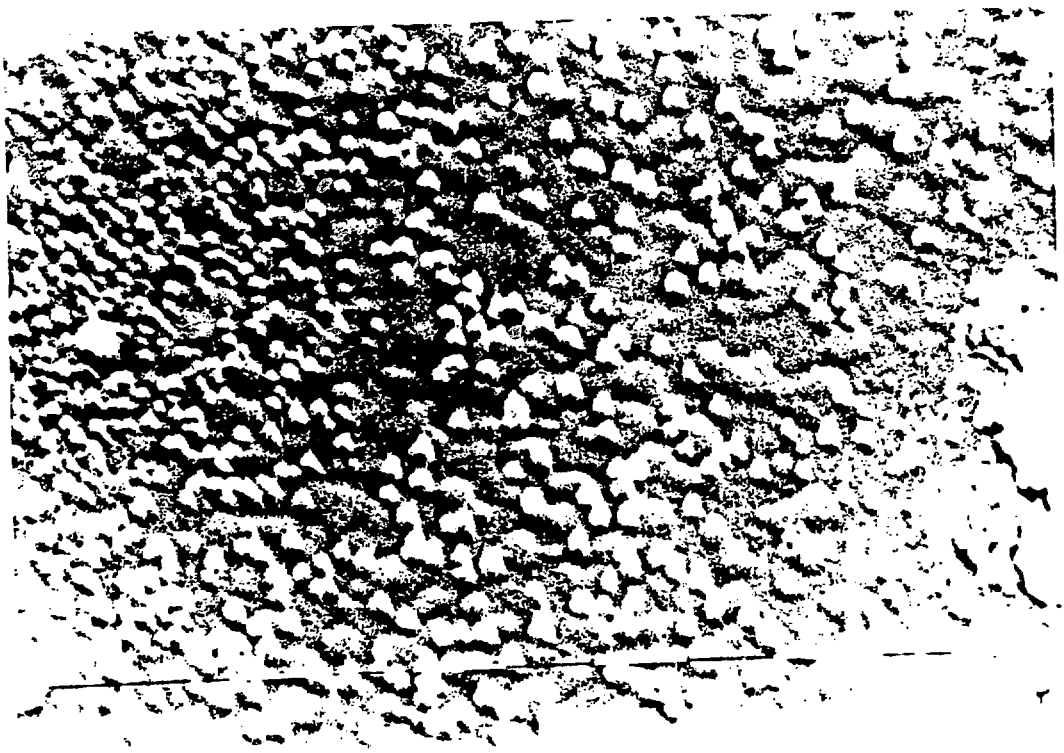

Fig. 12 Basalt glass nucleated at 700°C.

This seems to suggest that the phenomena of nucleation are related to a separation of phases, in which Ti and Fe seem to have a very important role, as well as Mg and Na, in which the clear and dark phases repetively are enriched. (RINCON and DURAN, 1982)

If we pay attention to figures 13 and 14, we see that the size of the nucleus grows with the time of treatment. These photographs correspond to a sample treated at 700ºC during 1 and 2 hours respectively. At the present moment, we are taking photographs (using SEM) of the samples nucleated at different temperatures and during different times. Thus, we shall get information about the kinetics of the nucleation phenomena.

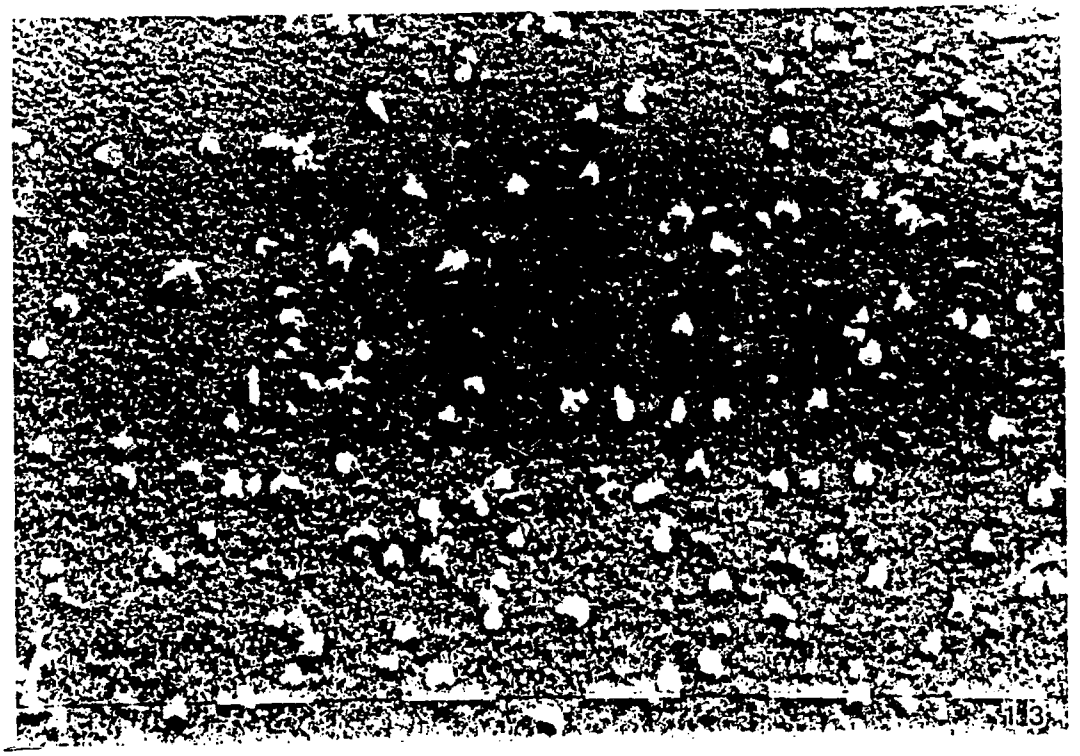

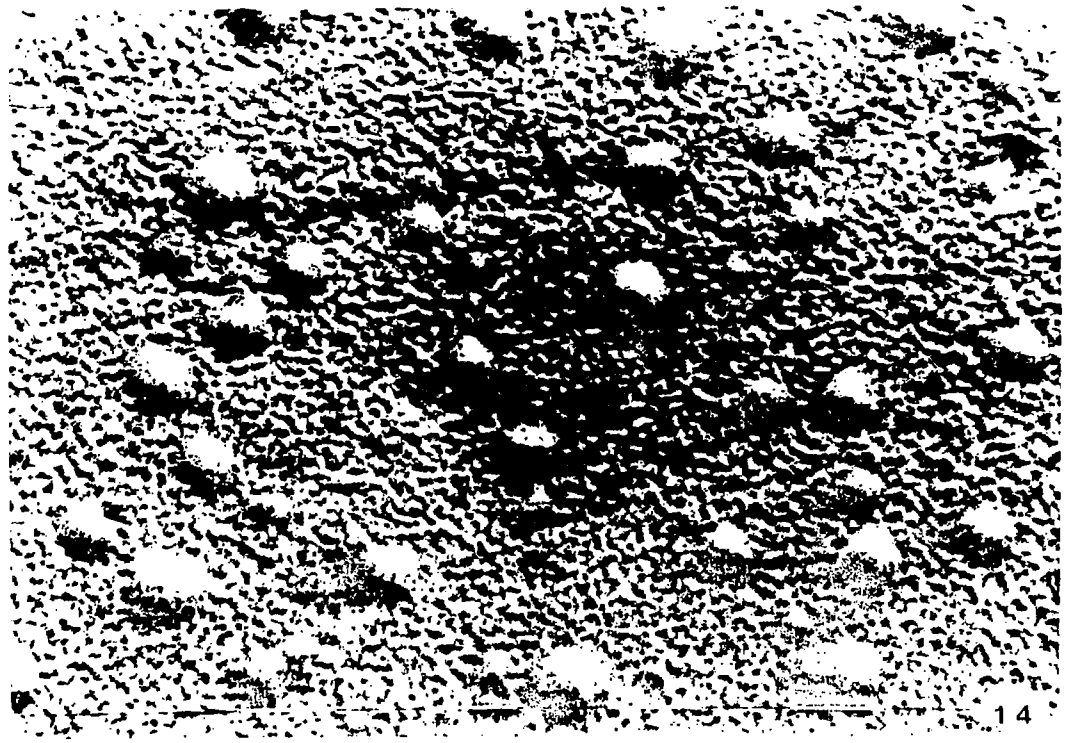

Fig. 13 and 14 Increase of the nucleus size with the time of treatment (700ºC for 1 hour and 700ºC 2 hours respectively).

This seems to suggest that the phenomena of nucleation are related to a separation of phases, in which Ti and Fe seem to have a very important role, as well as Mg and Na, in which the clear and dark phases repetively are enriched.

If we pay attention to figures 13 and 14, we see that the size of the nucleus grows with the time of treatment. These photographs correspond to a sample treated at 700ºC during 1 and 2 hours respectively. At the present moment, we are taking photographs (using SEM) of the samples nucleated at different temperatures and during different times. Thus, we shall get information about the kinetics of the nucleation phenomena.

BIBLIOGRAFIA

BAHL,D.,et. al. "Basalt glass-ceramics" . J.Australian Cer. Soc., vol. 10, 1974

BANDYOPADHAYAY, A.K., et. al. "Nucleation and crystallization studies of a basalt glass-ceramics by small-angle neutron scattering" J.Mat.Sci., vol.18, 1983

BEALL, G.H. and RITTLER, H.L. "Basalt glass-ceramic" Cer. Bull., vol.55, nº 6, 1976

GARCIA VERDUCH, A. "Materiales obtenidos a partir de rocas y escorias fundidas". Conferencia dictada en las Jornadas Científicas sobre Cerámica y Vidrio. Oviedo, 23-25 Junio, 1980

QUERALT, I. et al. "Mineralogía y composición química de basaltos españoles en relación con sus posibles aplicaciones vitrocerámicas". I Congreso Iberoamericano de Cerámica, Vidrio y Refractarios. Soc. Esp. Cer. y Vid., vol.II, 1983

THOMASSIN, J.M. and TOURAY, J.C. "Early stages of reaction between basaltic glass and water X-Ray Photoelectron and scanning electron microscopy data" Bull. Min., vol. 102, nº 5-6, 1978

ABRAMYAN, A.W. et al. "Rovno basalts as raw materials for making stone-ceramic products by slip-casting" Glass and Ceramics, vol. 24, nº 8, 1967

WATANABE, T.A. and ZANOTTO, E.D. "Obtençao de vitro ceramicos e estudo comparativo de resistencia a compressao em relaçao a materiais sinterizados" Cerámica, vol. 25, nº 115, 1979

DIKEN, G.M. et al. "Devitrifiable systems for construction ceramics" Sil. Ind. vol. 2, 1976

DVORKIN, L.I. and GALUSHKO, I.K. "Fritted basalt enamel" Sprech. Keram. Glas. Em. Sil., vol 105, nº 21, 1972

CHICK, L.A. et al. "Basalt glass-ceramics for the immobilization of transuranic nuclear waste" Cer. Bull. vol. 62, nº 4, 1983

NEWKIRK, H.W. et al. "Synroc thecnology for immobilizing U.S. Defense Waste. Cer. Bull, vol. 61, nº 5, 1982

SASAKI, N. et al. "Alteration of glass and crystalline ceramic nuclear waste forms under hydrothermal conditions" Ceramic Bull., vol. 62, nº 6, 1982

MORSE, S.A. "Basalt and phase diagrams" Ed. Springer-Verlag, New York, 1980

RINCON, J.Mª, DURAN, A. Separación de Fases en Vidrios. El Sistema Na_2O-B_2O_3-SiO_2. Ed. Soc.Esp.Ceram.Vidr., Madrid, 1982.

Formation of NZP Ceramics for the Immobilization of Radionuclides

Jaime Alamo
Departamento de Química Inorgánica. Universidad de Valencia

ABSTRACT

The problem of Radioactive Waste Management is briefly outlined from the crystal chemical point of view. Some alternatives (glasses and ceramics) are compared and the synthesis and properties of NZP ceramics (*) are reviewed.

RESUMEN

Se expone brevemente el problema de la inmobilización de los radioisotopos presentes en los residuos nucleares desde el punto de vista cristaloquímico. Se comparan algunas alternativas (vidrios o cerámicas) y se resume la síntesis y propiedades de las cerámicas NZP (*).

THE RAD-WASTE PROBLEM

The technological development of nuclear power yields a radioactive waste that although, it is a small quantity considering the whole process and its benefits, its ultimate disposal is concerning scientists, politicians and the society.

The highest level waste is related to the spent nuclear fuel rods and their reprocessing, whose dangerousness and time of activity does not allow to be kept in the biosphere.

The isolation and inmobilization requires a security system based on superposed multibarriers that slow down (several centuries, o millenium) the degradation imposed by the geological agents (1). The first is a geological barrier, like a salt dome or an old mine or a deep bore hole. The last is a chemical barrier acting at an atomic level and it is called radiophase. Between other barriers account for the possible weakness of sensible parts or for geological actions that could happen. Among others they are the sintering or peletization of radiophases, their coating and/or in-

(*) The experimental work on NZP ceramics has been carried out by the author & al. at the Materials Research Laboratory. The Pennsylvania State University USA.

clusion in a corrosion resistant metallic matrix, and sealing in a stainless-steel storage canister.

The global solution requires the participation of scientists from multidisciplinary fields in addition to politicians and the society.

Here the main concern is the inner chemical barrier: the radiophase. Its election will have to quantify the following properties.

1. Thermodynamical stability including i) leachability in a large range of pressure, temperature and pH and ii) long-time metamictic degradation.

2. Ability to keep in the structure all or most of the radionuclides.

3. Compatibility with each other radiophase to be tailored for the system during processing and storing.

4. Waste loading, i.e. the maximum percentage of high level waste (HLW) in the radiophase.

5. Simplicity of the process, ease of control and ability to neutralize composition fluctuations in the HLW.

The crystal chemical problem for a phase candidate to radiophase is to be able to arrange at the same time all the radionuclides present in the HLW (2). The composition in a typical commercial radioactive waste is presented in table 1., and the coordination number required by the oxhydric polyhedra around the different radionuclides is showed in Fig. 1. To this variety of coordination requirement, fluctuations in the HLW composition and the radioactive evolutions like $^{137}Cs \longrightarrow Ba$ or $^{90}Sr \longrightarrow Zr$ add more difficulties to the adjustment of chemical formula. It is a real crystal chemical challenge to arrange all the radionuclides in a radiophase.

Other practical problem is that only a few Laboratories are equipped to handle the radioactive waste. Normal labs have to operate with non-radioactive simulated waste (3).

ALTERNATIVE RADIOPHASE CANDIDATES

Several kind of resistant materials are being tested as candidates to radiophase, like cements, glasses, glassceramics and crystalline ceramics. Our purpose is just to compare their stability in relation to their structure.

Table 1. Purex Process Waste PW-4b composition.

Element	atomic %
Zr	13,7
Mo	12,2
Nd	9,2
Ru	7,6
Cs	7,0
Ce	6,6
Fe	6,4
Pd	4,1
Sr	3,5
Ba	3,5
P	3,2
La	3,1
Pr	3,0
Tc	2,8
Sm	1,8
Y	1,8
Te	1,5
Cr	1,5
U	1,4
Rh	1,3
Rb	1,3
Np	1,1
--	---
--	---
--	---

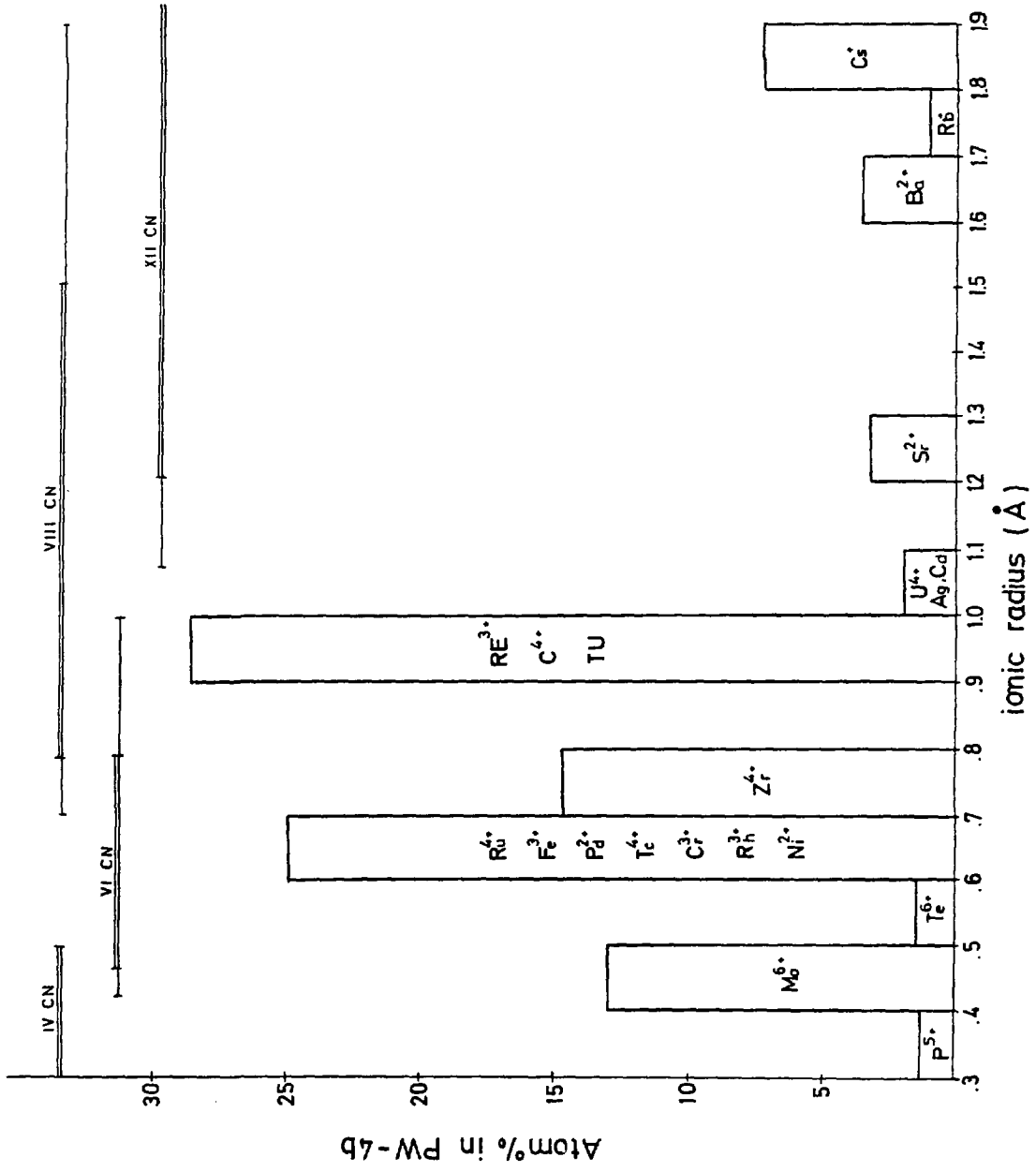

Fig. 1.- Atom distribution and coordination number preferred by the cations typically present in comercial radioactive wastes.

Cements are the less resistant phases and their leachability varies highly with the pH of water. Although special cements may play some role in the multibarrier system, or in medium or low level systems, they are not good candidates to radiophase.

Borosilicate glasses show excellent characteristics and have been largely tested but they are thermodynamically metastable and devitrification after a long time may destroy their radiophasic characteristics. Fig. 2 shows the dependence of free energy versus temperature for different materials. Also metamictic degradation have to be considered for phases including radionuclides and so, the evolution of free energy after centuries. Unfortunately, only a few minerals can provide information about the inalterability of their structures against the metamictic process, and extrapolation to other phases, glasses or crystals, is very difficult.

At the other hand crystalline phases are normally more restrictive about chemical stoichiometry, because of coordination and electrical balance requirements. So many phases will appear in the treated waste. The two systems best studied are not an exception. In the aluminosilicate formulation (4) appear pollucite, apatite, monazite, schelite, sodalite, fluorite, zirconia, RuO_2 and spinel. And in the SYNROC formulation (5) appear fluorites, perovskites, rutile, hollandite, magnetoplumbites and alloys.

The problem in these cases is to tailor the chemical additives to keep the radionuclides in the different radiophases forming a dense sintered ceramic body. Each of the phases have to be studied and tested separately. Then the compatibility relationships and atom partition between them have to establish the laws of a perfect tailoring of the chemical additives necessary to reach the equilibrium with the best performing radiophases. The formation of an extra phase with a higher leachability would lower down the global protection reached by the multiphasic system.

THE NZP STRUCTURE

$NaZr_2(PO_4)_3$ is the prototype of a singular structure for especial ceramic applications (6-12). This structure, NZP-type, can arrange a large variety of elements different in size and charge, so that it is also a candidate to radiophase, which provides a single phase waste form by itself at moderate loading rates. But getting this requires a good knowledge of the NZP structure and the crystallochemical affinity of the radio elements for the different atomic sites.

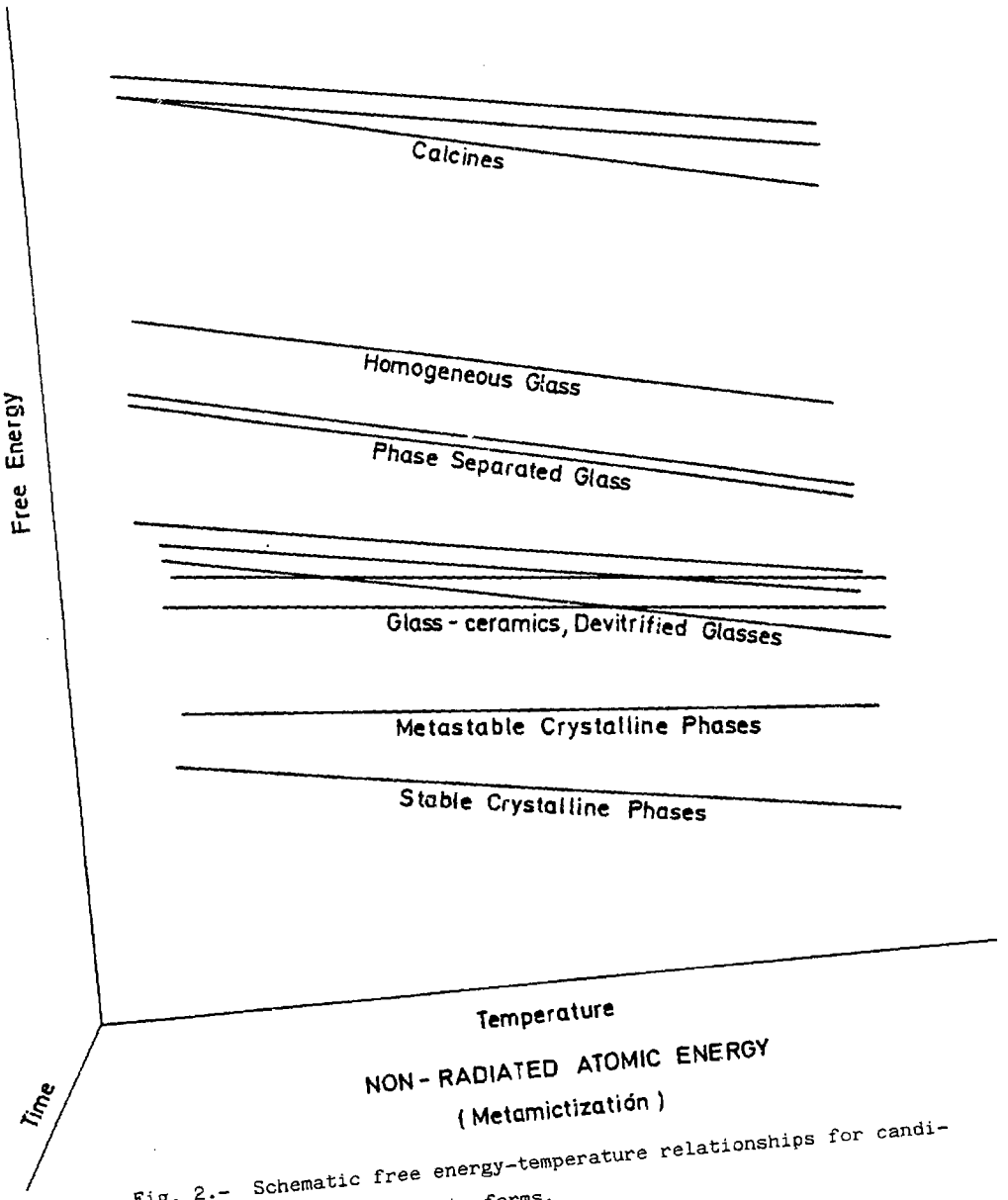

Fig. 2.- Schematic free energy-temperature relationships for candidate nuclear waste forms.

The NZP structure have a skeleton built up by ZrO_6 octahedra and PO_4 tetrahedra (Fig. 3-4) sharing corners, so that strong bonds maintain a high stability and low leachability in the phase. Zr can be substituted by other tetravalent or not to big trivalent cations maintaining the skeleton stability. At the same time these polyhedra can rotate around their vertices modifying the size of all the holes present in the skeleton.

In the structure (symetry $R\bar{3}c$), the $(Zr_2(PO_4)_3)^{-1}$ skeleton has three important kind of holes: (M_1) the octahedral one (symetry $\bar{3}$) filled with Na in the prototype. The prismatic one (symetry 32) formed by the three phosphates, that is normally vacant but plays an important role in the skeleton flexibility (10). And three more (M_2) octahedral ones (symetry 1) that are irregular and can be filled when necessary to keep the electrobalance.

The formula for the skeleton, including the holes, can be written in the following way $(M_1)_1(M_2)_3A_2(XO_4)_3$ where the holes can be filled more or less according to the nature of all the present atoms. Examples like $ZrNb(PO_4)_3$ or $Zr_2(PO_4)_2(SO_4)$ show that the holes can be empty. In compounds like $Ca_{1/2}Zr_2(PO_4)_3$ or $Zr_{1/4}Zr_2(PO_4)_3$ M_1 the holes are partially filled. In the compound $Na_4Zr_2(SiO_4)_3$ all they are filled. M_1 holes are occupied normally by mono and divalent ions, but tri and tetravalent ions can be also present in small proportion. M_2 holes are good for small monovalent ions, and for appropriate compositions they connect themselves building up a three dimensional network of channels (10) that allow a good ionic conductivity (6). The A site in the skeleton can be occupied by trivalent to pentavalent ions, and the X site by tetra to hexavalent ions.

NZP CERAMIC RADIOPHASES

The experimental work done around this phase for the immobilization of radionuclides (11-12) fall into three categories. First, synthesis of NZP phases with simple stoichiometry in order to determine their stability and leachbility, specially $CsZr_2(PO_4)_3$ and $SrZr_4(PO_4)_6$ as $^{137,134}Cs$ and ^{90}Sr radionuclides are of most interest in being immobilized in the radio waste forms.

Second, synthesis of NZP solid solutions of previous compounds with divalent and trivalent ions in order to establish the ion partition into different sites in the structure. And third, synthesis of NZP phases following crystal chemical models based on the ion partition and starting from simulated PW-4b waste and appropiate chemical additives at loading proportions in the range 10-30%..

All the synthesis were made by sol-gel techniques, i.e., mixing in solution with nitrates and occasionally organic precursors, gelling, desiccating to a xerogel and then heating in alumina crucibles to a series of temperatures (up to 1100ºC). Powders were characterized by x-ray diffractometry and SEM-EDX techniques. Hydrothermal runs were performed at 200º and 300ºC on fired powders.

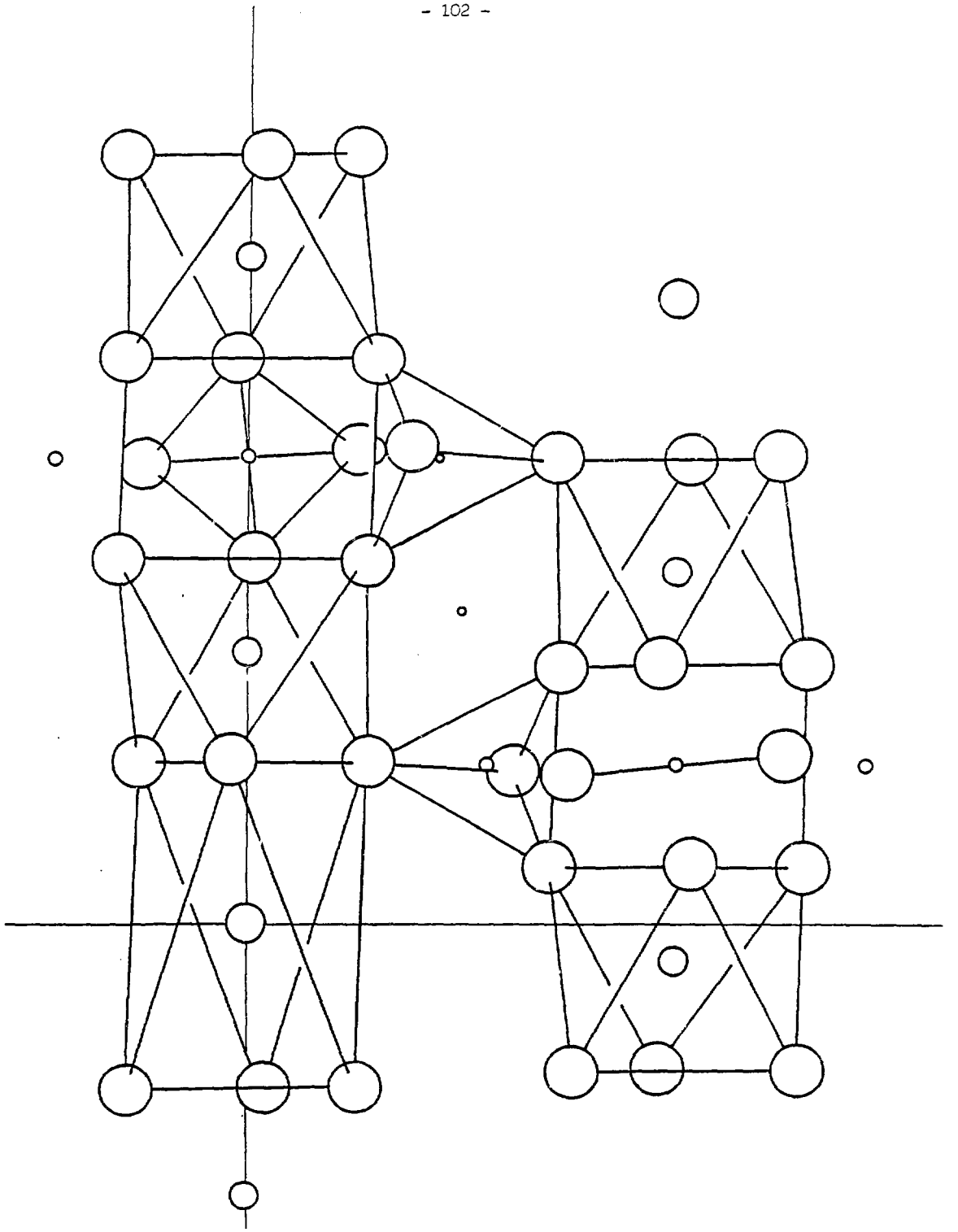

Fig. 3.- Partial projection of the $NaZr_2(PO_4)_3$ structure in the **b** direction.

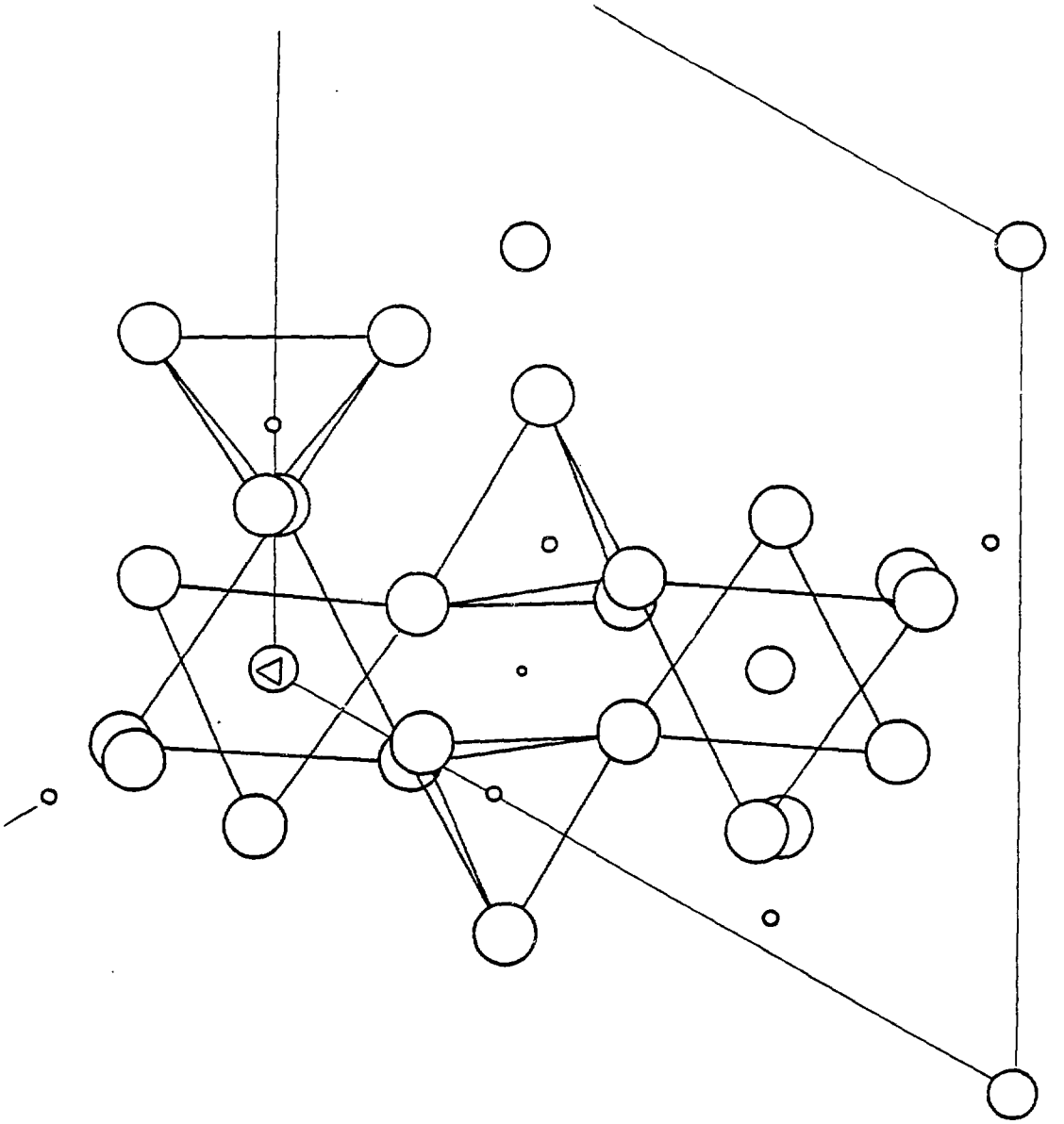

Fig. 4.- Projection of the same polyhedra as in Fig.3, now in the c direction.

The leach behavior and refractoriness of simple composition NZP phases were very satisfactory. Solid solution phases showed that all radionuclides could be trapped into the NZP host, but the alternative sites did not appear to be cleary differentiated by the atom partition and several models were tried with a simulated PW-4b waste. Fig. 5 summarizes the phase formation plotting against the P/Na and Zr/Na molar ratio of the additives.

Ceramic waste forms with a loading 10% in weight were single phase with occasionally trace amounts of monazite. With 20% loading it gives somewhat higher amounts of monazite. Fortunately for the whole process, the monazite phase is a uniquely resistant ceramic phase specially able of immobilizing actinides and totally compatibl with the NZP phases.

DISCUSSION

Single phase waste forms were privative of glasses until this discovering. Crystallinity offers an additional long time stability to that offered by glasses. Ultimate waste forms must be the best, the more resistant at the same time they have easy controlled preparation. In this sense the remarkable features of the NZP ceramic waste forms are threefold:

(1) The enormous compositional flexibility with the highly desirable monazite as the only second phase.

(2) The low firing temperatures needed for generating good crystallinity in these materials.

(3) The potencial use of the sol-gel and hence filter-bed technology based on the thoroughly studied Zr-P-O gels.

The experimental work done on NZP ceramics as radiophase is not enough to evaluate all its properties since the complexity of this ceramic application requires the best knowledge of how every radionuclide is controlled to a fixing site in the structure and so it is immobilized. But these preliminary results show that NZP radiophases are a serious candidate for nuclear waste immobilization.

REFERENCES

1. G.J. McCarthy, "High-level Waste Ceramics. Materials considerations, Process Simulation and Product Characterization.", Nuclear Technology 32 (1977), 1, 92-105.

2. Rustum Roy, "Rational Molecular Engineering of Ceramic Materials", J.Am. Ceram. Soc. 60 (1977), 7-8, 350-363.

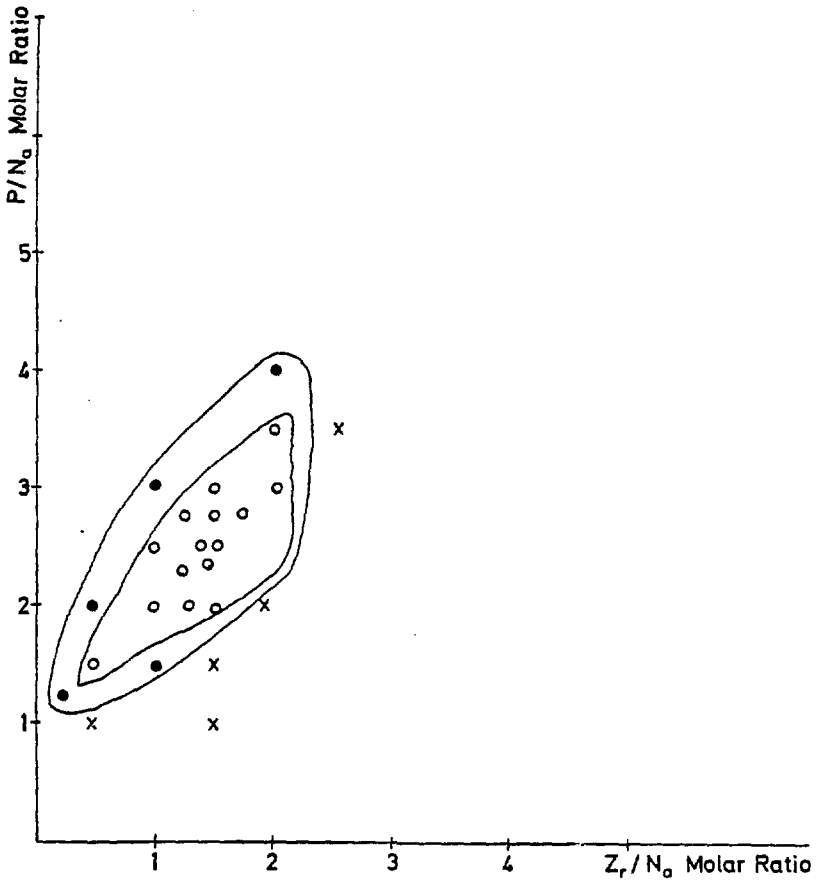

Fig. 5.- Map of NZP radiophases showing a single phase (o) and two phases (•) regions. Outside, ZrP_2O_7 and unknown phases are also present. Atom ratio refer to chemical added to the simulated waste.

3. G.J. McCarthy and M.T. Davidson,"Ceramic Nuclear Waste Forms: I, Crystal Chemistry and Phase Formation", Am. Ceram. Soc. Bull. 54 (1975), 782-786.

4. G.J. McCarthy, "Crystal Chemistry and Phase Formation in Developmental Supercalcines", report # COO-2510-14. The Pennsylvania State University report.

5. T.J. White, R.L. Segall, and P.S. Turner, "Radwaste Immobilization by Structural Modification-the Crystallochemical Properties of SYNROC, a Titanate Ceramic", Angew. Chem. Int. Ed. Engl. 24 (1985), 5, 357-365.

6. H.Y. Hong "Fast ion conduction in the $Na_{1+x}Zr_2Si_xP_{3-x}O_{12}$ system" Mater. Res. Bull. 11 (1976), 173.

7. J. Alamo and R. Roy, "New Ultra Low Expansion Ceramics in the system Na_2O-ZrO_2-P_2O_5-SiO_2" J. Amer. Ceram. Soc. 63 (1984), C78.

8. R. Roy,D.K. Agrawal, J. Alamo and R.A. Roy, "CTP): A new structural family of near-zero expansion ceramics." Mater. Res. Bull. 17 (1984), 471.

9. J. Alamo and R. Roy, "Crystalline phases in the ZrO_2-P_2O_5 system." J.Amer. Ceram. Soc. 63 (1984), C80.

10. J. Alamo and R. Roy, "Crystal chemistry of the $NaZr_2(PO_4)_3$, NZP or CTP, structure family" J. Materials Sciencie 21 (1986), 444-450.

11. R. Roy, E.R. Vance and J. Alamo, "(NZP) a new radiophase for ceramic nuclear waste forms" Mater. Res. Bull. 17 (1981), 585-589.

12. R. Roy, L. Yang, J. Alamo and E. R. Vance "A single phase (NZP) ceramic radioactive waste form", in "Proceedings of Scientific Basis for nuclear Waste Management VI", edited by D.G. Brookins (Plenum, New York, 1983) p.15

HEAT TRANSFER IN VITRIFIED RADIOACTIVE WASTE

Palancar, M.C., Luis, M.A., Luis, P.,
Aragón, J.M. and Montero*, M.A.

Dpt. Fisicoquímica de los Procesos Industriales (Chemical Reaction Engineering). Facultad de Ciencias Químicas. Universidad Complutense de Madrid. 28040Madrid (Spain).

(*)Consejo de Seguridad Nuclear

ABSTRACT

An experimental method for measuring the thermal conductivity and convection coefficient of borosilicate glass cylinders, containing a simulated high level radioactive waste, is described. A simulation of the thermal behaviour of matrices of solidified waste during the cooling in air, water and a geological repository has been done.

The experimental values of the thermal conductivity are ranging from 0.267 to 0.591 w/m K, for matrices with simulated waste contents of 10 to 40% (the waste is simulated by no radioactive isotopes). The convection coefficient for air/cylinders under the operating conditions used is 116 w/m^2 K.

The simulated operation of cooling in air shows that about 1-2 days are enough to cool a solidified waste cylinder 0.6 m diameter from 900 to 400ºC. The cooling under water from 400 to near 80ºC is faster than in air, but sharp temperature gradients within the matrices could be expected. The simulation of geological repositories lead to some criteria of arranging the matrices for avoiding undesirable high temperature points.

1.- INTRODUCTION

The management of spent nuclear fuel leads commonly to solid materials of high radioactive level which should be stored in geological repositories. As these materials are heat sources, several thermal phenomena should be considered for designing this type of storage. The studies of such phenomena are mainly related to the measure and prediction of temperature distributions; the knowledge of this is necessary to predict the future behaviour of the waste and its sourroundings. For longtime prediction purposes, it is necessary to elaborate appropiated thermal models which, in first approximation, are based in general principles such as the equation of the energy conservation and kinetic laws of heat transfer. The most realistic models should take into account that the presence of radioactive compounds will complicate the thermal behaviour of the system due to two phenomena which are difficult to correlate with time: the heat generation, that is depending of the nature of the radionuclides present in the waste at each time, and the changes of estructural properties of the waste (and maybe its sourroundings) which, at its turn, could drastically affect the thermal and physicochemical properties of the system.

From the above considerations it is clear that it is not easy to develop rigurous and complete models for the prediction of temperature distributions in radioactive waste and repositories. Such models should be made from the conjunction of several submodels and empirical correlations. Thus, it should be necessary to have information about the effects of the temperature and radiations on properties such as thermal conductivity, emisivity, density, specific heat, convection coefficients and mechanical and structural characteristics. This information gives a way to introduce the corresponding change of variables and parameters in the general equations of the model.

In this paper a technique for measuring the thermal conductivity and the convection coefficient of cylindrical matrices of solidified radioactive wastes is described. It is also presented an approach to the elaboration of predictive models of temperature distribution in matrices and geological repositories; the proposed model is relatively simplified since that it is supposed all the parameters constant with time and temperature and a simple law to describe the heat generation of the radioactive waste.

2.- EXPERIMENTAL DETERMINATION OF THERMAL PARAMETERS

The measurement of thermal parameters is based in the principles cited in the previous paragraph. The heat balance for a volume element V is:

Net output heat flowrate from V	=	Net generated heat within V	-	Accumulated heat in V	(1)

This general balance will take the form of a particular mathematical expression when the characteristics of the volume element and its contiguous ones as well as the heat transfer mechanisms were known. The method and operating conditions for the measurement of a given thermal property should be selected in such a manner that the mathematical expressions and the experimental procedure were as simple as possible.

2.1.- Thermal conductivity

The mechanism of heat transfer between volume elements of a solid is the conduction. The expression 1 takes the form:

$$(K \nabla T) = \rho c_p \frac{\partial T}{\partial t} \qquad (2)$$

for an isotropic solid without internal heat generation and cylindrical symmetry. The solution of eq. 2, obtained by the procedure described by JODRA (1), under the boundary conditions shown in Table I is:

$$T-T_a = \frac{(T_o - T_a).a^2}{R} \cdot \sum_{i=1}^{\infty} \sum_{j=1}^{\infty} \frac{J_o(\zeta_i.r)}{J_o(\zeta_i.R).(\zeta_i^2 + a^2)} \cdot \frac{\cos(\eta_j . z)}{\left[L_z.(\eta_j^2 + a^2) + a\right].\cos(\eta_j . L_z)} \exp(-\alpha.c^2.t) \quad (3)$$

where ζ_i , η_j are the roots of:

$$a \cdot J_o(\zeta_i.R) = \zeta_i \cdot J_1(\zeta_i \cdot R)$$

$$\eta_j \cdot tg(\eta_j.L_z) = a$$

and

$$c^2 = \zeta_i^2 + \eta_j^2$$

Eq. 3 is used to calculate the thermal conductivity of the solid from one temperature datum.

TABLE I.- Boundary conditions of eq. 2

Time	B. Conditions
≤ 0	The whole solid at uniform temperature, T_o
>0	The solid is sourrounded by a fluid of uniform temperature, T_a Solid/fluid heat transfer is by convection.

The experimental equipment necessary to have the boundary conditions of Table I and to measure the temperature of the solid is relatively simple: a furnace to heat the solid sample, a device providing a current of air at constant temperature and flowrate, termocouples and temperature recorder.

2.2.- Convection coefficient

The convection is the heat transfer mechanism between a solid and a flowing fluid when radiative heat transfer is negligible. As the convection coefficient do not depend on the intrisic solid characteristics, a solid of the same shape and size and at the same surface temperature than the original sample could be used for the measurement of such a coefficient. If the solid used for this measurement is of high conductivity we may suppose no temperature gradients inside it; therefore, the eq.1 takes the form:

$$q = \rho V \; c_p \; \frac{d T}{d \tau} = h \; S \; (T - T_a) \qquad (4)$$

where q is the heat tranferred from the solid to the fluid per unit of time; q is referred to the whole cylinder since that in this case the volume element of eq. 1 can be extended to the cylinder volume due to the temperature uniformity in it. The integration of eq. 4 gives:

$$\ln \; \frac{T_o - T_a}{T - T_a} = \frac{h \, S}{\rho V \; c_p} \, t \qquad (5)$$

Eq. 5 is used to calculate the convection coefficient, h, from cooling curves and given the values of S, ρ, V and c_p. The experimental equipment for this type of measurements could be the same described in the above paragraph.

2.3.- Results for vitrified radioactive waste

The thermal conductivity and convection coefficient of cylinders of vitrified radioactive waste (1.8 cm diameter, 6 cm height) have been found by the methods previously decribed. The material is a borosilicate glass added with a mixture of several metal oxides which simulates a typical LWR high level waste (considering security phactors, no radioactive isotopes have been used). The composition and preparation procedure of this glass can be found in PALANCAR(2).

Cylinders of pure copper of the same size than the glass ones were designed for the measurement of the convection coefficient.

The temperature measurement is made by means of thermocouples (cromel-alumel), which were disposed in the cylinders in such a manner that contact resistences were minimized; more details about this technique can be seen in LUIS(3).

In Table II the thermal conductivity of five samples are shown. For the operating conditions of cooling (the same for all the cylinders) the convection coefficient was 116 w/m^2 K. All the experimental values of thermal conductivity and convection coefficient are valids for temperature range of 25-250ºC.

TABLE II.- Thermal conductivity

waste (%)	10	15	20	30	40
K (w/m K)	0.267	0.331	0.407	0.591	0.523

3.- SIMULATION OF THERMAL BEHAVIOURS

The thermal behaviour of cylindrical matrices of glass solidified radioactive waste (waste contents: 10, 20, 30%) has been simulated for three different sceneries: a) cooling in air, b) cooling under water and c) cooling in a geological repository. The simulation gives temperature distributions in the matrices at any time. In the case c the temperature distributions in the geological material are also calculated. The mathematics of the method involve the resolution of eq.2 which, in this case, has an extra term which account for the heat generation of the radioactive waste. The particular boundary conditions will be given in the next paragraphs.

Cylindrical matrices 0.6 m diameter and 2.4 m height of borosilicate glass with waste contents ranging from 10 to 30% have been supposed for the simulation. It has also been supposed that the heat generation of the waste follows the expression proposed by GOLDSTEIN(4):

$$q \quad (w/m^3 waste) = 7.314\ 10^3 \exp(-0.024\ t') \qquad (6)$$

were t' is the age of the waste in years.

3.1.- Cooling in air

This simulation is a simplified explanation of the thermal behaviour of vitrified waste after the process of solidification, MENDEL(5). The boundary condition of eq. 2 is imposed by the supposition of heat transfer by convection on the external surface of cylinders. The integration gives the following expression for the temperature profile in the cylinders:

$$T-T_a = \frac{4\,a^2(T_o-T_a)}{R} \sum_{i=1}^{\infty} \sum_{j=1}^{\infty} \frac{J_o(\xi_i r)}{(\xi_i^2 + a^2) J_o(\xi_i R)} \cdot$$

$$\frac{\cos(n_j z)\; e^{-\alpha \sigma^2 t}}{\left[L_z (n_j^2 + a^2) + a\right] \cos(n_j L_z)} + \frac{4\,a\,\alpha\,V}{R\,K}\, q_c\, e^{-K'(t'-t)}$$

$$\sum_{i=1}^{\infty} \sum_{j=1}^{\infty} \frac{\xi_i J_o(\xi_i r)}{(\xi_i^2 + a^2)\left[J_o(\xi_i R)\right]^2} \frac{\cos(n_j z) J_i(\xi_i R)\left(e^{-K't'} - e^{-\alpha \sigma^2 t}\right)}{\left[\cos(n_j L_z)\right]\left[L_z(n_j^2 + a^2) + a\right]\left[\sigma^2 \alpha - K'\right]} \qquad (7)$$

A detailed description of the procedure followed for obtaining eq.7 is given in PALANCAR(6). In Table III the time required to cool three different matrices is shown. As can be observed, the cooling time is about 1-2 days; this time increases with the waste contents in the matrix.

TABLE III.- Time required to reach 400ºC at the center of the matrix.

waste(%)	time (h)
10	25
20	36
30	41

3.2.- Cooling under water

This is a typical step in the management of solidified waste, GOLDSTEIN(4). We have simulated the cooling of matrices, initially at 400ºC, during its stay in a pool of water, which is supposed to be at 80ºC and with enough agitation to maintain the superficial temperature of cylinders at 80ºC.

With these conditions, the mathematical model leads to the following expression, PALANCAR(6), which gives the temperature distribution in the cylinder:

$$(T - T_a) = \frac{4(T_o - T_a)}{L_z R} \sum_{i=1}^{\infty} \sum_{n=o}^{\infty} \frac{J_o(\xi_i r)}{J_1(\xi_i R)^2} \frac{\operatorname{sen}(\eta_n z)}{\xi_i \eta_n}$$

$$\left[1 - \cos(\eta_n L_z) J_1(\xi_i R)\, e^{-\alpha \sigma^2 t}\right] +$$

$$\frac{2 Q_o\, e^{-K'(t'-t)} V\alpha \left[e^{-K't} - e^{-\alpha \sigma^2 t}\right]}{K\left[\sigma^2 \alpha - K'\right]} \qquad (8)$$

Eq. 8 has been used to calculate a lot of temperature values at different radial and axial coordinates in the cylinder at times from 1 to 16 hours. The most significative results are related with the formation of strong internal temperature gradients. For example, after one hour of cooling, there are temperature differences (center-external surface of the cylinder) of 46C, 495 and 560ºC for waste contents of 10, 20 and 30%, respectively. These differences, greater than the initial one (320ºC), could indicate that during a period of time the generation of heat within the matrix is very high and an accumulation of heat is produced.

3.3.- Cooling in a geological repository

The cooling of solidified waste matrices during their storage in a geological repository has been simulated. A granitic formation at initial temperature of 25ºC has been supposed. The calculation of temperature distributions is made in

two steps, which involves two systems of increasing complexity:

a) repository with only one matrix
b) repository with an arrangement of n matrices in the same horizontal level.

The thermal behaviour of the case a is treated by considering that it is a system of two solids, one being a source of heat (the matrix) and the other a homogeneous solid without heat generation in which the first solid is enclosed. Negligible contact resistences and heat transfer by only conduction are supposed. Thus, the equations involved are: eq. 2 for the granitic material and eq. 2 plus a heat generation term for the matrix. A detailed description of the resolution of this model can be found in PALANCAR(6).

The temperature distributions obtained for the case a are used to calculate, by the principle of superposition, the distributions of case b.

Two different types of arrangements have been considered in case b : triangular and in line; the influences of the number of matrices and distances between them have been studied for both arrangements. The prediction of the highest temeperature in the system could be the most remarkable information that has been obtained by this simulation. This temperature has been represented in fig. 1 for some arrangements and distances between matrices. As it could be easily expected, the maxima of temperature are found in the center of the matrices located in the central zone of the arrangement.

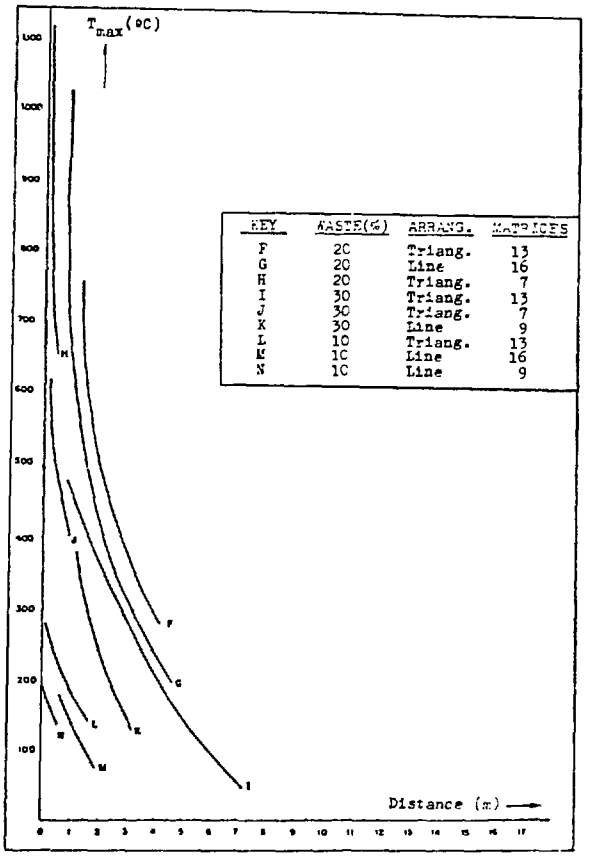

KEY	WASTE(%)	ARRANG.	MATRICES
F	20	Triang.	13
G	20	Line	16
H	20	Triang.	7
I	30	Triang.	13
J	30	Triang.	7
K	30	Line	9
L	10	Triang.	13
M	10	Line	16
N	10	Line	9

Fig. 1.- Maximum temperature at the center of matrices.

NOTATION

a = Heat transfer coefficient/conductivity of solid, h/k

cp = Specific heat of solid, (J. Kg^{-1} . K^{-1})

h = Heat transfer coefficient in the film around the solid, (W. m^{-2}. K^{-1})

J_0, J_1 = Bessel functions

K = Thermal conductivity of solid, (W. m^{-1}. K^{-1})

L_z = Height of solid cylinder/2, (m)

Q_o = waste heat generation at age zero, (w/m^3).

r = Radial distance from center of solid, (m)

R = Radius of solid, (m)

S = Surface area of solid, (m)

T = Temperature of solid at position (r,z,t), (K)

T_a = Bulk fluid temperature, (K)

T_o = Initid temperature of solid, (K)

t' = age of the waste (s, yr)

t = Time, (s)

V = Volume of solid, (m^3)

z = Longitudinal distance from medium plain of solid, (m).

α = Thermal diffusivity, (m^2. s^{-1})

$\eta_n = (2\ n + 1)\ / L_z$; n being a whole number.(m^{-1})

η_j = see eq. 3

ξ_i = see eq. 3

REFERENCES

1.- Jodra, L.G., Luis, P., Aragón, J.M. and Palancar, M.C.; Anal. Quim. 80 (1), 94 (1984).

2.- Palancar, M.C. and Aragón, J.M.; "Estudio de conductividades térmicas y caracterización de materiales cerámicos utilizados para la solidificación de productos irradiados". Report 1982 to Instituto de Estudios Nucleares, JEN. Madrid.

3.- Luis, M.A.; "Preparación y caracterización de vidrios de borosilicato para la inmovilización de residuos radiactivos de alto nivel". Trabajo de Licenciatura, Univ. Complutense de Madrid, Facultad de Ciencias Químicas, 1982.

4.- Goldstein, S.O. and Quignet, N.; "Etude de la diffusion de la chaleur dans un dépot de déchets THA en formation geologique granitique". Communication at 2nd French-Russian Seminar. Fontenay-aux-Roses, France. June 23-28, 1980.

5.- Mendel, J.E. et al.; "Annual report on the characterization of high level wastes glasses". BNWL 2252-UC-70. Richland (Pacific Northwest Lab.), Washington 1977.

6.- Palancar, M.C. and Aragón, J.M.; "Inmovilización de residuos radiactivos en vidrios y modelos térmicos de almacenamiento definitivo". Report 1983 to Instituto de Estudios Nucleares, JEN. Madrid.

CHEMICAL DURABILITY OF SILICOBORATE GLASSES

Rodríguez, M.A.; Nieto, M.I.; Rubio, J; Fernández, A; Oteo, J.L.
Instituto de Cerámica y Vidrio, CSIC

ABSTRACT.-

A general view of the durability in silicoborate glasses is presented with more enphasis on the etching factors (chemical composition, lattice structure, pH...) the techniques used for this study and the experimental results. Likewise, the research presently developed in this area at the Instituto de Cerámica y Vidrio, CSIC, is related to the applications. Future research in this field is also mentioned.

RESUMEN.-

Se presenta en esta conferencia una panorámica general sobre la atacabilidad química de los vidrios silicobóricos haciendo hincapié en los factores que influyen en el proceso de ataque (composición química, estructura reticular, pH del medio, etc...), las técnicas empleadas para su estudio y los resultados obtenidos, ya sea producto de las revisiones bibliográficas o de la investigación propia. Asímismo, se especifican las lineas en las que se encuentran las investigaciones del grupo de trabajo y aplicación de los resultados obtenidos, para finalmente mencionar las futuras lineas de actuación del equipo.

1.- INTRODUCTION

As it is well known, the physicochemical knowledge of the glass surface is highly critical, in order to study the different problems of interaction glass-environnement or glass-water solutions.

In the recent years it has been possible to carry out research in this field thanks to the surface techniques recently developed (1,2). However, it is worth point out that all these techniques are not adequate to study the leaching of glasses; thus ,for example, the Reflection IR Spectroscopy can provide valuable information, but only in perfectly polished surfaces. Therefore, in this case the surface roughness disables the use of the RIR Spectros-

copy.

Other methods used in less extension provide good information on the surface, like the absorption methods (3,4) which can determine the following two parameters:

- The specific surface and the existence or lack of porosity
- The absorption isostheric heats with organic absorbates.

As a result of the application of these methods it has been shown that glass surface composition is completely different of - the bulk composition (1,2,5). These difference are the consequence of the glass processing, as well as of the interaction of the glass with the environment.

I.1. Effect of the solution pH and the etching time.-

Generally, it is assumed that glasses with silica formator - react with water solutions according to:

a) Desalkalinization reactions, which take place at pH < 9 and controlled by ionic interchange mechanisms between the glass alkali ions and the H^+ of solution, where the diffusion is controlled by a time square root law.
b) SiO_2-lattice solution reactions, which take place by breaking of the Si-O-Si bonds in the interface solution-glass. These reactions dominate at pH > 9 and are kinetically controlled by a linear dependence with reaction time (7,8).

These general ideas can be acepted for every glass although for those with more than one formator, as in the case of borosilicate ones, it is necessary to prevent the existence of special characteristics.

I.2. Effect of the glass composition.-

In general, the glasses with high content of modifiers are resistent to the lattice dissolution processes (pH > 9) and the glasses with high content of formators are resistent to desalkalinization processes.

The increasing alkali content enhances the etching by water - solutions, being more helpfulthose glasses with alkali having a - higher diffusion coefficient. In the case of glasses with more than one alkali (mixed alkali glasses), the corrosion rate decreases - compared with glasses containing one alkali oxide (1,5).

It is necessary to point out thar SiO_2 substitution by Al_2O_3 in a silica glass involves the $[AlO_4]$ groups formation reducing the leaching rate of alkali ions, and the transition of the desalkalinization processes to the lattice dissolution is carried out at a pH higher than 9 (1). However, when the $Al_2O_3/R_2O \approx 1$, the Al^{3+} ion operates as modifier and the acid leaching increases.

I.3. Effect of the SA/V ratio.-

Recent experiments performed by El Shamy and col (9) have demonstrated that the reaction velocity increases when the ratio :

Surface area of etched glass/etching solution Volume is higher. This variation is not proportional in all cases so that the etching process is greatly increases if powder glass is used in spite of large surfaces. The powder glass produces concentration domains originating local increases of the SA/V ratio (1).

I.4. Effect of the temperature.-

The etching process is a kinetic process (10) which can be expressed is an Arrhenius equation; therefore, a hight increase of temperature gives rise to an enhancemente of the reaction velocity. However, the data are not extrapolated at any temperature, since the temperature is very high, not only the etching process is accelerated, but the mechanism changes as it was demonstrated by Clark and Hench (5).

I.5. Effect of the glass morphology.-

The glass-in-glass or liquid phase-separation in boroslicate glasses is an important phenomenon which can affect the chemical durability. This phase separation appears in a composition designed inside the miscibility gap or it is due to thermal treatments that promote the phase-separation (11). It is evident that etching magnitude depends strongly on the borosilicate glass microstructure; thus, with a continuous borate matrix easily leached the resulting glass generates some porosity.

II. STUDY OF REACTIONS BETWEEN BOROSILICATE GLASSES AND WATER SOLUTIONS.-

The following surface analysis methods have been used to study the etching processes:

- Spectroscopic methods. Transmission IR Spectroscopy due to the difficulties of the Reflexion IR Spectroscopy on roughness surfaces.
- Absorption methods. Specific surface determination and absorption isothermes.
- Microscopy. Transmission and scanning electron microscopy. The former one for checking the existence of phase separation and the latter one for following of the process.

These methods are complemented by the analytical data from the etching solution.

II. 1. pHmetrics determinations.-

In our experiments the leaching process has been followed by pH determinations, having observed a hard decreasing of the protons concentration in the leaching solution in the first steps of the reaction. This reaction can be due to the ionic exchange with alkalis or to the proton retention on the glass surface. As it can be observed in Fig. 1 the pH jump is greater when initial pH of etching solution is higher, being maximum when distilled water is employed.

In order to chek the reason for this phenomenon, the concentration increase of Na^+ ions in the etching solution has been determined simultaneously, by using a selective electrode of sodium. As it is shown in Fig. 2, the pH variation is not related to the slow increase of the Na^+ concentration in the etching solution. This effect seems to demonstrate that an electroabsoption of H^+ exists in good agreement with other authors (12,13).

II.2. IR Spectroscopy.-

Traditionally the IR Spectroscopy has not been widely used on the study of the chemical durability of glasses. This is due to the intrinsic difficulties with glass samples, such as high extintion coefficients, bands overlapping, etc... In the case of borosilicate glass as mixed lattice glasses the number of papers is too low.

The published papers have been developed in two defined lines: on the one hand, the study of "water" addition to the lattice (middle and nearest IR) and on the other hand, the following of the glass structure evolution as a consequence of chemical etching.

With respect to the study of hydroxil bands, the Scholze and

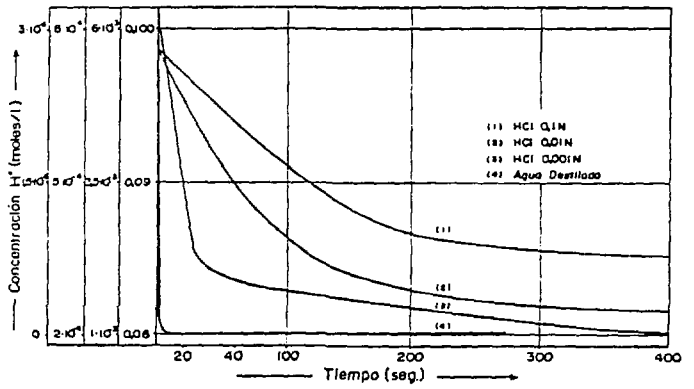

Fig. 1.- Variation of the H^+ concentration versus the etching time of a borosilicate glass.

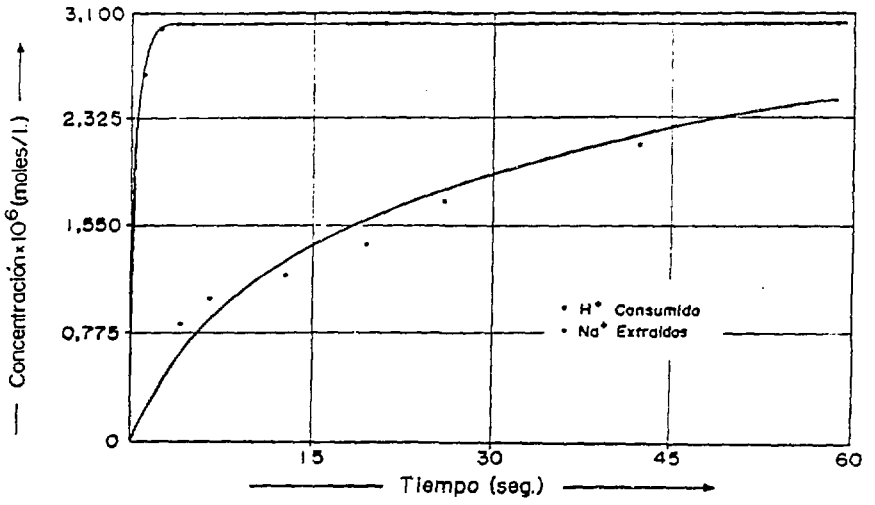

Fig. 2.- Variation of the H^+ concentration used and the leached Na^+ versus the etching time of a borosilicate glass.

col. papers (14,15) must be mentioned performing the spectra by - thin foil, analyzing the bands to 3450 and 1630 cm^{-1} corresponding to the O-H stress and the H-O-H strain, distinguishing between - both OH species (free OH and bonded OH by hydrogen bridge) which appear overlapped at 3400 cm^{-1}.

The Nogami and Tomozawa paper (16) report the calculation of - the water diffusion coefficient in the glass when it is submitted to a water stream saturated atmosphere.

Hench and col. (17) obtained important results with respect to the glass structure evolution during etching by using the Reflexion IR Spectroscopy. The change of the bands frequencies with consecutive etching has been followed by the Reflexion IR Spectroscopy. First of all, they studied (18) the qualitative evolution of the IR Spectrum with the increasing etching time without quantification due to the roughness changes altering the optical properties. The spectra evolution on sodocalcium glasses shows a great increment - of the band intensity at 1080 cm^{-1} (Si-O-Si stress) and the decreasing one at 960 cm^{-1} (Si-O not bridging stress). Likewise, they - observed a displacement in function of alkali percentage exsolved by leaching (19).

The necessity of using glass powder for controlling the SA/V ratio and later study of the specific surface evolution, directed our research to the transmission IR Spectroscopy. In this way, the effect of roughness change disappears form the analyzed surface, - although other problems will arise.

The high extintion coefficients of the structural bands makes it necessary to use small quantities of sample. For this reason, - the KBr dilution methods has been used implying complications of - the quantitative analysis due to the different optical characteristics of KBr+glass powder samples. So, it has been necessary to use internal standards. Otherwise, accumulations of data and later differentiation of water contained in KBr have been carried out.

In order to solve the overlappings several deconvolutions have been performed from the theoretical components by using the integrated intensity as a quantification parameter. Following this procedure a semiquantitative study has been carried out on the structural evolution of leached borosilicate glass (20). In Fig. 3 the evolution of different hydroxils present in a glass E submitted at several -

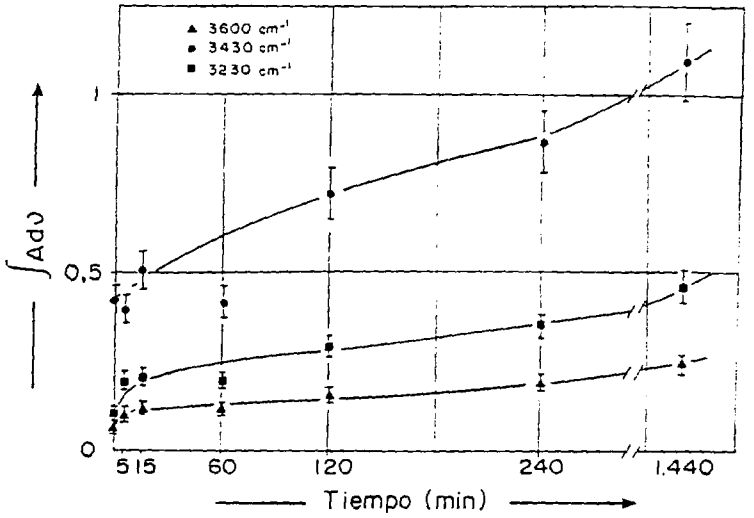

Fig. 3.- Variation of the integrated intensity of O-H vibrations of the E-glass versus the etching time.
de ataque.

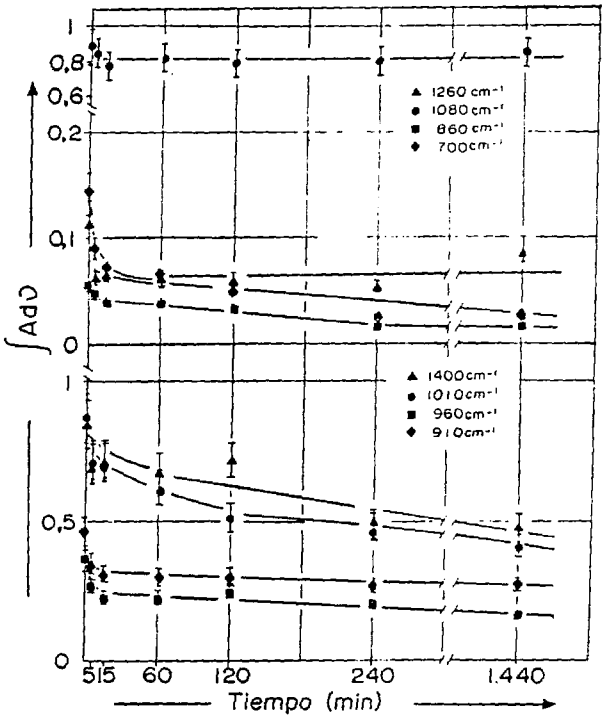

Fig. 4.- Evolution of the integrated intensities of the structural vibrations of the E-glass versus the etching time.

etching times with a solution of pH=1 can be observed.

In Fig. 4 the evolution of different structural bands of glass E is collected during the acid leaching. It is worth pointing out the constancy of the 1080 cm^{-1} band. Likewise, a decrease of the integrated intensity of boron bands is observed. This decrease is not equal in all bands, which involves a different extraction of these groups.

II.3. Determination of the absoption isothermes.-

The determination of the absoption isotheric heats is the most conventional method to know the reactions between glasses and water (21). These heats can be determined by Calorimetry or Chromatography. In the case of materials with low values of specific surface, like glasses, the Chromatography gives the more adequate results because at enable us to calculate heats from small quantity of absorbed products (22). For this reason a dynamic method for the obtention of absorption isothermes has been updated by connecting a micro computer giving rise to 300 point in a short time (23).

The isostheric heat is the thermodynamic magnitude which describes from a quantitative point of view the interactions between the absorbent (glass) and the absorbate (gas or vapour). From the absorption isothermes the entropie and the Gibbs free energy corresponding to the absorption process can be calculated and thus, it is possible to obtain know on the thermodynamics of surface.

With more alaborated calculations performed on the isothermes the energy distribution on the solid surface for a determined absorbate can be obtained which gives an idea of the energy range for absorption depending on the chemical nature of the solid and absorbate (24).

All these mentioned parameters give different values depending on the chemical composition of the surface. Therefore, the control of these parameters during the etching can provide a good information over the surface changes. In Figs. 5 and 6 the isothermes -- corresponding to n-hexane absorption in a sodium borosilicate glass are represented the same as the variation of isotheric heats calculated from the isothermes respectively. In Fig. 7 the variation of the retention volume of n-hexane over a E glass is shown in function

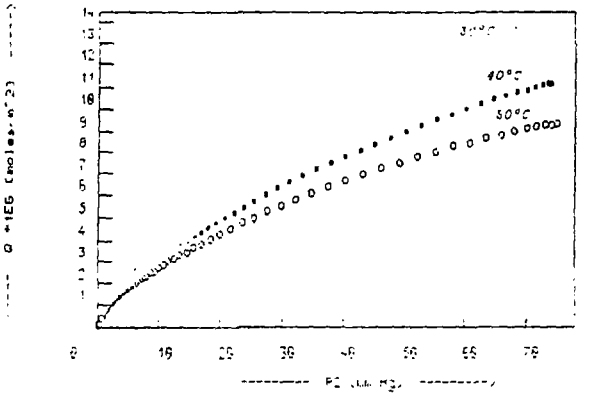

Fig. 5.- Absorption isothermes of n-hexane on a sodium borosilicate glass.

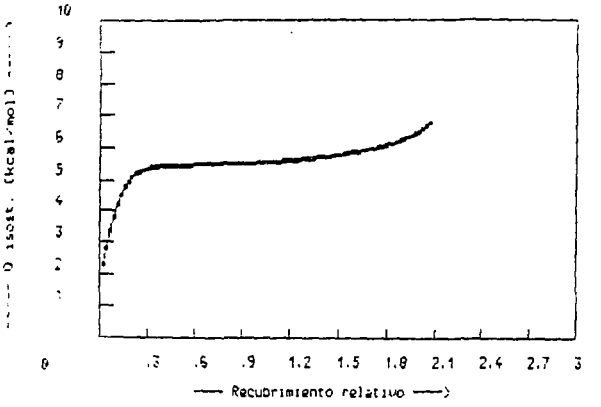

Fig. 6.- Variation of the absorption isostheric heat of n-hexane on a borosilicate glass versus the coating degree.

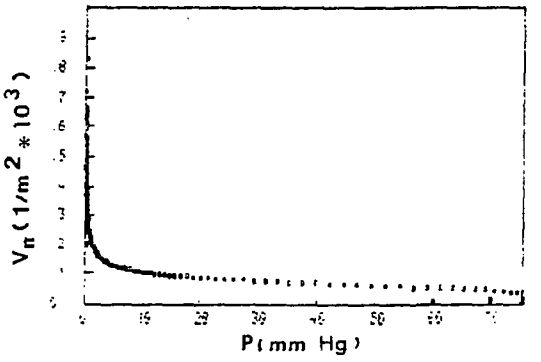

Fig. 7.- Variation of the retention volume of n-hexane on a E-glass.

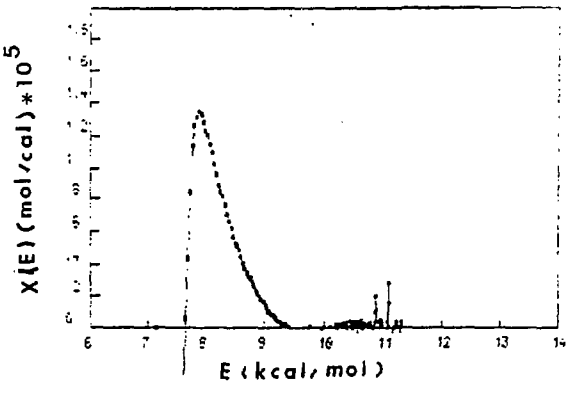

Fig. 8.- Variation of the energy distribution for the n-hexane-E--glass isotherme.

of the n-hexane pressure. Fig. 8 shows the energy distribution function obtained from the retention volume for the system n-hexane - E glass.

In Fig. 9 the variation of the isostheric heats on several borosilicate glasses versus the modifier oxide content in order to point out the effect of the surface composition is shown. In Fig.10 the variation of the isostheric heat versus the acid etching time (pH=1) for the E glass is represented. The observation of these curves gives us information on the strong surface changes produced as a consequence of leaching and their dependence with the etching conditions (temperature and time).

II. 4. Microstructure characterization by SEM and S_S determination.-

The specific surface of the starting material is a critical parameter which must be known in order to determine the SA/V ratio and therefore the etching magnitude. However, glasses show a very little SA and its determination by conventional methods is not possible. For this reason, a new measurement method was updated in our laboratory based in the dynamic method of nitrogen absorption developed by Nelsen and Eggertsen (25) which enables us to determine accurately (3% error) specific surfaces lower than 1 m^2/gr.

Fig. 11 represents the evolution of the specific surface of a E-glass submitted at different etchings (pH=1) versus the etching time (26). As it can be observed the specific surface increases -- continuously modifiying the etching conditions obtaining values at higher temperatures of 100 m^2/gr. This tremendous increase could be due to the grain destruction but granulometry shows that there are no variations. On the other hand, the nitrogen absorption-desorption measurements enable us to observe that nitrogen exolved is lower when absorption-desorption cycles increase, as it can be seen in Fig. 12. When the sample is degasified a second time the first value of the nitrogen desorbed is obtained according to degasification temperature an time.

From the former observations it can be concluded that a porosity generated by the etching process exist. Since the SEM observations do not show surface alterations it was concluded that the generated porosity is too little and can only be detected by nitrogen absorption as a very sensitive method.

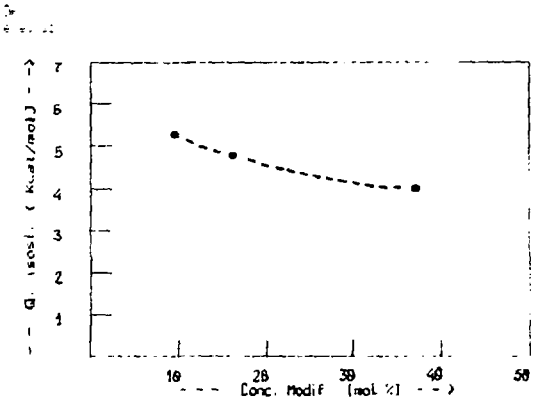

Fig. 9.- Variation of the isostheric heats of n-hexane on several borosilicate glasses versus the content of modifier.

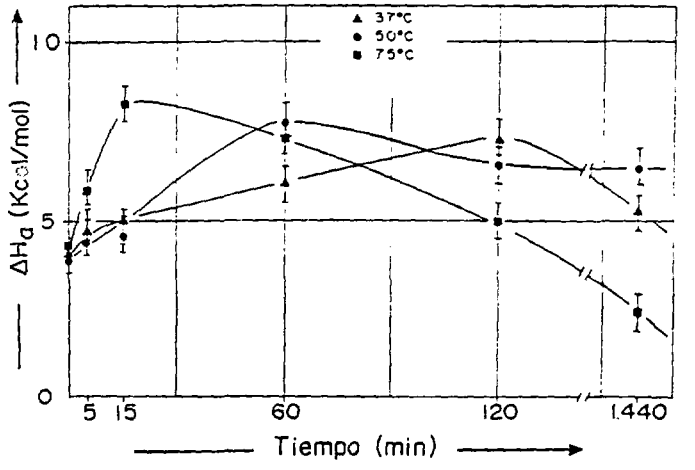

Fig. 10.- Variation of the isostheric heat of n-hexane on a E-glass versus the etching time for an acid solution (pH=1).

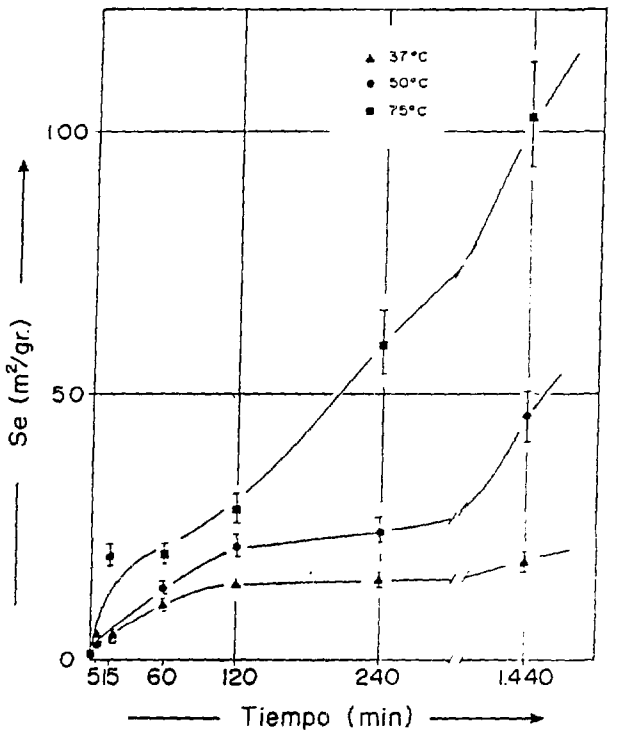

Fig. 11.- Variation of the specific surface of E-glass versus the etching time.

II.5. Kinetic model for acid etching.-

According to different authors, the acid etching in silicate or borosilicate glasses is governed by difusion processes. Hence, the Fick law must give the rate of the process. The Lyle paper (27) was one of the first in this way. But, later different models have obtained more coherent results (28,29). In this sense, Rodriguez (20) has developed a rate semiempiric equation derived from the Fick law taking into account not only the diffusion process, but also the pH value of the etching solution. From this equation it has been possible to calculate the velocity constants. Later, a simulation of the process has been carried out by using a discrete simulation method bases on the Monte-Carlo procedure.

As an example of application of this model to a borosilicate - glass, the Figs. 13,14 and 15 show the B, Na and H^+ concentrations during etching. The points represent the pH measurements obtained on different reaction times. The continuous curve corresponds to the foreseen values by the model. As it can be observed the agreement is good enough, except in the H^+ case which implies the necessity - of considering other factors in this case, while for extractions the model proposed fits well.

III. FUTURE TRENDS.-

The subjects of future research of this group with respect of glasses durability are listed below:

1. Borosilicate (E-glass) fiber leaching with double focus:
   a) In order to increase their compatibility with organic polymers applied to the obtention of composites fiber/plastic.
   b) In order to promote the oxide implantation and the build-up of surfaces with different properties.
2. Study of the chemical etching of borosilicate surfaces treated with organosilanols, as a part of the durability studies on composites.
3. Simulation of the chemical etching mechanisms from the structural point of view.

It is also foreseen to carry out the following research:

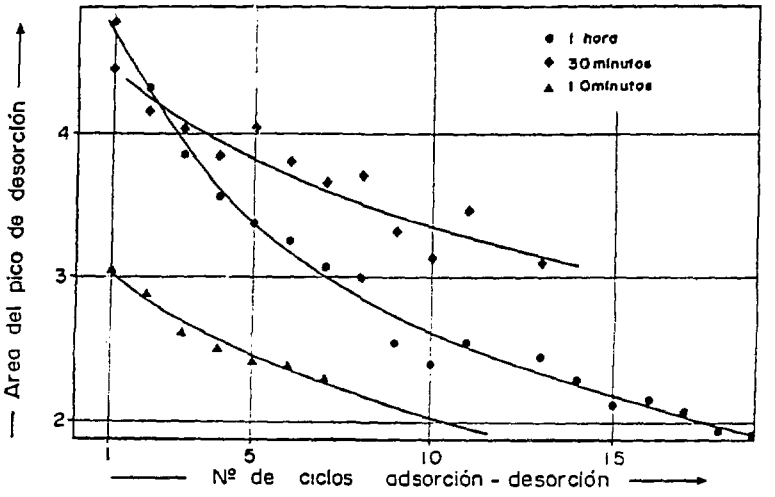

Fig. 12.- Evolution of absorbed nitrogen on E-glass etched versus the cycle number of absorption-desorption.

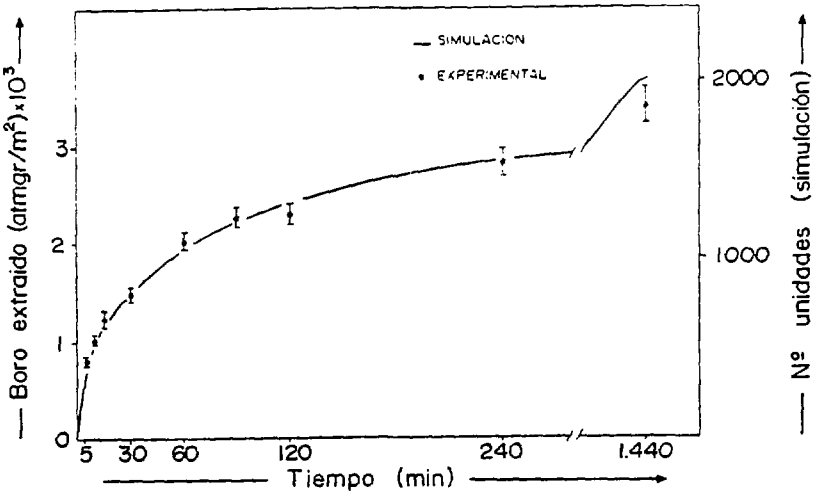

Fig. 13.- Variation of the B concentration extracted by chemical - etching according to proposed model. Values obtained by chemical analysis.

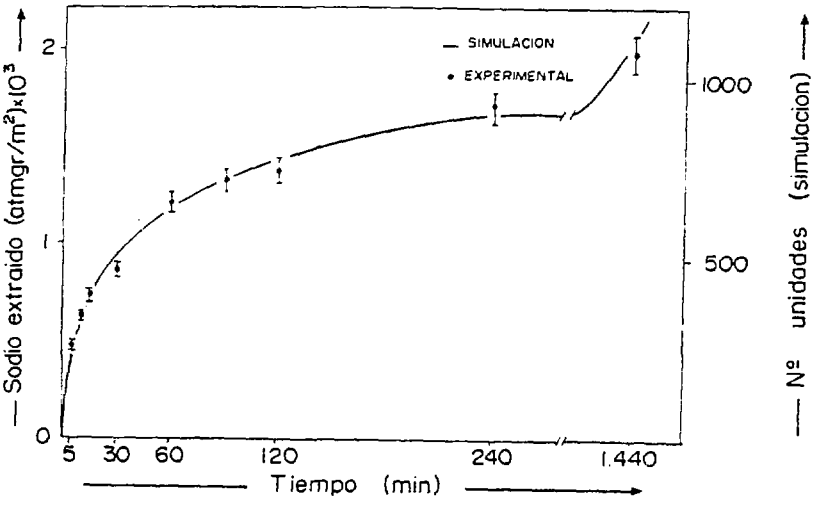

Fig. 14.- Variation of Na concentration extracted by chemical etching according to the proposed model. Values obtained by chemical analysis.

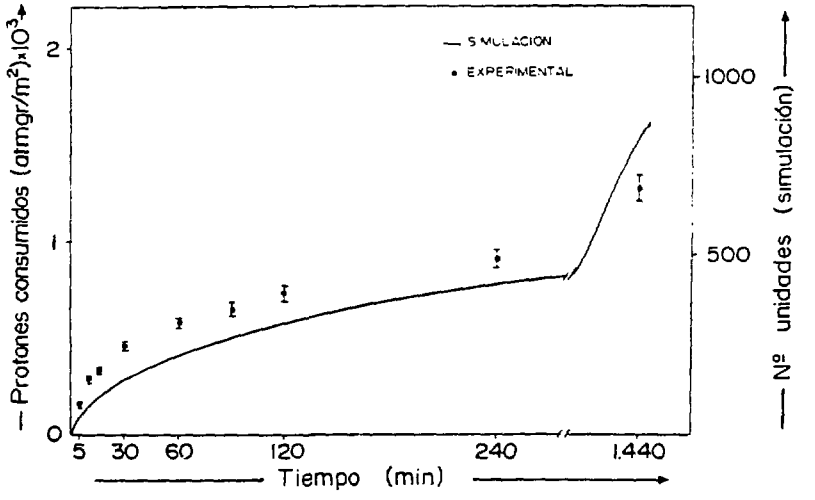

Fig. 15.- Variation of H^+ concentration leached according to proposed model. Values obtained by chemical analysis.

1. Development of dynamic method to measure the porosity of powder materials with lower specific surface.
2. Development of instrumentation to measure dynamically the absorption physics-chemical parameters.
3. Development of software for data adquisition on the data accumulation for simulation.

REFERENCES

1.- HENCH L.L. Physical Chemistry of Glass Surface. J.Non-Cryst. Solids, 25 (1977), 343-369.

2.- RYND J.P., RASTOGI A.K. Characterization of Glass Surfaces by Electron Spectroscopy. Surf.Sci., 48 (1975), 22-43.

3.- NIETO Mª.I., DIEZ J.C., OTEO J.L., DABRIO M.V. A Chromatographic Method for the Determination of Low Surface Areas. Chromatographia 12 (1979), 2, 111-116.

4.- DIEZ J.C., NIETO Mª.I., OTEO J.L., DABRIO M.V. Determinación de las isotermas de absorción por un procedimiento cromatográfico. Anales Soc.Esp.Fis.Quím. 74 (1978) 4, 641-647.

5.- HENCH L.L., CLARK D.E. Physical Chemistry of Glass Surface J. Non-Cryst. Solids, 28 (1978), 83-105.

6.- SCHOLZE H., HELMREICH D., BOKARDJIEV I. Untersuchungen über das Verthalten von Kalk-Natron-gläsern in Verdünnten Saüren. Glastech. ber., 48 (1975), 237-247.

7.- EL-SHAMY T.M., LEWINS J., DOUGLAS R.W. The dependence of the pH of the descomposition of glasses by aqueous solutions. Glass - Technol., 13 (1972), 81-87.

8.- YOUSSEFI A., PAUL A. Resistence chimique de quelques verres du système $Na_2O.CaO.SiO_2$. Verres Réfract., 32 (1978), 663-668.

9.- EL-SHAMY T.M.m DOUGLAS R.W. Kinetics of the reaction of water with glass. Glass Technol., 13 (1972), 77-80.

10.- PAUL A. Chemical durability of glasses; a thermodynamic approach. J.Mat.Sci., 12 (1977), 2246-2268.

11.- RINCON J.Mª, DURAN A. Separación de Fases en Vidrios. El Sistema $Na_2O-B_2O_3-SiO_2$. Ed. Soc.Esp.Ceram.Vidr., Madrid, 1982.

12.- SULLIVAN T.M. MACHIELS A.J. Influence of the electric double layer on glass leaching. J.Nonc-Cryst.Solids, 55 (1983), 269-282.

13.- HORN J.M., ONODA G.Y. Surface charge of vitreous silica and silicate glasses in aqueous electrolyte solutions. J.Am.Ceram.Soc., 61 (1978) 523-527.

14.- SCHOLZE H. Chemical durability of glasses. J.Non-Cryst.Solids, 52 (1982) 91-103.

15.- SCHOLZE H. Evidence of Control of Sissolution Rates of Glass by H^+ Mobility. J.Am.Ceram.Soc., 60 (1977), 186.

16.- NOGAMI M. TOMOZAWA M. Effect of Stress on Water Diffusion in Silica Glass. J.Am.Ceram.Soc., 67 (1984), 151-154.

17.- DILMORE M.F., CLARK D.E., HENCH L.L. Chemical durability of - $Na_2O.K_2O.CaO.SiO_2$ Glasses. J.Am.Ceram.Soc., 61 (1978), 439-443.

18.- SANDERS D.M., HENCH L.L. Mechanism of Glass Corrosion. J.Am. - Ceram.Soc., 56 (1973), 373-377.

19.- CLARK D.E., ETHRIDGE E.C., DILMORE M.F., HENCH L.L. Quantitative analysis of corroded glass using infrared frecuency shifts. Glass Technol, 18 (1977), 121-124.

20.- RODRIGUEZ M.A. Contribución al estudio de las reacciones de vidrios silicobóricos con disoluciones acuosas ácidas. Tesis Doctoral. Univ. Complutense. Madrid (1985).

21.- KISELEV A.V. Surface chemistry adsorption energy and adsorption equilibria. Q.Rev.Chem.Soc., 15., 99-124.

22.- SEWELL P.A. Physical adsorption on massive glass surfaces. Glass Technol., 8 (1967), 108-112.

23.- RUBIO J., RODRIGUEZ M.A., DIEZ J.C., OTEO J.L. Determinación de calores isostéricos en vidrios silicobóricos. Bol.Soc.Esp.Ceram. Vidr., (en prensa).

24.- RUDZINSKI W., WAKSMUNDZKI A., LEBODA R., JARONIEC M. New possibilities of investigating adsorption phenomena by gas chromatography: Estimation of adsorbent heterogeneity from the pressure dependence of retention data. Chromatographia, 7 (1974),11, 663-668.

25.- NELSEN F.M. EGGERTSEN F.T. Anal.Chem., 30 (1958), 1387.

26.- GOMEZ J. Contribución al estudio de las reacciones del vidrio E con disoluciones acuosas ácidas. Tesina. F. Ciencias. U. Autónoma de Madrid. (1984).

27.- LYEE A.K. Theoretical aspects of chemical attack of Glasses by Water. J.Am.Ceram.Soc., 26 (1943), 201-204.

28.- MULAIRE W.M., FURTH W.F. WESTWOOD A.R.C., Influence of surface potential on the kinetics of glass reactions with aqueous solutions. J.Mat.Sci., 14 (1979), 2659-2664.

29.- BOKSAY Z., BOUQUET G., DOBOS S. Diffusion processes in the surface layer of Glass. Phys.Chem.Glasses. 8 (1967), 140-144.

Alteration of Natural Glass in Radioactive Waste Repository Host Rocks: A Conceptual Review

by

John A. Apps

The Lawrence Berkeley Laboratory

Earth Sciences Division

University of California

Berkeley, California 94720

January 1987

This work was supported by the U.S. Nuclear Regulatory Commission. through NRC FIN No. B 040-6 under Interagency Agreement DOE-50-80-97. through U.S. Department of Energy Contract No. DE-AC03-76SF00098.

Abstract

Alteration of National Glass in Radioactive Waste Repository Host Rocks: A Conceptional Review.

by

John A. Apps

The Lawrence Berkeley Laboratory

Earth Sciences Division

University of California

Berkeley, California 94720

The storage of high level radioactive wastes in host rocks containing natural glass has potential chemical advantages, especially if the initial waste temperatures are as high as 250 °C. However, it is not certain how natural glasses will decompose when exposed to an aqueous phase in a repository environment.

The hydration and devitrification of both rhyolitic and natural basaltic natural glasses are reviewed in the context of hypothetical thermodynamic phase relations, infrared spectroscopic data and laboratory studies of synthetic glasses exposed to steam. The findings are compared with field observations and laboratory studies of hydrating and devitrifying natural glasses. The peculiarities of the dependence of hydration and devitrification behavior on compositional variation is noted.

There is substantial circumstantial evidence to support the belief that rhyolitic glasses differ from basaltic glasses in their thermodynamic stability and their lattice structure, and that this is manifested by a tendency of the former to hydrate rather than devitrify when exposed to water. Further research remains to be done to confirm the differences in glass structure, and to determine both physically and chemically dependent properties of natural glasses as a function of composition.

Introduction

For various scientific and technical reasons, the deep burial of high level radioactive wastes in geologic repositories is now accepted as the most reasonable means for isolating these hazardous materials from the biosphere. Several countries are studying the design, construction and integrity of radioactive waste repositories in order to resolve the uncertainties attending this disposal option, to select sites, and to reassure the public that underground repositories will function properly.

Current U.S. practice is to design for maximum temperatures in the host rock to range from about 160 ° C in salt to 260 ° C in basalt, (Raines et al., 1981). These maxima would be attained close to the container host rock interface and occur between 35 and 60 years after burial of the waste, (Wang et al., 1979). The temp rature of the waste would still be 50 to 100 ° C above the ambient temperature of the host rock, some 1,000 years after burial, and the region affected by elevated temperature would extend up to 500 m from the waste containers. A substantial volume of rock could alter therefore hydrothermally. A repository designed to operate at temperatures to 250 ° C would be both more compact and potentially cheaper per unit of disposed waste than one designed to operate at lower temperatures. It would also possess the advantage that the higher temperatures would increase the reactivity of the host rock in the near field, and enhance the capacity of the rock to sorb and coprecipitate radionuclides.

Rocks containing either acid or mafic glass possess potential advantages over other rocks as hosts for radioactive waste. Because glasses are much less stable than most minerals, they will react with dissolving radioactive waste under hydrothermal conditions to produce secondary minerals, that would entrap harmful radioelements.

The alteration products of natural silicic glasses are normally zeolites, such as clinoptilolite or heulandite, and smectites, both of which possess the potential to sorb radioelements such as cesium, or strontium. When basaltic glass alters, it releases ferrous iron, which induces a low environmental oxidation state as a result of disproportionation reactions in which ferric ions enter into secondary nontronite, magnetite or hematite. The lowered oxidation state ensures that the actinides, such as uranium, neptunium, plutonium and americium are maintained in the +4 or +3 oxidation states, which are the least soluble. Technicium also is strongly sorbed when reduced to the +4 state. The lower oxidation state also favors the formation of pyrite, which can reduce selenium and precipitate it as a selenide.

At higher temperatures, basalt alteration is also favorable for the formation of secondary sphene, which will accept tin-126 (and actinides?), and for the formation of epidote, which is isomorphous with allanite, a well known potential host for actinides (U.S. D.O.E., 1980).

In the Western United States use could be made of glassy rocks at two potential repository sites, both of which are currently under active consideration. One is at the Hanford site in Richland, in the Pasco Basin of Washington, where the underlying rocks are composed of massive flood basalt flows. These flood basalts still contain a vitreous mesostasis where the glass varies from a few weight percent to as much as 20 weight percent. The cumulative thickness of the flows is nearly 5,000 feet and they are overlain by up to 700 ft. of surficial sediments. The other repository site is at the Nevada Test Site in Nevada. Here, widespread acid ash flows and welded tuffs have accumulated as a result of several immense caldera eruptions during the past 26 million years. Although most of the welded tuffs have devitrified, probably immediately following their deposition, many horizons are present where vitroclastic tuffs and vitrophyres still

remain substantially unaltered.

The basalts of the Pasco Basin are for the most part below the water table and are therefore saturated, whereas in Nevada, because of the nature of the terrain, the low rainfall, and the high evapotranspiration rates, the water table is often many hundreds of feet below the surface. The present candidate repository location at the Nevada Test Site therefore happens to be in the unsaturated zone above the water table.

In this paper I would like to discuss some aspects arising from the selection of rocks containing natural glass as hosts for a nuclear waste repository, particularly if the initial repository temperatures are as high as 250 ° C. In particular, I would like to address some of the contrasting alteration mechanisms between acid rhyolitic glasses and glasses of basaltic or mafic composition. There is substantial circumstantial evidence to suggest that their mode of alteration is very different and that this must be accounted for in the prediction of repository behavior in either basalt or acid tuff.

To investigate this issue requires a knowledge of glass alteration from experiment and theory, supplemented by field observations of natural glass altering under conditions similar to those expected in a repository. This approach must be taken in order to extrapolate observations of short term laboratory experiments, to natural processes taking place over periods of thousands of years; i.e. time spans comparable with that necessary to isolate radioactive waste from the biosphere.

Thermodynamics of Glasses in Relation to Hydration and Devitrification

Silicate glass is primarily a polymerized network of covalently bonded $[SiO_4]^{4-}$ tetrahedra, linked by their oxygen apices. Other cations can substitute

for Si^{4+} such as Al^{3+} and B^{3+}, and sometimes Fe^{3+}. The charge deficiency is made up by interstitial cations. The continuity of the network is disrupted by the presence of so called "network modifiers" such as the alkali metals, the alkali earths ions, and some transition group metal ions such as Fe^{++}. Some cations such as Zn^{2+}, or Pb^{2+} may occupy either the tetrahedral network or the interstitial sites.

Silicate glasses can be synthesized over a very large range of chemical compositions. However, the range of natural glass is restricted to SiO_2 contents ranging from 40 to 80 wt%, and with varying amounts of other network builders, principally Al_2O_3, and network modifiers such as Na_2O, K_2O CaO, MgO, and FeO. Together, these constituents usually make up over 95 wt% of the total composition.

Glasses are conceived to be supercooled liquids in which rotational and translational degrees of freedom among the constituent molecules have been quenched, leaving only vibrational modes. This picture is an over simplification as noted in several studies of the thermodynamic properties of glass, (e.g. Goldstein, 1975; Richet and Bottinga, 1983) but it suffices for this discussion.

The transition from supercooled liquid to glass is characterized by a substantial change in heat capacity, which closely approaches the change between the liquid and the solid crystalline equivalent. It may be viewed as a second order thermodynamic transition. Even though interpretation of the glass transition as a thermodynamically reversible phenomenon is controversial, it will be here so treated as a matter of interpretive convenience. The measured glass transition temperature may vary by as much as 100°C for a given silicate glass composition, due in part to the prior cooling history of the glass. A reversible transition is not observable because of the sluggishness of the reaction at the transition temperature, (Gibbs and DiMarzio, 1958). Hence true metastable thermodynamic

equilibrium is never attained, and measured thermodynamic and transport properties of a given glass are often dependent on its previous history. Yet an extensive literature reveals that glasses have relatively consistent physical properties, suggesting that a qualitative if not quantitative thermodynamic treatment is possible.

When exposed to water, glasses have a tendency to alter by a variety of temperature, composition, and system dependent mechanisms. Wu (1980) categorised glasses into four types depending on their behavior when exposed to steam at elevated temperature, viz, those that: (a), hydrate; (b), do not hydrate; (c). dissolve in the aqueous phase, and (d), devitrify or crystallize. Because all glasses could eventually crystallize to a more stable phase assemblage, the last category is a manifestation of more rapid crystallization kinetics.

To place these mechanisms into context and relate them to natural glass alteration, I will discuss some of the hypothetical phase relations that might be involved. Figures 1 – 4 are temperature composition diagrams portraying an arbitrary pseudo-binary system involving a stoichiometric anhydrous silicate as one end member, and water as the other end member. The temperature range extends from about –50 ° C to beyond the melting point of the stoichiometric crystalline silicate. The pressure is arbitrarily set between 1 bar and 400 bars, a range expected to include most waste repository conditions. The typical waste repository environment will encompass a temperature domain around the boiling point of water, the upper limit being determined by the design specifications of the repository.

Features common to all diagrams are a pseudo-binary immiscibility loop between vapor (steam) and liquid (silicate melt) phases, culminating in a critical phase, a solidus curve with respect to the stable essentially stoichiometric solid and the liquid (i.e. melt/water) phase, and a subsolidus pseudo-binary solvus

leading to the formation of coexisting supercooled water rich and water poor melts (or glasses). Evidence for the existence of the binary solvus is speculative and is based on the assumption that glasses have a finite and definable saturation limit with respect to hydration, and a finite equilibration solubility. Superimposed on the supercooled liquid field is the glass transition. Apart from the pseudo-binary miscibility loop, all stable phase transitions are drawn with light lines, whereas metastable transitions are drawn with heavy lines.

In Figure 1, it is assumed that the glass will hydrate to a significant extent. Hydrated glass may be produced either by quenching of a hydrous melt, along path, a´-b, or by hydration in contact with either a vaporous or a liquid aqueous phase along path a-b. Rhyolitic or rhyodacitic glasses most probably follow path a-b during hydration in closed systems, as will be discussed further on.

Figure 2 represents Wu's 2nd case in which an anhydrous glass exposed to a steam atmosphere will hydrate to an inconsequential extent before saturation, as indicated by path a-b. However, a "superhydrated" unstable glass could in principle be produced in the system by quenching a hydrated melt along path c-d. This case may be representative of very high silica glasses such as tektites or vitreous silica.

Silicate glasses containing high concentrations of alkali metals are represented in Figures 3 and 4. In these cases, the glass will actually liquify or dissolve in the presence of an aqueous phase. Figure 3 represents the situation of liquifaction in the presence of steam, as indicated along path a-d. The glass will first hydrate along a-b, then transition to a supercooled liquid, along b-c, finally becoming a stable liquid at c and eventually saturating at d with respect to the aqueous (steam) phase. Figure 4 shows the corresponding case in which the glass is dissolved by an aqueous liquid, along path a-b-c. These last two cases have not been observed to occur naturally, although they represent variations of the

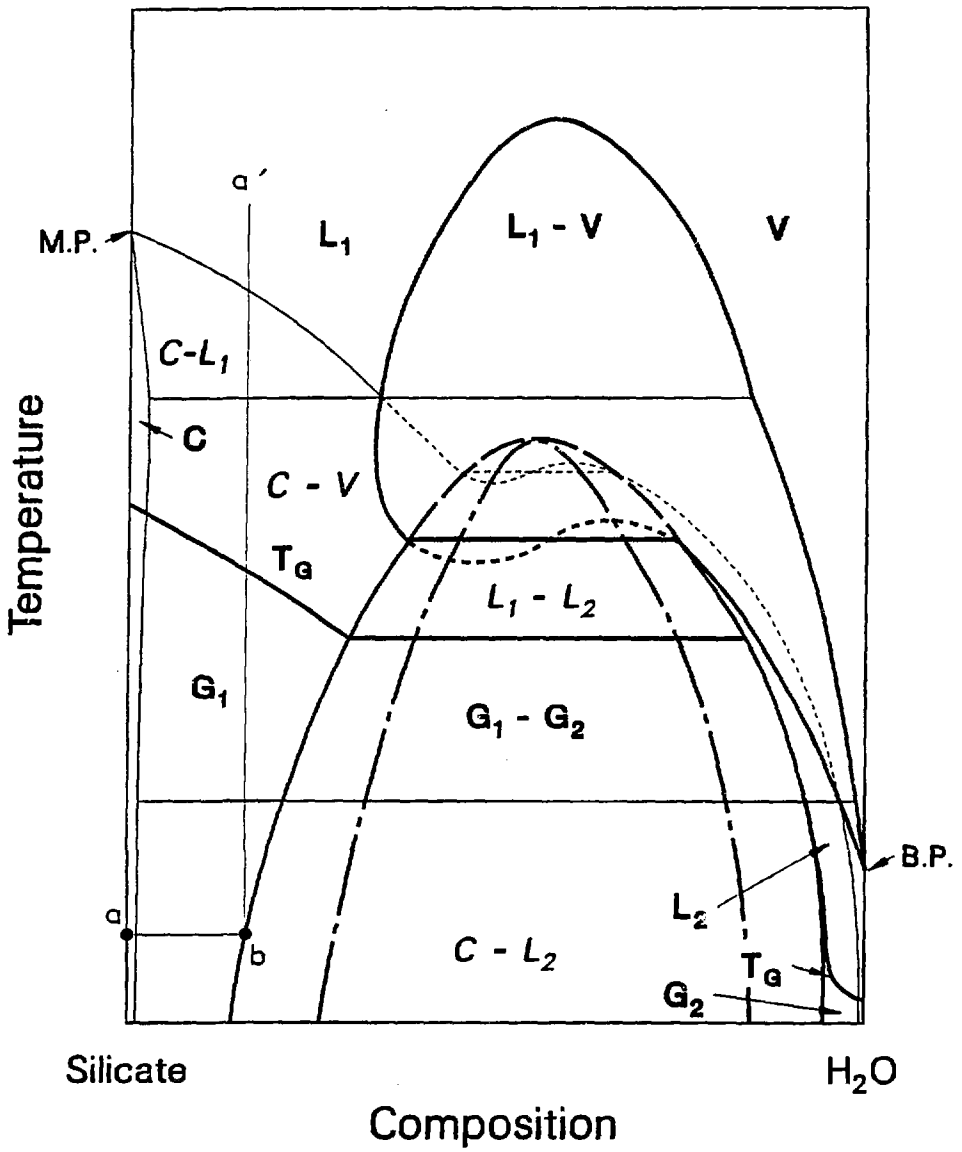

Figure 1. Hypothetical pseudobinary temperature-compositon diagram to illustrate the metastable field of hydrated silicate glass in equilibrium with the aqueous phase.

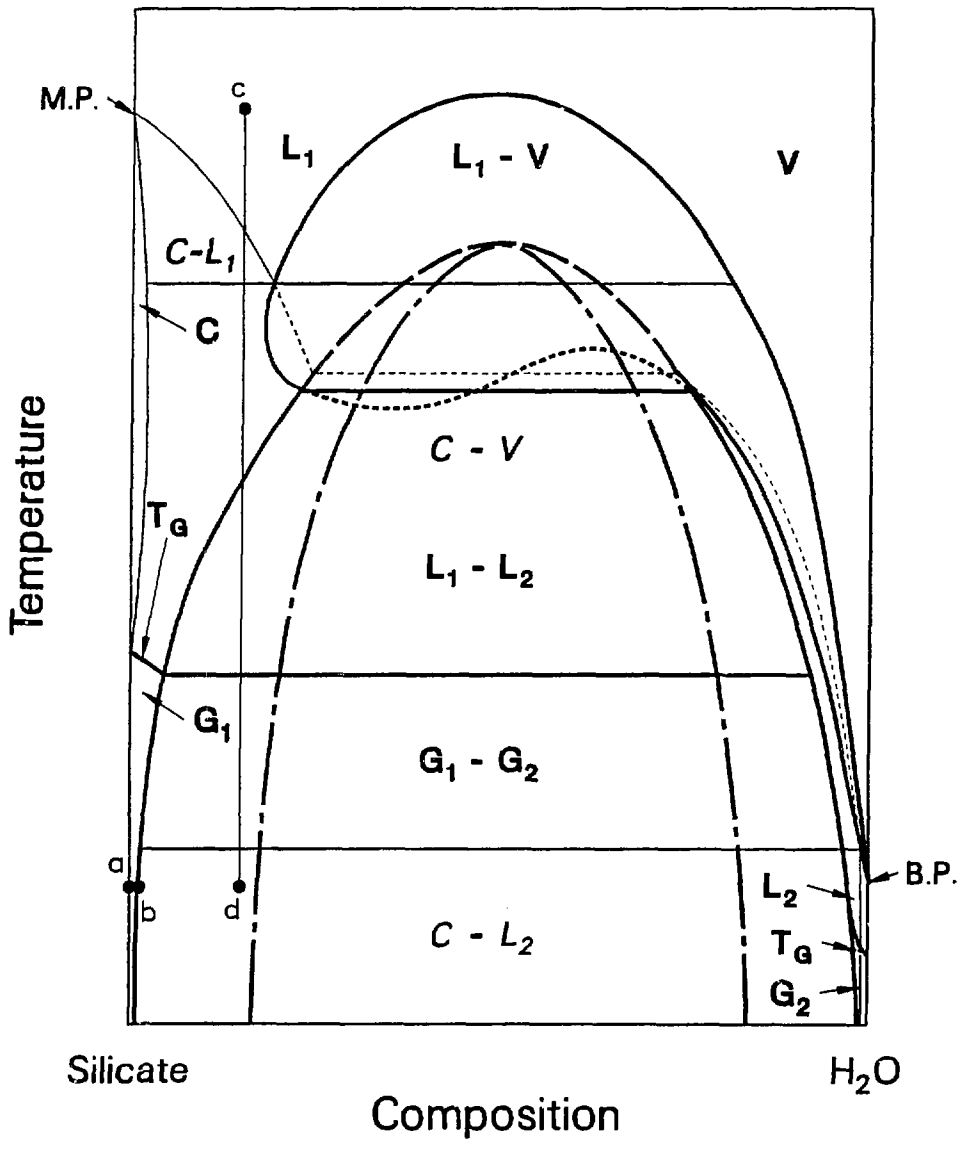

Figure 2. Hypothetical pseudobinary temperature-composition diagram to illustrate the metastable field of a non hydrated glass in equilibrium with the aqueous phase.

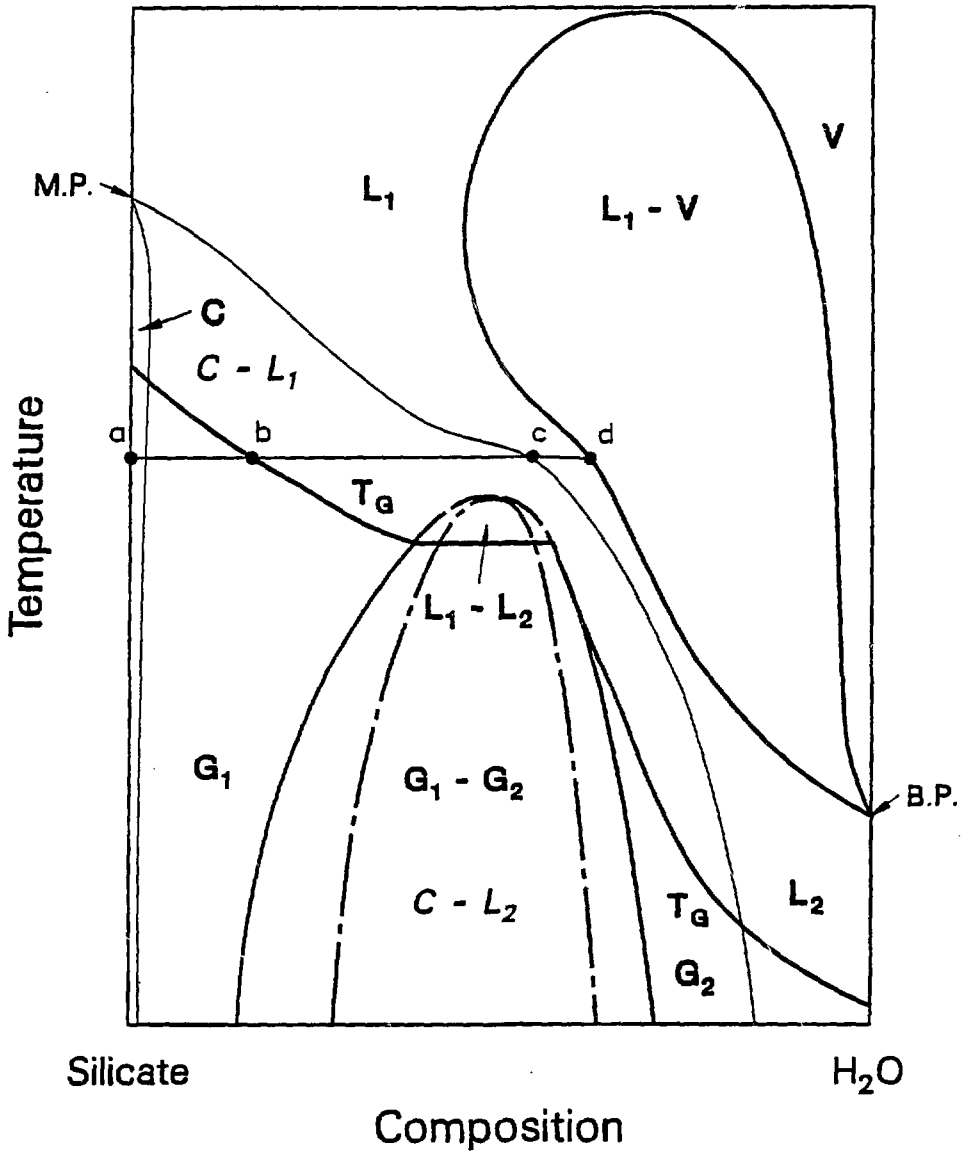

Figure 3. Hypothetical pseudo-binary temperature-composition diagram to illustrate the hydration and liquifaction of an alkali silicate glass by steam.

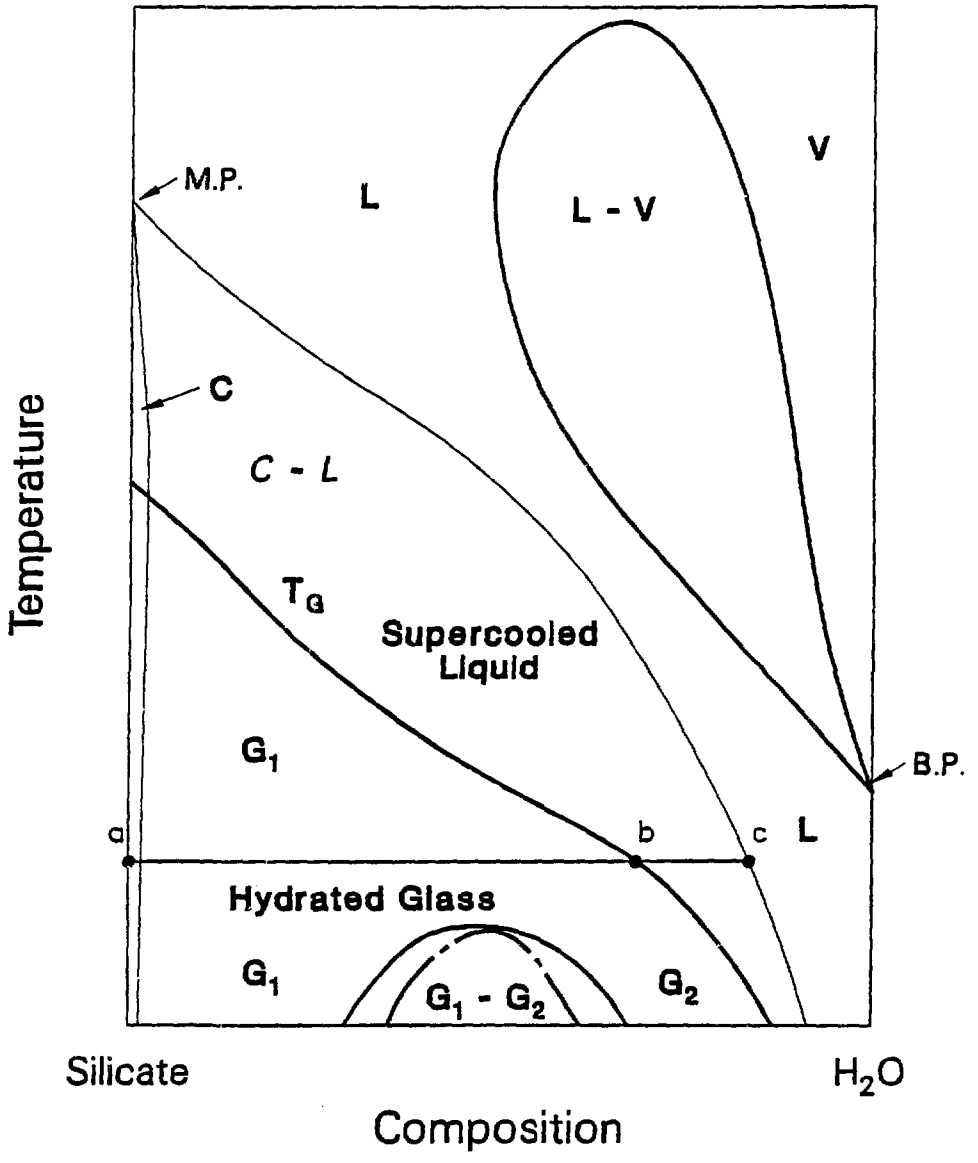

Figure 4. Hypothetical pseudo-binary temperature-composition diagram to illustrate the hydration and dissolution of an alkali silicate glass by a liquid aqueous phase.

third case listed by Wu.

There remains the question as to how Wu's fourth category can be fitted into this scheme. Furthermore, field and laboratory observations to be discussed below, suggest that basaltic glass would also fall into the same category. Here we must speculate that, with falling temperature, a hypothetical stoichiometric silicate mimicing a basaltic melt in composition would, on cooling, recrystallize to form a stable hydrated phase in the pseudo-binary cross section. We must further assume that metastable equilibrium hydration in the glass would be transient, because hydration would so lower the activation energy of devitrification, that devitrification would immediately follow. As it turns out, this is true to a certain extent, but other thermodynamic and structural factors also play a role as will be discussed further on.

Correlation of Extent of Hydration with Glass Composition

In the discussion which follows, a distinction is attempted between saturation hydration of a glass, and the rate of hydration. Unfortunately, in some glasses, hydration induces rapid devitrification, so the saturation hydration cannot be determined. In others, the rate of hydration may be so slow that saturation hydration cannot be achieved, either in the laboratory, or through prolonged exposure in the field. These differing properties often lead to ambiguities in interpretation, sometimes compounded by lack of a critical distinction being made in the literature.

Scholtze (1959a,b,c, and 1966) has measured changes in the infrared absorption spectra due to silanol groups on of a large range of weakly hydrated silica glasses, to study the effect of substituting various metal oxides for silica. Scholtze found that metal oxide substitution could be correlated with the fraction, r, of non hydrogen-bonded silanol groups, which is in turn, correlated

inversely with the polarisability of the oxygen ions in the lattice and the basicity of the glass.

As will be noted from Figure 5 (redrawn from Scholze, 1959b), network modifiers such as the alkali metals, potassium and sodium, have a powerful effect in decreasing r, whereas network builders such as aluminum have the opposite effect. Wu (1980) correlated r with the four response modes of glass when exposed to steam. Those glasses with r approaching unity did not hydrate, or at least were not observed to hydrate in the laboratory; those with intermediate r values i.e. $\approx$ 0.3 to 0.7 hydrated, but otherwise showed no other alteration, whereas those with low r factors, either dissolved completely as a liquid phase or devitrified, i.e. crystallised. Those with high alkali metal contents dissolved, whereas those with alkali earths contents devitrified.

Unfortunately, variation of r is not linear with composition, so it is not possible to predict the hydration behavior of the natural glasses from Scholtze's data. However, it is reasonable to assume that rhyolitic glass, with its higher silica and alkali metal content will have a higher r factor than basaltic glass with its lower silica content and significant enrichment in CaO and MgO. The former would therefore tend to hydrate, catalysed by the alkali metal cations, as suggested by Wu (1980), whereas the latter would tend to devitrify. This contrasting behavior is consistent with field and laboratory observations.

Field evidence also shows that rhyolitic and basaltic glasses behave quite differently regarding hydration and devitrification. Natural rhyodacitic and rhyolitic glasses containing between 65 and 80 wt% silica, will hydrate under earth surface conditions, apparently without destruction of the SiO_4, AlO_4 tetrahedral framework, and with only partial or even no loss of interstitial alkali cations. (Scheidegger and Kulm, 1975; Scheidegger et al., 1978; Jezek and Noble, 1979; Federman 1984; Forsman, 1984). According to Federman, (1984), rhyodacitic and

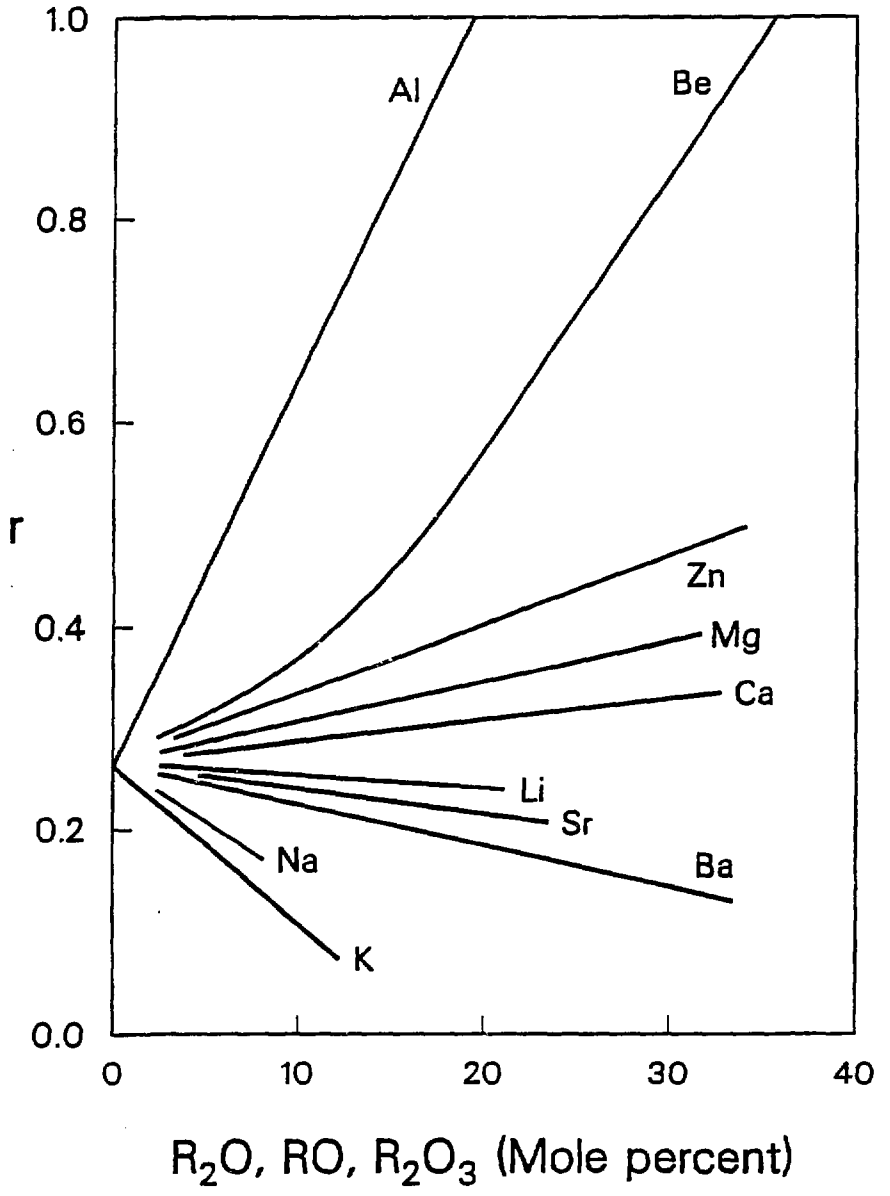

Figure 5. Correlation of non hydrogen-banded silanol groups in a 80 mole % SiO_2, 20 mole % Na_2O glass as a fraction of the mole percentage substitution of metal oxides for silica (after Scholze, 1959b).

rhyolitic glasses in abyssal tephra deposits from the Eastern Mediterranean, initially containing 0.3 to 1.0 wt% H_2O-, hydrate to between 4 and 5 wt% H_2O after 10^5 to 10^7 years. Scheidegger et al. (1978) and Ninkovich (1979) have made similar observations in their studies of ash layers in the Northwestern Pacific and Indian Oceans respectively. Such hydrated glasses may persist in nature for very long periods. Forsman, (1984) describes several ash beds from North Dakota containing "unaltered glass" ranging in age from Upper Cretaceous to Paleocene. The ash beds have been saturated with water during much of their history and are believed to be "superhydrated", as gas bubbles in the glass shards are now filled with water. It is probable that the glass was preserved partly because the aqueous phase also saturated metastably with respect to the glass structure, and that devitrification through dissolution and precipitation of secondary minerals was inhibited by the relatively low ambient temperatures.

Basaltic glasses containing 45 to 55 wt% SiO_2 in abyssal tephra also appear to persist in an essentially undevitrified state, at least up to 3.8 million years, (Scheidegger, 1973). In contrast to more silica rich glasses, they do not appear to hydrate, or perhaps hydrate at a much slower rate. Scheidegger (1973), found that basaltic glasses ranging in SiO_2 content from 47 to 51 wt% from the Cobb Seamount on the Juan de Fuca Ridge in the Pacific Ocean contained between 0.10 to 0.38 wt% H_2O+, essentially similar to glass from fresh basalt pillows, which, according to Moore, (1970), contain between 0.06 to 0.42% H_2O+. However, naturally occurring basaltic glasses containing up to 1.84% H_2O have been analysed, (Delaney and Karsten, 1981).

An even older basaltic glass of olivine tholeiite composition has been described by Muffler et al. (1969) in a late Triassic (180 my) "aquagene tuff" from southeastern Alaska. Although the tuff fragments display 30μm alteration rims, the bulk of the glass shows no apparent alteration. The H_2O- content of

the "unaltered" glass is 1.58 wt%, somewhat higher than that reported for the Cobb Seamount tephra, although the SiO_2 content is similar, i.e. 48 wt%.

While it is evident from field observations that the saturation hydration level of rhyolitic glasses is of the order of 5 wt% H_2O+ at 0 to 25 °C, the saturation hydration of basaltic glasses within the same temperature range is unknown. Stolper (1982) claims that water solubility in magmas is insensitive to composition. It is not clear whether the saturation concentration of water in glass is also insensitive to composition, and that basaltic glasses, given sufficient time would hydrate to the same water concentration as obsidians. In synthetic systems, which cover a wider range of compositions, it is known that vitreous silica hydrates less than alkali silicate glasses under comparable conditions. (Wu, 1980; Della Mea et al., 1984). This suggests that the saturation hydration in natural glasses could well be sensitive to composition. However, it is presently not possible to estimate whether a basaltic glass can hydrate to a significant extent.

Kinetics of Hydration and Devitrification

The rate of natural glass hydration has been determined both experimentally and from field observations. Although the hydration mechanism for basaltic glasses has not been unequivocally determined, as will be discussed further below, hydration in obsidians and perlites appear to be a diffusion controlled process following a parabolic rate law, (Friedman and Smith, 1960; Marshall, 1961; Friedman et al., 1966; Lofgren, 1968; Friedman and Long, 1976; Michels et al., 1983). This process is sufficiently uniform and slow at earth surface temperatures, that it has found application as a dating method for obsidian artifacts, (Friedman and Smith, 1960; Meighan et al., 1968; Michels et al. 1983), and for recent, i.e. up to 200,000 year old rhyolitic or obsidian flows, (Friedman, 1968; Pierce et al., 1976).

Rhyolitic glasses undergo significant density and optical changes when they hydrate (Lofgren, 1968). This leads to localized stress concentrations at the interface between the hydrated and unhydrated glass, which is sufficient in some cases to cause fracturing, or at least show optical strain (Lofgren, 1968). Evidence that hydration induces fracturing has also been observed by Morgenstein and Riley (1975) in basaltic glasses The fracturing permits access of water to the glass interior and facilitates transport of chemical components in and out of the glass, thus accelerating both hydration and devitrification.

According to Friedman and Long (1976), increasing SiO_2 and H_2O content in obsidian increases the diffusion rate of water, whereas increasing CaO, and MgO, decreases the rate of diffusion. Al_2O_3, FeO, Na_2O, and K_2O contents appear to have little effect on the rate, at least over the narrow range of compositions studied by the investigators. The effect of minor changes in CaO and MgO content is substantial, with the hydration rate declining from 5 $\mu m^2/10^3$ yr. to 0.2 μm^3 10^3 yr. at 10 ° C over a narrow SiO_2 compositional range between 72.2 and 76.9 wt% SiO_2. Extrapolation of hydration rates to basaltic glass composition is unfortunately not possible because of the scatter in Friedman and Long's data, the empirical correlation used, and the length of the extrapolation required. Their data strongly suggest, however, that basaltic glass hydration rates would be at least two and possibly three orders of magnitude slower than for a typical obsidian. This is consistent with the field observations of Scheidegger, (1973) that basaltic glasses several million years old have not hydrated. It might also be construed that the Triassic basaltic glass described by Muffler et al. (1969) has taken 180 million years to hydrate to no more than 1.6 wt% H_2O-.

In synthetic silica-metal oxide glass systems, the evidence of Yoko et al., (1983) and Moriya and Nogami, (1980) indicates that substitution of up to 10 wt% Al_2O_3, MgO or CaO for SiO_2 in a 20 wt% NaO_2 SiO_2 glass decreases the

hydration rate by as much as 500 times. However, the hydration process does not uniformly follow parabolic kinetics, suggesting that a simple diffusive hydration of the glass structure is no longer the principal alteration mechanism.

Another interesting observation, which may be germane, is provided by LaMarche et al. (1984), who attempted to hydrate a silica rich (80 wt% SiO_2) tektite glass containing 2.48 wt% MgO and 1.91 wt% CaO at 90 ° C. No surface hydration layer could be produced, consistent with field observations of weathered tektites. This could be interpreted either as evidence that the kinetics of hydration is slowed by the presence of MgO and CaO, or that the very high silica content prevents significant hydration, i.e. the tektite glass falls into non hydratable glass category of Wu (1980a).

In rhyolitic glasses, hydration facilitates the diffusion of some metal cations in and out of the glass. White and Yee (1986) find that the diffusion coefficients of rubidium, cesium, and strontium are markedly greater when exposed to the aqueous phase below 100 ° C than would be expected based on extrapolation of high temperature diffusion coefficients to the same temperature region. Field evidence, e.g. Jezek and Noble (1978) also report on the exchange of potassium for sodium in perlites. Thus the chemical composition of an exposed natural rhyolitic glass can change with time and therefore affect the mineral composition on devitrification.

While the evidence that basaltic glass will hydrate is equivocal at best, in contrast to rhyolitic glass, there is plenty of evidence that basaltic glass will devitrify to form secondary smectites and zeolites. In nature, basaltic glass originates in three ways;

1. Through the quenching of basaltic lavas in submarine environment. In this situation basaltic pillows are encased in a glassy rind known as sideromelane;

2. As air fall tephra.

3. As hyaloclastites. Hyaloclastites are most notably formed in Iceland, where the rapid injection of basaltic lava into ice or water leads to quenching and fragmentation.

The process by which basaltic glass alters to secondary minerals is known as palagonitization. It is most frequently studied under circumstances in which the glass is exposed to seawater under essentially "open system" conditions. Palagonitization is not a simple process in which water diffuses into the glass lattice, but instead may involve initial hydration of a thin rind less than 50 μm. thick. The thin rind induces high stresses in the adjacent unaltered glass, and leads to the formation of array of microcracks penetrating the glass ahead of the "hydration" zone, (Morgenstein and Riley, 1975). Rapid devitrification of the "hydrated" rind then produces a palagonite layer, which may be poorly coherent, spall and leave more fresh glass exposed for hydration.

Repeated cycles lead to the formation of a cumulative alteration layer that in some cases possesses characteristics remiscent of Liesegang banding. It is quite likely that a Liesegang alteration mechanism occurs in which counter diffusion of two or more components is involved (Fisher and Lasaga, 1981). Certainly the mineralogical and chemical evidence of the palagonitization of sideromelane in seawater indicates extensive exchange of elements between the glass and seawater (Staudigal and Hart, 1983).

Basalt glass alteration implies that the process of glass hydration will make devitrification possible i. . the activation energy barrier inhibiting devitrification will be removed, or at least decreased significantly. Unfortunately, the initial hydration process, has not been confirmed. It is not clear whether devitrification proceeds simultaneously with hydration or whether hydration precedes devitrification as is the case in rhyolitic glasses, or indeed whether hydration

occurs at all as suggested by the recent work of Crovisier et al. (1986).

Average alteration rates in basaltic glasses are difficult to establish, but several studies, including that by Morgenstein and Riley (1975) on basaltic glass artifacts from Hawaii, in which alteration rates are correlated with C-14 dating, that by Burnett and Morgenstein (1976) on submarine palagonites dated by means of the uranium decay series, and those correlating the age of exposure with the accumulation of manganese oxide layers (Bender et al., 1966, Moore, 1966; Hekinian and Hoffert, 1975, and Burnett and Morgenstein, 1976) indicate that the net rate of alteration is linear and not parabolic. The palagonite layer, does not therefore act as a rate-controlling diffusive barrier.

Experimental studies on basaltic glasses e.g. by Furnes (1975) and Crovisier et al. (1983) do not contradict available field evidence regarding the alteration mechanism, whereas the most recent experimental findings by Crovisier et al. (1986) supports the view that a linear alteration process is involved, at least at earth surface temperatures, in which there is no evidence of the formation of an initial hydration layer.

Rhyolitic glasses devitrify through nucleation, spinodal decomposition or through dissolution in and precipitation from the aqueous phase. The relative importance of the last process is strongly dependent on the environmental conditions. Field evidence in altering acid vitroclastic tuffs and basalts clearly shows, through the presence of secondary clays and zeolites in pores, fractures and vesicles, that is important in the 25–400 °C range, and probably dominants alternative devitrification mechanisms in many situations. An extensive literature exists describing the surface dissolution kinetics of glasses, but its review is beyond the scope of this paper.

High temperature nucleation above, or around the glass transition temperature leads to the formation of a characteristic spheroidal texture in which

cristobalite or quartz in association with feldspar forms radial aggregates. In anhydrous glasses, this process is slowed so substantially below 600 °C that it cannot be considered of relevance to a waste repository environment. However initial hydration of the glass permits devitrification to proceed at a greatly accelerated rate. Lofgren (1968) notes that hydrated glasses are characterized by the formation of "globulites". These minute spherical bodies have not been characterized so far, so it is impossible to assess whether they represent the initial stages of nucleation and devitrification in the hydrated glass. Nothing has been reported in the literature regarding the spinodal decomposition of hydrated glasses.

According to Friedman and Long (1984), hydration of rhyolitic glass will substantially decrease the activation energy of devitrification, thereby permitting measurable devitrification to proceed at much lower temperatures. These authors calculate that a hydrated rhyolitic glass will devitrify at 200 °C at about the same rate that an anhydrous glass will at 600 °C, (c.f. also Marshall, 1961). The relative rates of devitrification of natural glass in the host rock of a waste repository may therefore be strongly dependent on its hydration rate and saturation level. A rhyolitic glass will hydrate more rapidly than it will devitrify, whereas one could speculate that basaltic glass will devitrify as fast as it hydrates, so that the hydration rate becomes the rate limiting step in devitrification. Lofgren (1968) has tentatively established that rhyolitic glasses devitrify about four orders of magnitude slower than the hydration process. In contrast, nothing is known quantitatively about the relationship of hydration to devitrification in basaltic glass.

Evidence for Structural Differences between Rhyolitic and Basaltic Glasses

Field and laboratory studies, show that fundamental differences exist between basaltic and rhyolitic glasses in their manner of alteration in the presence of an aqueous phase. What this is due to cannot be conclusively resolved at this time, but there is both thermodynamic and spectroscopic evidence indicating that the differences may be attributed to a structural dissimilarity between the two glasses.

Navrotsky and her coworkers (e.g. McMillan et al., 1982; Navrotsky et al., 1982; Roy and Navrotsky, 1984; Navrotsky et al., 1985 a,b) have investigated the heats of solution in molten lead borate of glasses in the system SiO_2-$M_{1/n}^{n+}AlO_2$ where M = Li, Na, K, Rb, Cs, Mg, Ca, Sr, Ba, Pb. They find that the glass stability tends to increase with substitution of $M_{1/n}^{n+}AlO_2$ for SiO_2, apparently reaching a maximum when $X_{M_{1/n}^{n+}AlO_2} = 0.5$, i.e. the heat of solution, ΔH_{sol}, reaches a maximum value. They also found that, for a given value of $X_{M_{1/n}^{n+}AlO_2}$, ΔH_{sol} decreases progressively in the sequence Cs $\sim$ Rb $\sim$ K, Na, Li, Ba, Pb $\sim$ Sr, Ca, Mg. These observations may be interpreted to indicate that the alkali metals interact very weakly with the alumino-silicate framework structure whereas the alkali earths, particularly Ca and Mg interact much more strongly and tend to destabilize the structure. Navrotsky et al. (1982, 1985a) have derived the enthalpy of mixing binary composition plots from the heat of solution data. These show that compensated SiO_2-$M_{1/n}^{n+}AlO_2$ melt joins show a much smaller tendency towards liquid immiscibility than do the corresponding SiO_2-$M_{1/n}^{n+}O_{n/2}$ systems. However, this tendency increases progressively in the same sequence Cs, ... Ca, Mg noted above, with the potential for separation into respectively a very silica rich phase and a silica poor phase.

The significance of these findings in relation to rhyolitic and basaltic glasses is evident and consistent with independent lines of evidence. Clearly, the rhyolitic glass, whose aluminosilicate structure is charge compensated with the alkali metals, will be more stable and less likely to break down than a basaltic glass containing substantial amounts of alkali earths. The weaker structure of the latter would also have a tendency to react more rapidly and devitrify, thereby not giving it the opportunity to hydrate as with the former. The tendency towards immiscibility in the charge compensated alkali earth aluminosilicate melt systems also suggests that significant structural differences may exist between the two glasses, for which there appears to be independent supporting evidence.

X-ray scattering studies of albitic ($NaAlSi_3O_8$) and anorthitic ($CaAl_2Si_2O_8$) glasses by Taylor and Brown (1978a,b) and Taylor et al. (1980) show substantially different radial distribution functions for the two glasses. The investigators conclude that albite glass possesses a structure somewhat similar to a disordered cristobalite, being composed of linking six-membered tetrahedral rings. This structure is quite open and could allow the diffusive penetration of water or permit ion exchange of potassium for sodium. In contrast, anorthitic glass is perceived to contain 4-membered tetrahedral rings similar to the feldspar structure. The smaller ring size could inhibit diffusion of water and/or cations through the lattice. It is possible that the higher concentration of magnesium, calcium, and ferrous iron in basaltic glass as compared to rhyolitic glass, coupled with the lower silica content, could lead to structural differences analogous to those believed to occur between albite and anorthite glasses. Detailed studies to verify such structural differences remain to be conducted on a broader range of glass compositions.

Further circumstantial evidence that significant structural differences may exist in natural glasses of different chemical compositions is the existence of an

immiscibility phenomenon in the corresponding liquid state (Philpotts, 1976), and the evidence of spinodal decomposition in glasses. In the former case, Philpotts and his colleagues have made a thorough study of the formation of immiscible melts in basalts (Philpotts, 1977, 1978; Philpotts and Doyle, 1982). Although there is some question whether melt immiscibility occurs above or below the solidus, i.e. whether or not the melt was supercooled at the time, e.g. see Biggar, (1979); Freestone (1979), Philpotts and Doyle (1980), the fact remains that unmixing occurs, and that there is evidence of a discontinuity in the melt structure, which may also be reflected in a corresponding structural discontinuity between basaltic and rhyolitic glasses.

Evidence for spinodal decomposition in natural glasses in the composition range of interest is much more tenuous. However, Manankov (1979) has examined glasses of basic composition after annealing then at 500–750 ° C, and found that they decomposed spinodally into calcium rich and calcium poor phases. He associated this phenomenon with observations in igneous rocks where coherent breakdown of natural pyroxenes leads to phases respectively enriched and impoverished in calcium, e.g. albite (= plagioclase?) and pigeonite respectively. Similarly, Barron (1981), in modelling spinodal decomposition in synthetic silicate systems, concludes that a subsolidus diopide-quartz melt immiscibility occurs 100–150 ° C below the diopside liquidus in both diopside-nepheline-quartz and diopside-leucite-quartz systems. Again, we may note the potential immiscible separation of Ca(-Mg) rich and Ca(-Mg) poor silicate liquids.

Implication of Glass Composition and Structure on the Radioactive Waste Burial in Rocks Containing Igneous Glass

Hydrothermal alteration in a waste repository under present design concepts considered by the United States Department of Energy will range from ambient

temperature to as high as 250 ° C. Most field observations, and experimental studies of natural glass alteration are at near earth surface temperatures. No studies have been made on basaltic glass hydrothermal alteration at significantly elevated temperatures. In fact, almost nothing is known of the relative kinetics of hydration and devitrification with increasing temperature in such glasses. We must speculate that increasing temperature will accelerate these processes in basaltic glasses.

The composition of the glass mesostasis in basaltic rocks can be quite variable, depending on the history of the magma, and its mode of cooling. In large flood basalt flows, cooling is slow, and the residual magmatic liquid can become highly enriched in silica. Although the silica content of the glass mesostasis may be as low as 65% wt% SiO_2, some basalt flows in Iceland contain mesostasis glass with SiO_2 concentrations of as high as 80 wt% (Kacandes et al., 1986). This is precisely the range of silica concentrations over which melt miscibility may occur (Philpotts and Doyle, 1982). Thus the mode of hydrothermal alteration of glass in basaltic flows may vary depending on its composition.

We may summarize the available evidence for glass alteration mechanisms in a repository environment in schematic diagrams as illustrated in Figures 6 and 7 for rhyolitic and basaltic glasses respectively. These diagrams are subject to modification as various issues and uncertainties are resolved.

Conclusions and Recommendations

From the foregoing discussions, we can draw the following conclusions.

1. Experimental and infrared spectroscopic evidence shows that the extent to which silicate glasses hydrate appears to be dependent on their composition.
2. Laboratory evidence on synthetic silicate glasses suggests that those rich in MgO and CaO are likely to devitrify rather than hydrate.

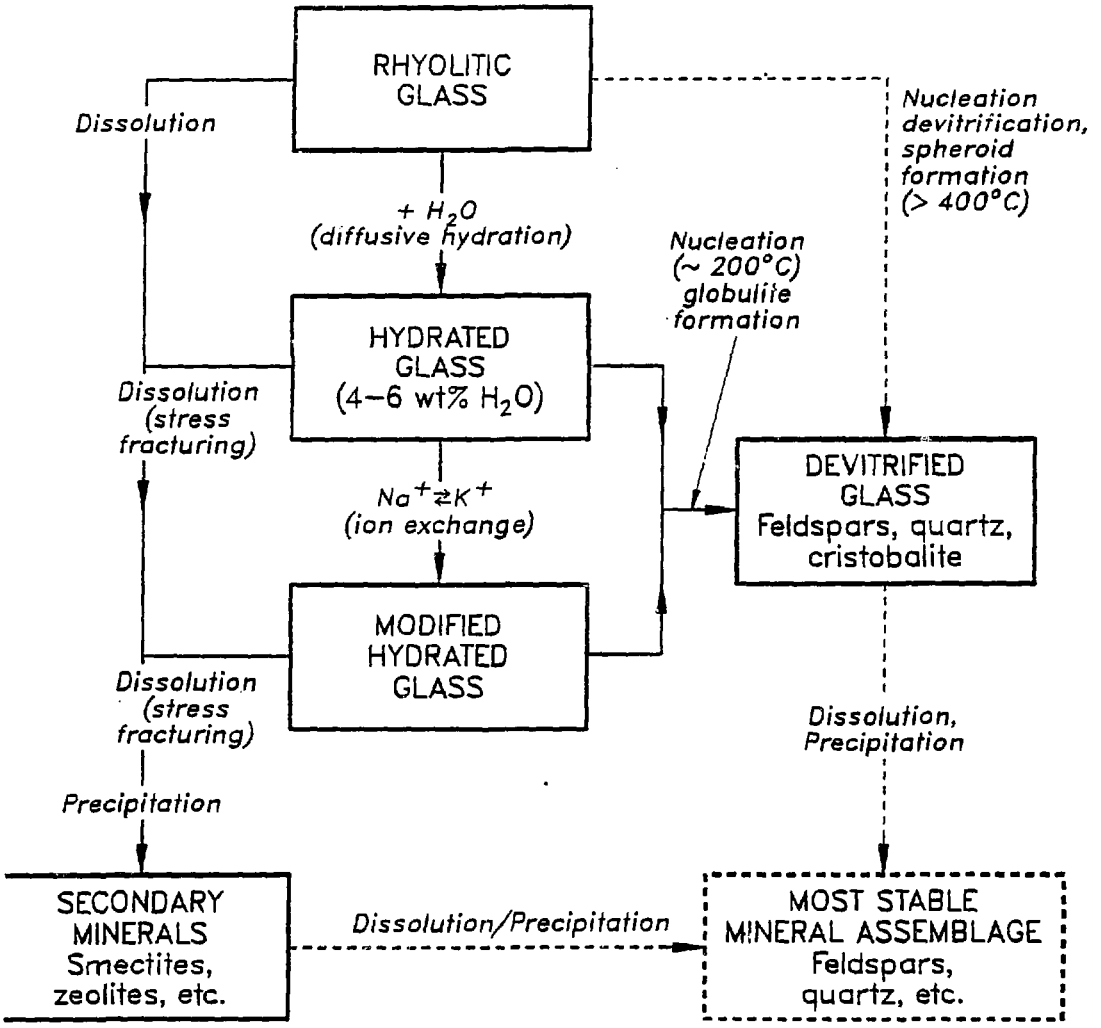

Figure 6. Schematic diagram to show the decomposition paths of rhyolitic glass when exposed to the aqueous phase.

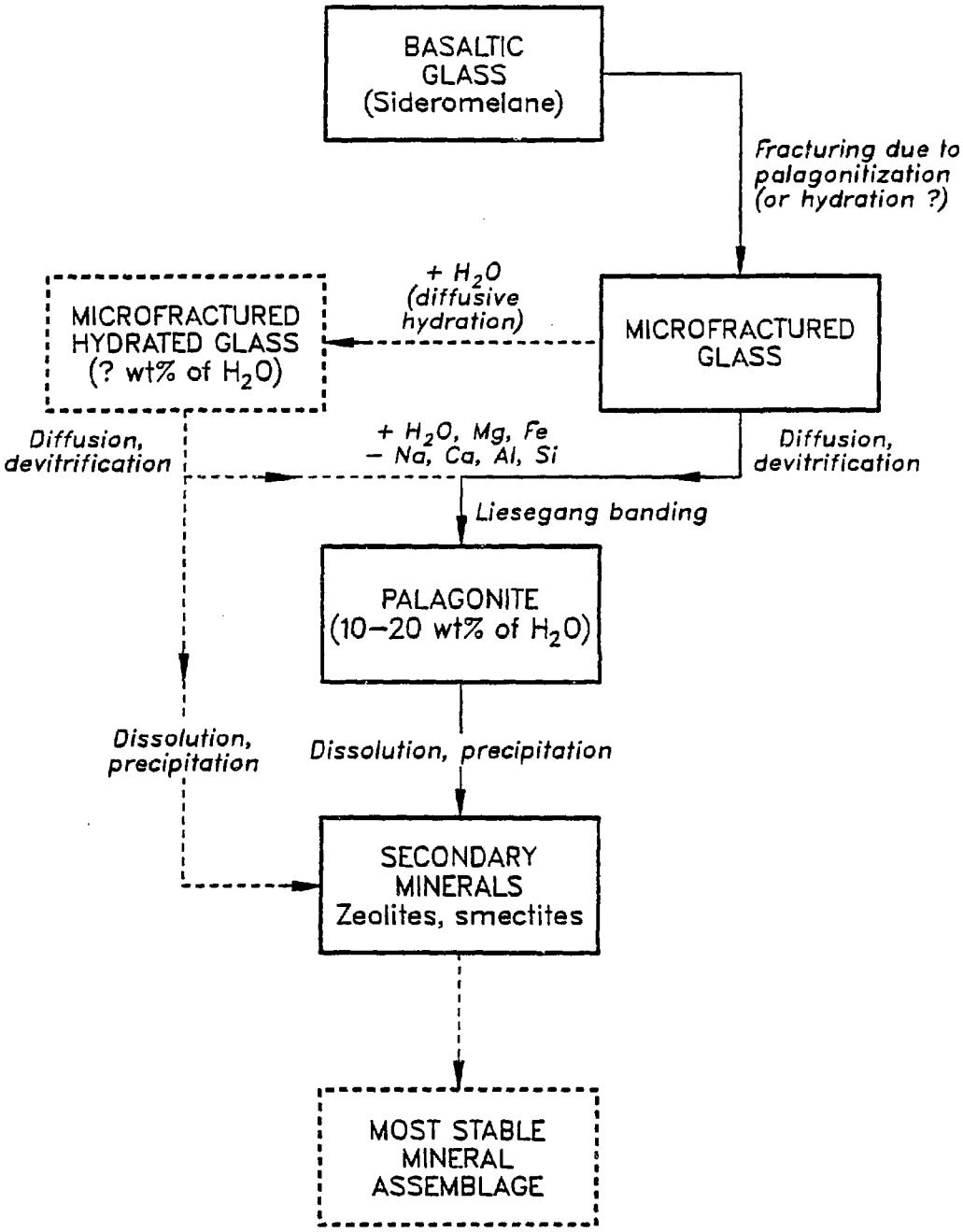

Figure 7. Schematic diagram to show the decomposition paths of basaltic glass when exposed to the aqueous phase.

3. Rhyolitic and rhyodacitic glasses can hydrate without apparent devitrification or breakdown of the glass structure.

4. Experimental evidence indicates that the hydration of rhyolitic glasses follows a parabolic role law, i.e. a diffusion controlled process is involved.

5. Rhyolitic and rhyodacitic glasses, when exposed to the aqueous phase under closed system conditions, at earth surface temperatures will hydrate to 5-6 wt% H_2O. In contrast, glasses of basaltic composition will either hydrate exceedingly slowly, or devitrify immediately upon hydration,

6. Circumstantial evidence suggests that increasing concentrations of MgO and CaO in alumino-silicate glass will substantially decrease the rate of hydration.

7. Basaltic glass, under open system aqueous conditions, will devitrify to form a weakly coherent rind of secondary clay minerals. The alteration front advances according to an effective zero order rate law, although a diffusion controlled process may be implicated in part due to the apparent formation or a Liesegang band texture. Evidence for glass hydration before devitrification is equivocal.

8. Hydration of a rhyolitic glass will greatly accelerate devitrification.

9. The reason for the different alteration mechanisms between rhyolitic and basaltic glasses may be due to differences in the structure of the glass as well as their polarisability.

10. Thermodynamic evidence suggests that the presence of alkali metal ions, eg Na^+ and K^+ in the interstices of charge compensated aluminosilicate glass structures tends to stabilize the tetrahedral framework, whereas the converse applies to alkali earth ions, e.g. Mg^{++} and Ca^{++}. This suggests that alkali metal aluminosilicates would be more likely to hydrate than alkali earth

aluminosilicates. Also, the latter would be more prone to devitrify than the former.

11. Thermodynamic evidence also indicates that alkali earth aluminosilicate melts have a tendency to display immiscibility phenomena in the silica rich region of binary SiO_2 - $M_{1/n}^{n+}AlO_2$ systems.

12. X-ray diffraction studies show that albite glass has a different structure from anorthite glass. This structural distinction may extend to similar differences between rhyolitic and basaltic glass structures.

13. Both petrographic observations and experimental phase equilibrium studies support the existence of an immiscible two liquid region at or below the solidus in differentiating basaltic magmas. This suggests the existence of structural differences between magmas of different silicic compositions, which might reasonably be expected to extend to structures of the corresponding glasses.

To provide convincing evidence of some of the tentative conclusions reached above will require further experiments.

An interesting approach would be to synthesize a range of glass compositions between rhyolite and basalt in composition, and then proceed with a complete characterization of their physical and transport properties, e.g. specific volume, heat capacity, compressibility, expansivity, electrical conductivity, refractive index. X-ray radial distribution functions and infrared spectra might also be measured with advantage. The goal for such characterization studies would be to establish whether a discontinuity exists in the properties of the glasses, and which reflects a structural difference, and at what composition this structural change occurs. Controlled experimental studies should then be made on selected glasses over a range of temperatures between 25 and 250°C to measure the rates of hydration, the saturation hydration, and the surface reaction rates with respect

to the aqueous phase.

With the results of such experiments in hand, it should then be possible to conduct modelling studies of the rate of alteration of the host rock glass in the immediate vicinity of the waste repository.

Acknowledgments

I am indebted to Mr. D. Snyder, University of California, Berkeley, and Dr. A. F. White, Lawrence Berkeley Laboratory for their critical review of this paper, and for helpful suggestions for its improvement.

This work was supported by the U.S. Nuclear Regulatory Commission, through NRC FIN No. B 040-6 under Interagency Agreement DOE-50-80-97, through U.S. Department of Energy Contract No. DE-AC03-76SF00098.

REFERENCES

Barron, L.M. 1981. The Calculated Geometry of Silicate Liquid Immiscibility. *Geochimica et Cosmochimica Acta* 45, p. 495-512.

Bender, M. L., Teh-Lung Ku, and Broecker, W. S., 1966, Manganese Nodules-Their Evolution. *Science* 151. p. 325-328.

Biggar, G.M., 1979. Immiscibility in Tholeiites. *Mineralogical Magazine* 43, p. 543-4.

Burnett, W.C. and Morgenstein, M., 1976. Growth Rates of Pacific Manganese Nodules as Deduced by Uranium-Series and Hydration-Rind Dating Techniques. *Earth and Planetary Science Letters* 33, p. 208-218.

Crovisier, J-L., Eberhart, J.P. and Honnorez, J., 1986. Dissolution of Basaltic Glass in Seawater; Mechanism and Rate. *Fifth International Symposium on Water-Rock Interaction, Reykjavik, Iceland. Extended Abstracts*, p. 142-145.

Crovisier, J.L., Thomassin, J.H., Juteau, T., Eberhart, J.P., Touray J.C., Baillif. P., 1983. Experimental Seawater-Basaltic Glass Interaction at 50 ° C: Study of Early Developed Phases by Electron Microscopy and X-ray Photoelectron Spectrometry. *Geochimica et Cosmochimica Acta* 47, p.377-387.

Delaney, J.R. and Karsten, J.L., 1981. Ion Microprobe Studies of Water in Silicate Melts: Concentration Dependent Water Diffusion in Obsidian. *Earth and Planetary Science Letters* 52, p. 191-202.

Della Mea, G., Dran, J.C., Petit, J-C., Bezzon, G., Rossi-Alvarez, C.R., 1984. New Data on Ion-Induced Modifications of Aqueous Dissolution of Silicates. *Materials Research Society Proceedings 26, Elsevier Science Publishing Co., Inc.* p. 747-754.

Federman, A., 1984. Hydration of Abyssal Tephra Glasses. *Journal of Non-Crystalline Solids* 67, p. 323-332.

Fisher, G.W. and Lasaga, A.C., 1981. Irreversible Thermodynamics in Geology, in *Reviews in Mineralogy*, v. 8, *Kinetics of Geochemical Processes*. (A.C. Lasaga and R.J. Kirkpatrick, Eds.), Ch. 5, p. 171-209.

Forsman, N.F., 1984 Durability and Alteration of Some Cretaceous and Pyroclastic Glasses in North Dakota. *Journal of Non-Crystalline Solids* 67, p.449-461.

Freestone, I.C., 1979. Immiscibility in Tholeiites. *Mineralogical Magazine* 43, p. 544-546.

Friedman, I.I., 1968. Hydration Rind Dates Rhyolite Flows. *Science* 159, p. 878-880.

Friedman, I.I. and Smith, R.L. 1960. A New Dating Method using Obsidian - Part I. The Development of the Method. *American Antiquity*, 25, p. 476-522.

Friedman, I. and Long, W., 1976. Hydration Rate of Obsidian. *Science* 191, p. 347-352.

Friedman, I., Long, W., Smith, R.L., 1963. Viscosity and Water Content of Rhyolite Glass. *Journal of Geophysical Research* 68, p.6523-6535.

Friedman, I., Smith, R., Long, W., 1966. Hydration of Natural Glass and Formation of Perlite. *Geological Society of America Bulletin* 77, p. 323-328.

Friedman, I. and Long W., 1984. Volcanic Glasses, their Origins and Alteration Processes. *Journal of Non Crystalline Solids* 67, p. 127-133.

Furnes, H., 1975. Experimental Palagonitization of Basaltic Glasses of Varied Composition. *Contributions to Mineralogy and Petrolology* 50, p. 105-113.

Gibbs, J.H. and DiMarzio E.A., 1958. Nature of the Glass Transition and the Glassy State. *Journal of Chemical Physics* 28, p. 373-383.

Goldstein, M., 1976. Viscous Liquids and the Glass Transition. V. Sources of the Excess Specific Heat of the Liquid. *Journal of Chemical Physics* 64, p. 4767-4774.

Hekinian, R. and Hoffert, M., 1975. Rate of Palagonization and Manganese Coating on Basaltic Rocks From the Rift Valley in the Atlantic Ocean Near 36 deg.50'. *Marine Geology* 19, p. 91-109.

Jezek, P. and Noble, D., 1978. Natural Hydration and Ion Exchange of Obsidian: An Electron Microprobe Study. *American Mineralogist* 63, p. 266-273.

Kacandes, G.H., Ulmer, G.C. and Grandstaff, D. E. 1986. Icelandic Geothermal Fields as an Analog for Nuclear Waste Isolation in Columbia Plateau (Washington, U.S.A.) Basalt. *Fifth International Symposium on Water-Rock Interaction, Reykjavik, Iceland. Extended Abstracts*, p. 302-305.

LaMarche, P.H., Rauch, F., Lanford, W.A., 1984. Reaction Between Water and Textite Glass. *Journal of Non-Crystalline Solids* 67, p. 361-369.

Lofgren, G. E., 1968. *Experimental Devitrification of Rhyolite. Glass.* PhD Dissertation, Stanford University, 99 p.

Manankov, A.V., 1979. Mechanism of Liquid Immiscibility in Silicate Systems. *Doklady Akademia Nauk SSSR* 246, p. 102-105.

Marshall, R.R, 1961. Devitrification of Natural Glass. *Geological Society of America Bulletin* 72, p. 1493-1520.

McMillan, P., Piriou, B. and Navrotsky, A., 1982. A Raman Spectroscopic Study of Glasses Along the Joins Silica-Calcium Aluminate, Silica-Sodium Aluminate, and Silica-Potassium Aluminate. *Geochimica et Cosmochimica Acta* 46, p. 2021-2037.

Meighan, C.W., Foote, L.J., Aiello, P.V., 1968. Obsidian Dating in Western Mexican Archeology. *Science* 160, p. 1069-1075.

Michels, J.W., Tsong, I.S.T., Nelson, C.M., 1983. Obsidian Dating and East African Archeology. *Science* 219, p. 361-366.

Moore, J.G., 1966. Rate of Palagonitization of Submarine Basalt Adjacent to Hawaii, *U.S. Geological Survey Professional Paper* 550-D, p. D163-D121.

Moore, J.G., 1970. Water Content of Basalt Erupted on Ocean Floor. *Contributions to Mineralogy and Petrology* 28, p,. 272-279.

Morgenstein, M. and Riley, T., 1974. Hydration-Rind Dating of Basaltic Glass: A New Method for Archaeological Chronologies. *Asian Perspectives* p. 145-159.

Moriya, Y. and Nogami, M., 1980. Hydration of Silicate Glass in Steam Atmosphere. *Journal of Non-Crystalline Solids* 39, p. 667-672.

Muffler, L.P., Short, J.M., Terry, E.G., Smith, V.C., 1969. Chemistry of Fresh and Altered Basaltic Glass from the Upper Triassic Hound Island Volcanos, Southeastern Alaska. *American Journal of Science* 267, p. 196-209.

Navrotsky, A., Peraudeau, G., McMillan, P. and Coutures, J.-P., 1982. A Thermochemical Study of Glasses and Crystals Along the Joins Silica-Calcium Aluminate and Silica-Sodium Aluminate. *Geochimica et Cosmochima Acta* 46, p. 2039-2047.

Navrotsky, A., Geisinger, K.L., McMillan, P. and Gibbs G. V., 1985. The Tetrahedral Framework in Glasses and Melts - Inferences from Molecular Orbital Calculations and Implications for Structure, Thermodynamics and Physical Properties. *Physics and Chemistry of Minerals* 11, p. 284-298.

Navrotsky, A., Hervig, R.L., Roy, B.N. and Huffman, M. 1985. Thermochemical Studies of Silicate, Aluminosilicate, and Borosilicate Glasses. *High Temperature Science* 19, p. 133-149.

Ninkovich, D. 1979. Distribution, Age and Chemical Composition of Tephra Layers in Deep Sea Sediments of Western Indonesia. *Journal of Volcanology and Geothermal Research,* 5 p. 67-86.

Philpotts, A.R., 1976. Silicate Liquid Immiscibility: Its Probable Extent and Petrogenetic Significance. *American Journal of Science*, 276, p. 1147-1177.

Philpotts, A.R., 1977. Silicate Liquid Immisibility in Tholeiitic Basalts. *Journal of Petrology* 20, p. 99-118.

Philpotts, A.R., 1978. Textural Evidence for Liquid Immiscibility in Tholeiites *Mineralogical Magazine* 42, p. 417-425.

Philpotts, A.R. and Doyle, C.D., 1982. Effect of Magma Oxidation State on the Extent of Silicate Liquid Immiscibility in a Tholeiitic Basalt. *American Journal of Science* 283, p. 967-986.

Philpotts, A.R., and Doyle, C.D., 1980. Immiscibility in Tholeiites: a Discussion. *Mineralogical Magazine* 43, p.939-940.

Pierce, K.L., Obradovich, J.D., Friedman, I., 1976. Obsidian Hydration Dating and Correlation of Bull Lake and Pinedale Glaciations near West Yellowstone, Montana. *Geological Society of America Bulletin* 87, p. 703-710.

Raines, G.E., Rickertsen, L.D., Claiborne, H.C., McElroy, J.L. and Lynch, R.W., 1981. Development of Reference Conditions for Geologic Repositories for Nuclear waste in the USA. *Scientific Basis for Nuclear Waste Management.* (John G. Moore, Ed.), Plenum Press, New York, p. 1-10.

Richet, P. and Bottinga, Y., 1983. Verres, Liquides et Transition Vitreuse. *Bulletin Mineralogique* 106, p. 147-168.

Roy, B.N. and Navrotsky, A., 1984. Thermochemistry of Charge-Coupled Substitutions in Silicate Glasses. The Systems $M^{n+}_{1/n}AlO_2$–SiO_2 (M = Li, Na, K, Rb, Cs, Mg, Ca, Ba, Pb). *Journal of the American Ceramic Society.* 67, p. 606-

610.

Scheidegger, K.F., 1973. Volcanic Ash Layers in Deep Sea Sediments and their Petrolgical Significance. *Earth and Planetary Science Letters* 17, p. 397-407.

Scheidegger, K.F., Jezek, P.A., Ninkovich, D., 1978. Chemical and Optical Studies of Glass Shards in Pleistocene and Pliocene Ash Layers from DSDP Site 192, North-West Pacific Ocean. *Journal of Volcanology and Geothermal Research* 4, p. 99-116.

Scheidegger, K.F., and Kulm, L.D., 1975. Late Cenozoic Volcanism in the Aleutian Arc: Evidence from Ash Layers in the Northeastern Gulf of Alaska. *Geological Society of America Bulletin* 86, p. 1407-1412.

Scholze, H., 1959. Der Einbau des Wassers in Gläsern I. *Glastechnische Berichte* 32, p. 81-88.

Scholze, H., 1959. Der Einbau des Wassers in Gläsern II. *Glastechnische Berichte* 32, p. 142-152.

Scholze, H., 1959. Der Einbau des Wassers in Gläsern III. *Glastechnische Berichte* 32, p. 278-280.

Scholze, H., 1966. Gases and Water in Glass. *The Glass Industry*, p. 546-551. 622-628, 670-675.

Staudigel, H. and Hart, S., 1983. Alteration of Basaltic Glass: Mechanisms and Significance for the Oceanic Crust-Seawater Budget. *Geochimica et Cosmochimica* 47, p. 337-350.

Stolper, E., 1982. Water in Silicate Glasses: An Infrared Spectroscopic Study. *Contributions to Mineralogy and Petrology* 81, p. 1-17.

Taylor, M. and Brown, G., 1978. Structure of Mineral Glasses-I. The Feldspar Glasses $NaAlSi_3O_8$, $KAlSi_3O_8$, $CaAl_2Si_2O_8$. *Geochimica et Cosmochimica* 43, p. 61-75.

Taylor, M. and Brown, G., 1978b. Structure of Mineral Glasses-II. The SiO_2-$NaAlSiO_4$ Join. *Geochimica et Cosmochimica* 43, p. 1467-1473.

Taylor, M. and Brown, G. and Fenn, P., 1980. Structure of Mineral Glasses-III. $NaAlSi_3O_8$ Supercooled Liquid at 805 ° C and the Effects of Thermal History. *Geochimica et Cosmochimica* 44, p. 109-117.

U.S.DOE, 1980. Minerals that could be Used to Contain Radionuclides. *Management of Commercially Generated Radioactive Waste.* Final Environmental Impact Statement, Volume 2, Appendices, U.S. Department of Energy DOE/EIS-0046F p. p1-p52.

Wang, J.S.Y., Tsang, C.F., Cook, N.G.W. and Witherspoon, P.A., 1979. A Study of the Regional Temperature and Thermodynamic Effects of an Underground Repository for Nuclear Waste in Hard Rocks. Lawrence Berkeley laboratory Report LBL-8271 Rev., 60 p.

White, A.F. and Yee, A. 1986. Near-Surface Alkali Diffusion into Glassy and Crystalline Silicates at 25 ° C to 100 ° C, in *Geochemical Processes at Mineral Surfaces.* (J.A. Davis and K.F. Hayes, Eds.) *A.C.S. Symposium Series* 323. The American Chemical Society, Washington, D.C. Chapter 28, p. 587-598.

Wu, C.-K., 1980. Stable Silicate Glasses containing up to 10 Weight Percent of Water. *Journal of Non Crystalline Solids* 41, p. 381-398.

Yoko, T., Huang, Z., Kamiya, K., Sakka, S., 1983. Hydration of Silicate Glasses by Water Vapor at High Temperatures. *Glastechnische Berichte* XIII Internationaler Glaskongress, July 4-9, 1983, Hamburg. Deutschen Glastechnischen Gesellschaft, Frankfurt am Main, p. 650-655.

RADIATION DAMAGE IN NUCLEAR WASTE GLASS

Jeffrey F. DeNatale
Department of Mechanical Engineering
University of California
Davis, California, 95616

Abstract

Silicate glass is a promising material for the containment of nuclear wastes. The need for an accurate characterization of the waste properties makes an understanding of the radiation response of the glass an important issue. There are a number of ways in which the self-generated radiation may affect the glass, both in terms of its structure and chemistry. There are also a number of different techniques for characterizing these effects and it is important to be aware of their limitations and the significance of these measurements.

The radiation damage to simulated nuclear waste glass appears as the decomposition of the glass. This is often accompanied by the formation of sub-micron oxygen bubbles and the development of an amorphous phase separation. This type of damage has been observed under electron, gamma and ion irradiations, and a comparison of the separate responses can be used to quantitatively determine the radiation effect in nuclear waste glasses.

The proposed use of a borosilicate matrix for the immobilization of high level nuclear waste is associated with its ease of processing and the view of its structure as highly entropic. Thus, it can accomodate the large and varying number of constituents in the waste stream, particularly those with high alkali content for which no appropriate ceramic has been found. The issue of the radiation damage to alkali-silicate glasses is therefor particularly appropriate.

The wastes themselves are highly toxic and long lived, requiring isolation from the biosphere for times on the order of 10^5 years. Because of these long containment times, accurate characterization of the waste form properties is essential and any deterioration in these properties could potentially have major implications on the waste retention. The self generated radiation is one such factor, since radiation is known to be capable of inducing significant changes.

The storage materials for commercial nuclear wastes must witnstand extremely large radiation exposures, which arise from the decay of fission products (Cs, Sr) and actinides (U, Np, Pu, Am, Cm). The fission product decay produces primarily beta-gamma events and atomic transmutations (such as $^{90}Sr \rightarrow {}^{90}Y \rightarrow {}^{90}Zr$).
The actinides are responsible for the alpha decay, which produces an high-energy alpha particle and a heavy, low energy recoil nucleus. The actinides will also produce a

minor amount of damage from (α,n) reactions. Figure 1 and Table 1 illustrate the large numbers of these reactions that are anticipated for commercial wastes. For the case of defense wastes these values will be lower by approximately two orders of magnitude but still these doses are not negligible.

There are a number of different ways in which irradiation can affect a glass. Of these, displacement and ionization damage represent the major sources of structural alteration, and atomic transmutation only a minor component of the structural rearrangement. The effects of solution radiolysis will only affect the stability of the glass during leaching and thus are confined to the glass surfaces.

Displacement damage occurs when an incident particle transfers sufficient kinetic energy to an atom to displace it from its lattice site. These displaced atoms, if imparted with sufficient kinetic energy, may cause subsequent displacements leading to the formation of so-called collision cascades. This process occurs through interactions with the nuclei of the target atoms, and hence these events are often referred to as nuclear interactions. The interstitials and vacancies so formed, if sufficiently mobile, may aggregate and lead to the formation of extended defects which may alter the density and other physical properties of the material. The sensitivity of a material to displacement damage is generally quantified by a

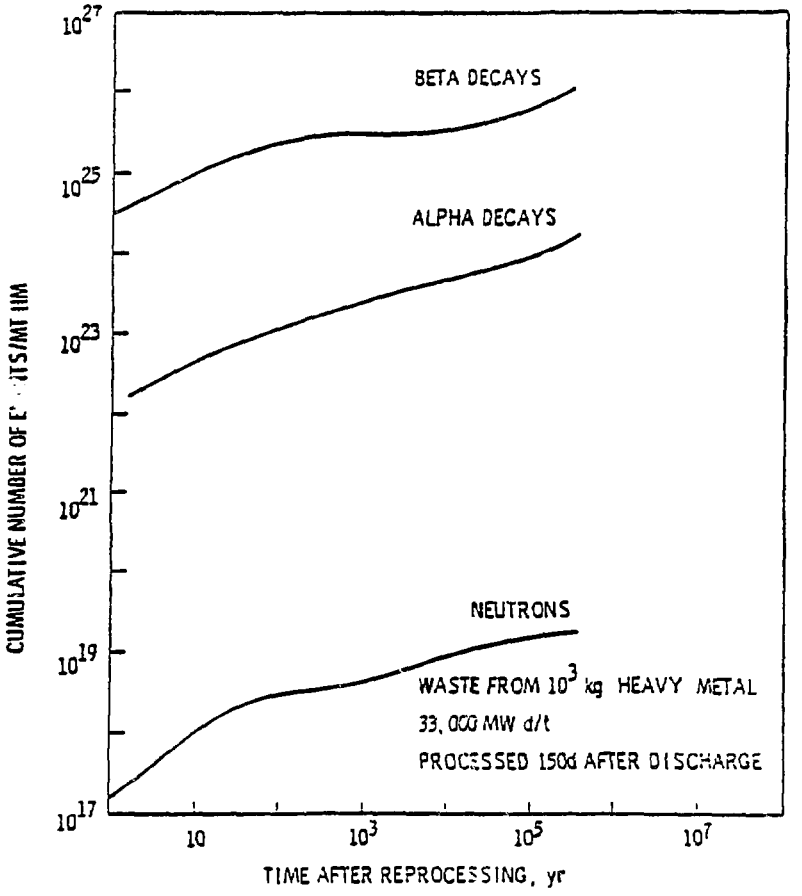

1. Cumulative numbers of decay events for a commercial high level waste [18].

Table 1:

ATOMIC DISPLACEMENTS IN COMMERCIAL HIGH LEVEL WASTE

Radiation	Energy	Displacements per Decay	Energy Lost in Elastic Collisions
Alpha Particles	6 MeV	140	6-8 keV
Alpha Recoil	100 keV	1500	100 keV
Beta	>0.5 MeV	0.13	<0.1 keV
Gamma	2 MeV	---	<<0.1 keV

characteristic displacement cross section, which will depend on the amount of energy needed to remove an atom from its site. The amount of structural damage induced may be conveniently represented in terms of the proportion of lattice atoms displaced from their sites, referred to as displacements per atom (dpa).

The alpha recoil nuclei represent the major source of the displacement interactions in the waste. The alpha particles in comparison lose only a small fraction of their energy to displacement processes, and the role of beta particles is much less still. The gamma quanta will be negligible in terms of producing displacement damage, which arises only through the generation of secondary electrons. Neutrons, while individually effective in producing atomic displacement, are comparatively minor in terms of the total amount of damage generated in the waste [1]. The comparison of these processes is illustrated in figure 2 and table 2.

The other means of inducing significant structural damage is by ionization damage, or radiolysis. This arises from interactions of the incident radiation with the orbital electrons of the target atoms and if one of these interactions leads to the creation of a localized excitation, the decay may occur mechanically, resulting in a bond fragmentation. The sensitivity to this type of damage is highly material specific, in contrast to displacement damage which occurs in all materials for

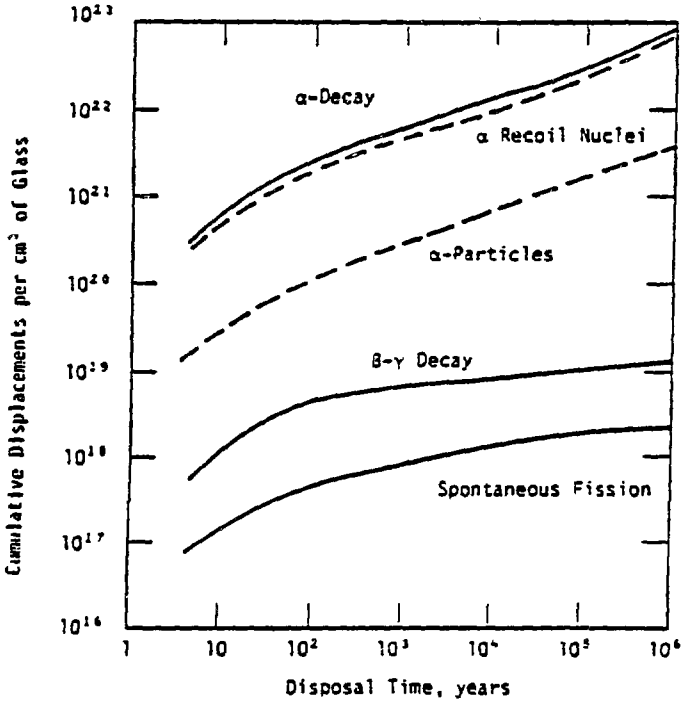

2. Cumulative atomic displacements due to the different decay reactions for a commercial high level waste [18].

sufficiently energetic particles. The sensitivity to ionization damage is primarily related to the ability of the material to delocalize the excitation energy. For metals these interactions are quickly dissipated, and hence the influence of ionization damage to metals may be ignored. For organics [2] and many ceramics, however, these interactions often represent the major source of damage. The structural influence of radiolysis may be quantified by the radiolytic yield, G, which represents the number of bond fragmentation events resulting from the absorption of 100 eV of ionizing energy [3].

The sources of ionizing radiation in commercial wastes are illustrated in figure 3. Beta-gamma decay is the major source of ionization events in the waste for the first 1000 years of storage, after which alpha decay becomes dominant.

A comparison between the two types of damage is not without complication because of the differences in their formation mechanisms. The comparison in terms of the energy deposition into the two processes, which is shown in figure 4 for commercial waste, is therefore rather arbitrary but it is apparent that ionization effects could be significant if a means exists for converting the excitation energy into structural damage [1].

Another influence of the radiation to the waste material is through solution radiolysis. This arises from the interaction of the self-generated ionizing radiation with any water that may contact the glass. This

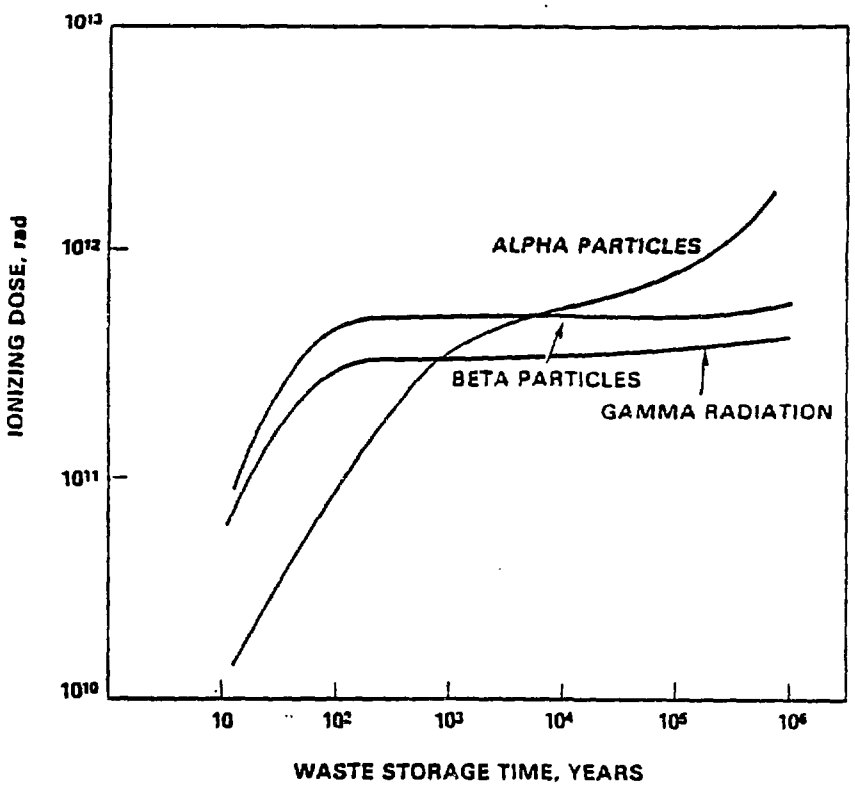

3. Sources of ionizing radiation in a commercial high level waste [19].

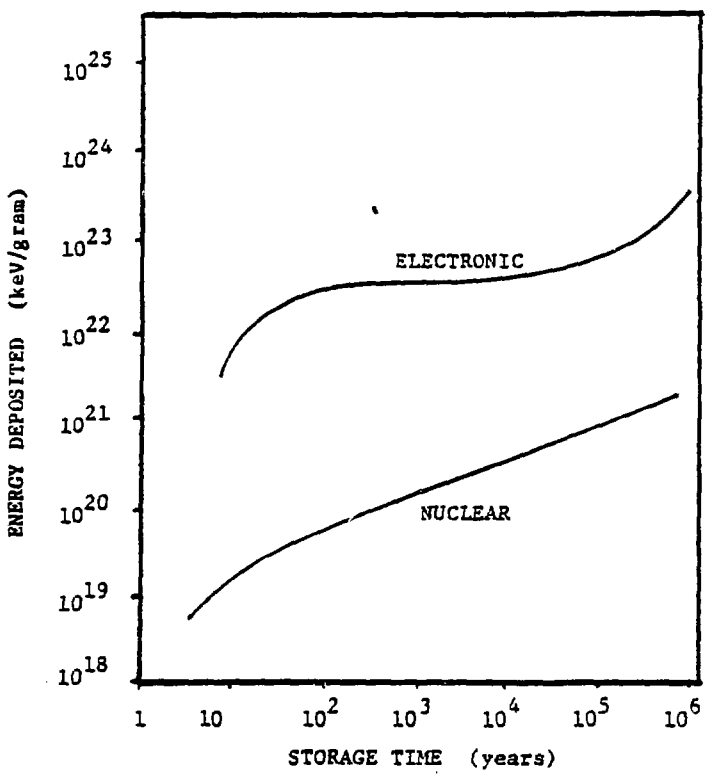

4. Comparison of energy deposition into nuclear and electronic processes for a commercial high level waste.

interaction may lead to the formation of active species and enhancement of the solution-surface reactions. This may be especially severe in the case of air-saturated solutions, since this allows the formation of nitric acid as one of the radiolysis products. The enhancement of the solution-surface reactions by the presence of ionizing radiation has been shown by both in-situ studies [4] and by bulk investigations [1,5].

Atomic transmutation may also represent a source of damage to the waste storage material, arising primarily from the decay of ^{137}Cs and ^{90}Sr. This may cause changes in the coordination, bonding, valence, and size of the atomic species. These effects may be especially important in crystalline ceramics with site specific incorporation of radionuclides. Although the importance of this effect in amorphous silicates has not yet been characterized, the structural significance is small in comparison to the thousands of interactions associated with each energetic particle.

Finally, helium pressurization arising from alpha decay may lead to cracking of the waste form. This is important since it introduces additional surface area to any groundwater that may contact the waste, increasing the net leaching process proportionately.

Approaches to Investigation

There are a number of different approaches to the

evaluation of radiation damage in a radioactive waste storage material. These fall into the general categories of internal and external techniques. While all may be useful, one must be aware of the limitations of each in the interpretation of the results and the selection of complementary techniques.

Internal Techniqes

Actinide Doping

Actinide doping is one of the most widely used simulation techniques. This method involves incorporation of a short lived actinide such as ^{244}Cm or ^{230}Pu into the waste material to accelerate the damage by alpha decay. This technique has a number of advantages, such as the ability to provide both ionization and displacement effects through alpha particles and recoil nuclei. It also is quite isotropic, resembles the actual waste behavior, and provides for the helium generation the actual waste will encounter. It is of limited value, however, in extracting fundamental information on the radiation response, and requires glove box handling in the preparation and analysis of specimens. One must also take care to insure that the correct isotope distribution is achieved, again a point of major importance for crystalline materials.

External Bombardment Techniques

Ion Irradiation

Bombardment with high energy ions may be a useful technique for investigating the fundamental damage to a waste material. It is convenient since one may choose the ion species and energy to give the desired distribution of energy into nuclear and electronic processes. This can be used to identify the origin of damage effects by seeing if the damage correlates to the nuclear or electronic energy deposition density [6]. The major limitations of this technique concern the shallow ion range, the introduction of impurities from the ion beam itself, and the highly directional flux. These factors must be addressed in the extrapolation of ion damage results, however, since they may lead to deviations from bulk behavior [1,7].

Gamma Irradiation

Gamma irradiation may also be a valuable tool for investigating the process of damage to the waste material. While the damage induced may be significantly different than that which the actual waste will experience, the gamma irradiation provides an intense source of ionizing radiation, allowing one to identify the specific defects and damage responses associated with ionization interactions.

Electron Irradiation

In-situ electron irradiation provides a means of

characterizing many of the parameters that the damage depends upon. By performing the studies in an HVEM one can reduce the influence of thin film effects on the damage aggregation, and extract useful information about the temperature, energy, and flux dependances of damage. One must address the limitations of this approach in the extrapolation to bulk material response, however, since there may be differences in the defect distributions and kinetics [8]. Similarly, since high energy electrons are a source of both ionization and displacement events, it may be difficult to distinguish the separate effects of each.

The other atomistic approaches to the analysis of nuclear waste glasses involve the use of spectroscopic techniqes to characterize the local changes in atomic arrangement with the progression of damage. This approach has proven valuable in the characterization of simpler systems such as vitreous silica, and while it may provide some useful chemical information, its limitations with regards to the description of aggregated defect behavior hinders its value in the application to such complex systems.

The approach to characterization of radiation effects in nuclear waste glasses has been mostly to monitor the responses of their bulk properties with increasing radiation exposure. There are a number of different bulk properties that are affected by radiation. These include density, stored energy, mechanical behavior, and resistance

to chemical attack (leachability). Most of these properties show a saturation effect, though the dose at saturation may depend on the experimental conditions. Bulk investigations are convenient, and may provide useful information although they can be misleading, as in the case of density measurements when aggregated defects have formed. In addition, since the measurements reveal nothing about the chemistry or structure of the material, they provide no indication of the fundamental response of the glass.

In order to generate a quantitative description of the way in which radiation affects nuclear waste glasses, the distinction between ionization and displacement effects, which can often produce similar damage structures, must be made. To characterize the separate effects of each, a range of radiation types must be used to provide a variation in the energy deposition into the two processes. The work presented here describes the application of this approach to waste glass behavior using complementary techniques to characterize the fundamental damage process. The particular glass used is a simulated commercial waste storage glass developed by Battelle Laboratories for Purex wastes (PNL 76-86) [9,10].

In situ electron irradiations can be used to characterize the microstructural defects that form in the waste glass under high energy irradiation, and these studies, performed at the National Center for Electron

Microscopy using 1500 keV electrons, showed that two major aggregated defects are formed: sub-micron gas bubbles and an amorphous phase decomposition.

Irradiation of the glass at elevated temperatures to fluences in excess of abot $6x10^{20}$ electrons per square centimeter leads to the formation and growth of oxygen bubbles within the glass [10,11]. With further irradiation, these bubbles can grow quite large through coarsening and coalescence, inducing large volume expansions of the glass in the later stages of growth, figure 5.

The sensitivity of PNL 76-68 glasses to bubble formation is a function of temperature, and they are most sensitive at approximately 250 °C, figure 6. Little damage is incurred at room temperature in this particular glass and although for other types of glass this peak may shift or broaden, the general shape of the curve is quite reproducable [12]. The characterization of the temperature dependance of damage is an extremely important parameter in the interpretation of radiation damage effects in waste forms due to the increased temperatures the storage materials will encounter.

Irradiation may also induce an amorphous phase separation, figure 7, not attributable to thermal effects [10,11]. Analysis of this separation using X-ray energy dispersive spectroscopy has shown the segregation to involve redistribution of the heavy metals to one phase at

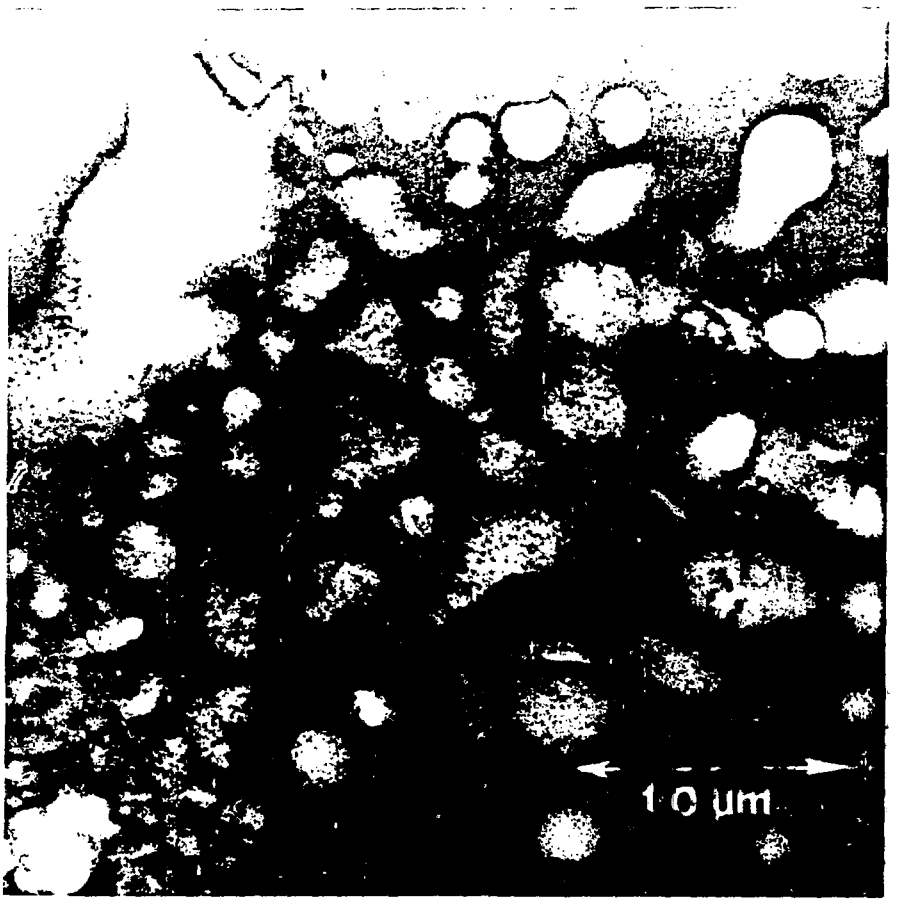

5. Bubble formation in a simulated PNL 76-68 waste glass irradiated with high energy electrons.

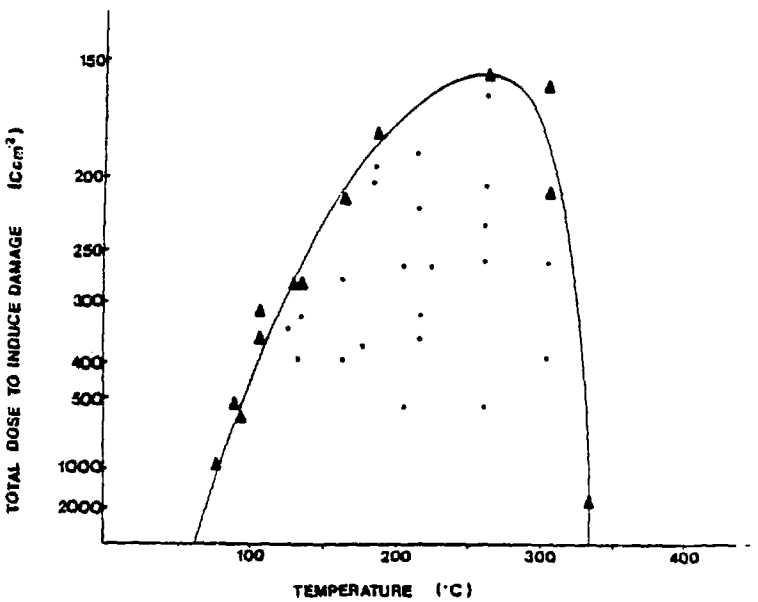

6. Temperature dependance of the dose necessary to form bubbles by electron irradiation in the waste glass.

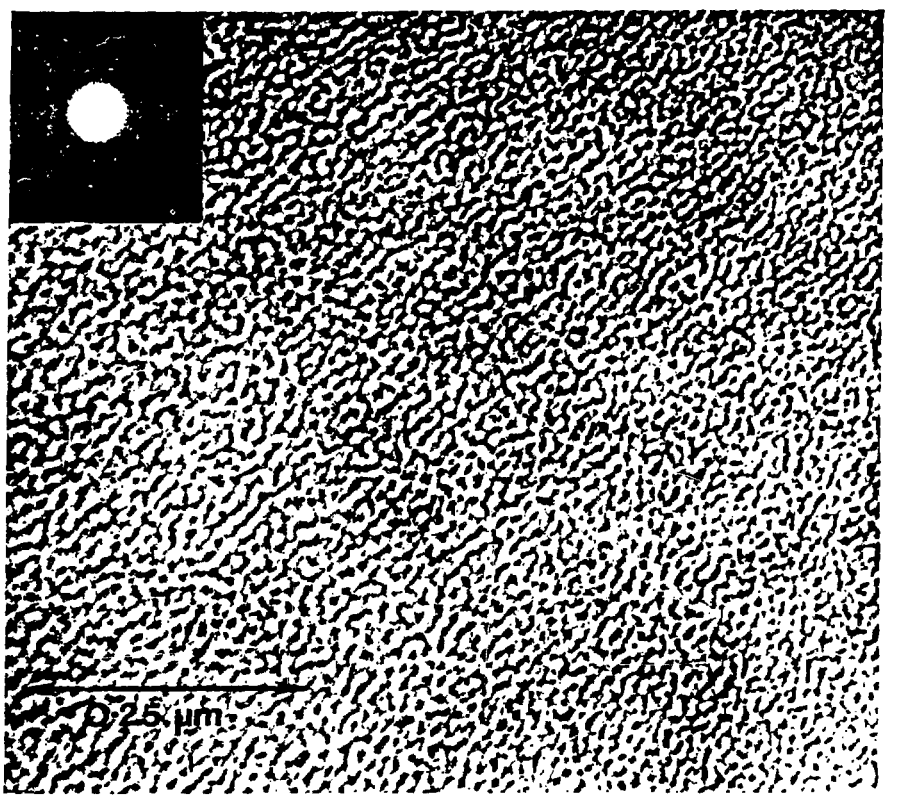

7. Phase separation in the waste glass induced by electron irradiation.

the expense of the other, as would be consistent with the mass thickness contrast observed [11]. This separation is often observed in the later stages of bubble growth, and can produce some interesting interactions, particularly the regression and ultimate disappearance of previously formed bubbles [11]. It is believed that this occurs through the introduction of a path of higher diffusivity, allowing the interior gas to escape. Indeed, a quantification of this observation produces a diffusion coefficient consistent with molecular oxygen in high silica glass, and the introduction of such a rapid transport path may be important to the leaching behavior.

In the past, there have been observations of related damage in electron irradiated glasses. Todd and Lineweaver [13] originally reported the generation of molecular oxygen in electron irradiated glasses, which required the presence of additional cation species in the silica network. Later microstructural observations of bubble formation noted that their rapid formation rates were inconsistent with the limited mobility of oxygen in silica glass [14]. This anomaly can be resolved, however, by a cation controlled process in which the bubbles form by the collapse of the oxygen rich network following a local cation depletion [11]. This importance of the cation species is contrasted by the behavior of vitreous silica, which neither forms bubbles nor evolves oxygen under electron irradiation. This underscores an important point, namely that the

fundamental radiation responses of vitreous silica and modified silicate glasses are distinctly different. Work by Arnold [6] has shown a similar difference in their responses to heavy ion irradiation.

Formation of the bubbles is not unique to the waste glasses and has been observed in binary alkali silicates as well. A comparison of the behaviors of sodium, lithium and potassium containing glasses has shown the formation of the bubbles to be correlated with the difference between the cation diffusivity and that of molecular oxygen, consistent with the proposed aggregation mechanism.

To characterize these bubbles, one must identify whether they arise from the ionization or displacement component of the electron beam. From the rates at which they form, it is found that one cannot generate enough displacement activity in the glass to account for the damage by a direct displacement mechanism [15]. Thus, one can conclude that the primary damage event is radiolytic in nature, and simulations of this effect must consider the ionization component of the waste spectrum.

The importance of the ionization component is supported by the response of the glass to gamma irradiation. Samples were iradiated using a ^{60}Co source to a total dose of 9.1×10^{9} Rads and an examination of the foils showed that one could indeed generate this same type of porosity, figure 8 [16]. The uniformity of the damage in the gamma irradiated sample is

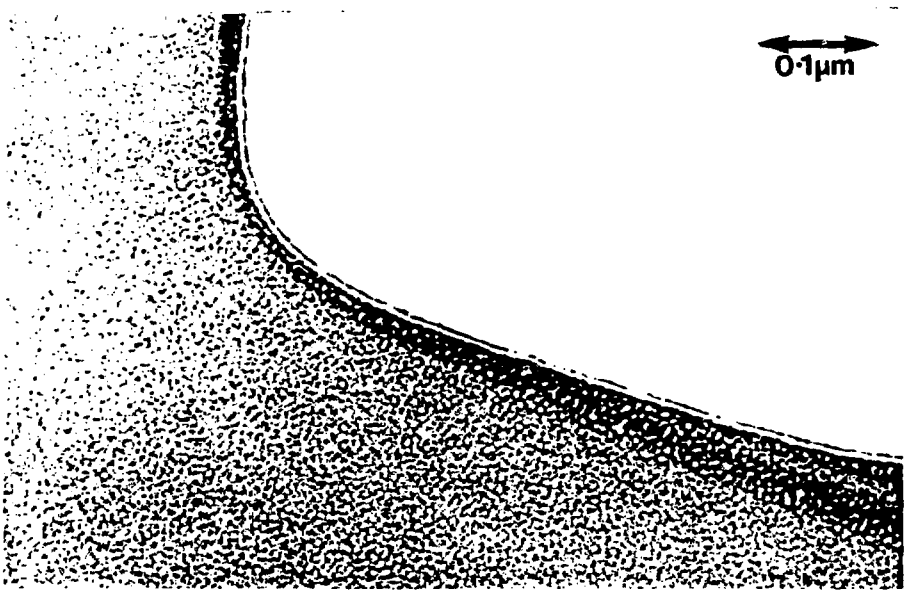

8. Bubble formation in the waste glass induced by gamma irradiation to a dose of 9.1×10^{9} rads.

significantly higher than for the electron case, and this is easily attributable to the differences in their irradiation intensity distributions.

One other major distinction between the electron and gamma responses comes in the quantification of the damage sensitivity. By calculating the amount of oxygen released from the network for the applied ionization dose, one can calculate the efficiency of bubble formation. If we assume that the primary damage events in the two cases can be described by the same radiolytic yield, then the bubble formation by gamma irradiation is found to be more efficient by approximately two orders of magnitude over the electron case. The difference is likely attributable to the large difference in dose rate between the two irradiations, which is consistent with the radiation responses of other materials [17]. This large difference in the quantitative assesment of damage illustrates the importance of identifying how strongly the damage behavior may be influenced by variables such as the irradiation flux.

It is unlikely that the synergistic effects of the various processes will be significant in the waste glass and this is supported by the response of the glass to heavy ion bombardment, where one introduces an intense displacement component along with the ionization. Again, a similar porosity develops in the glass after most types of ion bombardment. While irradiation with inert gas ions

also induces an additional component of the porosity due to gas implantation, this is not the case with lead ion irradiation. An example of the microstructure formed after irradiation with 250 keV lead ions to a fluence of $5x10^{14}$ ions per square centimeter is shown in figure 9. The ionizing dose corresponding to this fluence is approximately 10^{10} Rads, and it is noteworthy that irradiation to a comparable dose with gamma rays produces a very similar microstructure, even with an enormous difference in the amount of displacement activity. Quantification of the damage sensitivity shows the lead ion response to be intermediate between those of the gamma and the electron irradiations.

From a comparison of the electron, gamma, and ion irradiations we may deduce a number of important points about the behavior of the waste glass. Firstly, the ionization component is the important factor in the formation of microstructural damage. While displacement effects may contribute to some structural damage, their role at the microstructural level is minor. Secondly, The sensitivity of the glass to this type of damage is higher than was previously believed based solely on the electron damage results. The effects of the development of porosity to waste storage behavior can be expected to occur early enough in storage to be of concern. This is apparent from the brief storage time required to accumulate an ionization dose of 10^{10} Rads (see figure 3). This also indicates

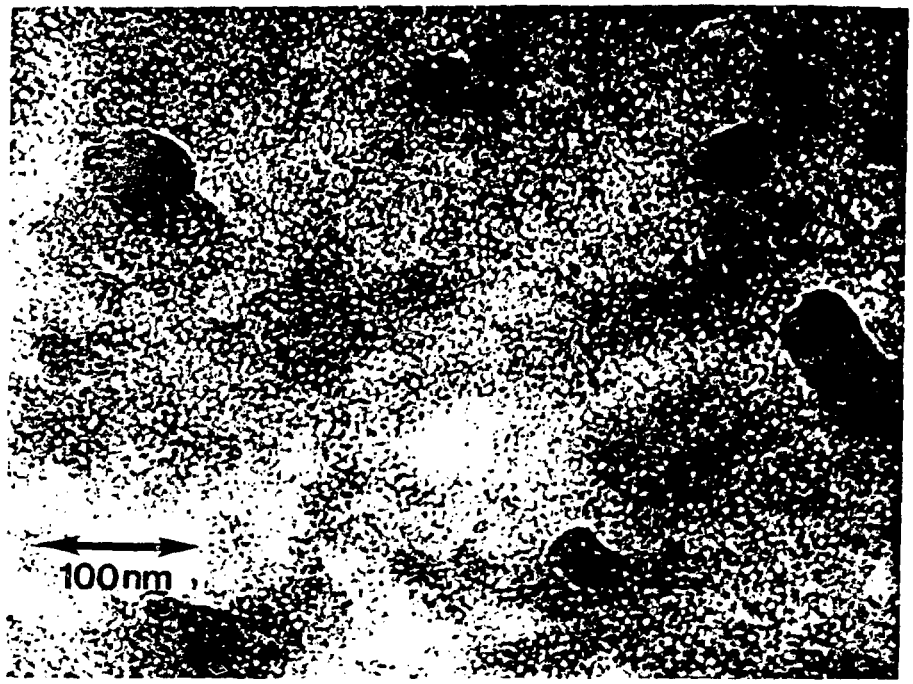

9. Bubble formation in the waste glass induced by irradiation with 250 keV lead ions to a fluence of $5x10^{14}$ ions per square centimeter.

that this type of damage will be significant in some glasses even for the lower radioactivities appropriate to the storage of defense wastes.

Conclusions

Radiation damage is an important consideration for any nuclear waste storage material, and there are a variety of different techniques that may be applied to the characterization of such damage. By understanding the basic processes of radiation damage and the limitations of the various techniques, one may be able to quantitatively predict the damage of these materials.

The microstructural investigations presented here illustrate the approach for a simulated commercial waste storage glass. Here, electron, gamma, and ion irradiations were performed in order to characterize the process of network decomposition in these glasses, information that would have been inaccessible to simple bulk property measurements. The results further illustrate the importance of characterizing the dependances of damage on temperature and dose rate. Extrapolation of any accellerated simulation data to actual waste storage conditions without an understanding of this behavior would be tenuous at best.

The author wishes to thank Dr. K.H. Westmacott and Professor G. Thomas at the National Center for Electron Microscopy for use of those facilities, Dr. N. Bibler at Savannah River Laboratories for conducting the gamma irradiations, and Dr. G.W. Arnold for his assistance on the ion irradiations. I also wish to thank Dr. D.G. Howitt for his invaluable assistance in the direction of this work and for comments on this manuscript. Support for this research was provided by the United States Department of Energy under contract number DE-AT03-79ER10437.

REFERENCES

[1] W.G. Burns, A.E. Hughes, J.A.C. Marples, R.S. Nelson and A.M. Stoneham, J. Noncryst. Solids 107 (1982) p. 245.

[2] D.G Howitt and G. Thomas, Rad. Effects 34 (1977) p. 209.

[3] D.G. Howitt, "Radiation Effects Encountered by Inorganic Materials in AEM," from Analytic Electron Microscopy , Eds. D.C. Joy, A.R. Romig, and J.R. Goldstein, Plenum Press, (in press).

[4] D.K. McElfresh, J.F. DeNatale, E.P. Butler and D.G. Howitt, Rad. Effects 79 (1983) p. 285.

[5] G.L. McVay and L.R. Pederson, J. Am. Ceram. Soc. 64 (1981) p. 154.

[6] G.W. Arnold, Scientific Basis for Nuclear Waste Management -VIII, Eds. C.M. Jantzen, J.A. Stone and R.C. Ewing, (Materials Research Society, 1985) p. 617.

[7] A.M. Ougouag and A.J. Machiels, Scientific Basis for Nuclear Waste Management -VII, Ed. G.L. McVay, (Material Research Society, 1984) p. 797

[8] J.J. Laidler F.A. Garner and L.E. Thomas, "Simulation Experiments with the High Voltage Electron Microscope" in Radiation Damage in Metals , Eds. N.L. Peterson and S.D. Harkness (ASM, 1976) p. 194.

[9] J.E. Mendel et al., "Annual Report on the Characteristics of High-Level Waste Glass," BWNL-2252, June, 1977.

[10] J.F. DeNatale and D.G. Howitt, Bull. Am. Ceram. Soc. 61 (1982) p. 582.

[11] J.F. DeNatale and D.G. Howitt, Nucl. Instr. and Meth. B1(1984) p. 489.

[12] A. Manara, M. Antonini,P. Campagni, and P.N. Gibson, Nucl. Instr. and Meth. B1 (1984) p. 475.

[13] B.J. Todd, J.L. Lineweaver, and J.T. Kerr, J. Appl. Phys. 31 (1960) p. 51.

[14] J.Y. Laval and K.H. Westmacott, Inst. Phys. Conf. Ser. 52 (1980) p. 295.

[15] J.F. DeNatale and D.G. Howitt, Proc. Seventh int. Conf. on High Voltage Electron Microscopy, August 1983, Berkeley, California. Eds. R.M. Fisher, R. Gronsky and

K.H. Westmacott, LBL-16031 (1983) p. 193.

[16] J.F. DeNatale and D.G. Howitt, Rad. Effects. In press.

[17] P.W. Levy, J.M. Loman and J.A. Kierstead, Nucl. Instr. and Meth. B1 (1984) p. 549.

[18] F.P. Roberts, R.P. Turcotte, and W.J. Weber, "Materials Characterization Center Workshop on the Irradiation Effects in Nuclear Waste Forms, Summary Report." PNL-3588, Pacific Northwest Laboratory, 1981

[19] W.J. Weber and F.P. Roberts, "Radiation Effects" in "State of the Art Review of Materials Properties of Nuclear Waste Forms," Eds. J.E. Mendel et al. PNL-3802, Pacific Northwest Laboratory, pp. 6.1-6.52.

AUTHOR INDEX

SUBJECT INDEX